DOE/ET-53088-234 IFSR #234

Turbulence in Toroidally Confined Plasma: Ion-Temperature-Gradient-Driven Turbulence; Dynamics of Magnetic Relaxation In Current-Carrying Plasma

G. S. Lee

Institute for Fusion Studies
The University of Texas at Austin
Austin, Texas 78712-1060

May 1986

TURBULENCE IN TOROIDALLY CONFINED PLASMA :
ION-TEMPERATURE-GRADIENT-DRIVEN TURBULENCE;
DYNAMICS OF MAGNETIC RELAXATION
IN CURRENT-CARRYING PLASMA

APPROVED BY SUPERVISORY COMMITTEE :

Marshall N. Rosenbluth

Patrick H. Diamond

Richard L. Dewar

Jack B. Swift

R. D. Hazeltine

DEDICATION

To my parents,

and my wife Kyesun.

TURBULENCE IN TOROIDALLY CONFINED PLASMA : ION-TEMPERATURE-GRADIENT-DRIVEN TURBULENCE; DYNAMICS OF MAGNETIC RELAXATION IN CURRENT-CARRYING PLASMA

by

GYUNG SU LEE, B.S.

DISSERTATION

Presented to the Faculty of the Graduate School of

The University of Texas at Austin

in Partial Fulfillment

of the Requirements

for the Degree of

DOCTOR OF PHILOSOPHY

THE UNIVERSITY OF TEXAS AT AUSTIN

May, 1986

ACKNOWLEDGEMENTS

It has been a great privilege to work with and learn from Dr. Patrick H. Diamond. I wish to express my deepest appreciation to him for the inspiration of his ingenuity and incisive attitude as a research scientist and as a teacher.

I am deeply indebted to Professor Marshall N. Rosenbluth for his support and advice during the course of this project. I would like to thank Professor Fredrick L. Hinton for his support during the first year at Austin. I would like to express my gratitude to Professor H. L. Berk, Professor J. B. Swift and Dr. R. D. Hazeltine for serving on my dissertation committee. I also have benefited from many discussions with Drs. P. W. Terry, J. N. Leboeuf, T. S. Hahm and Z. G. An.

I wish to express my gratitude to the many people at the Institute for Fusion Studies for their friendship, for sharing of knowledge and for all the assistance they have given me. In particular, I thank Suzy Crumley and Laura Patterson for helping me put it all in perspective.

I wish to thank my officemates and fellow graduate students, Dr. Y. M. Li, Dr. T. H. Chiueh, Dr. R. D. Sydora, G. G. Craddock, J. H. Han, S. B. Kim and O. J. Kwon for their warm friendship.

Finally, I thank my parents and my wife Kyesun for their continous support and comprehension during all these days.

TABLE OF CONTENTS

LIST OF FIGURES

Figure Page

CHAPTER 1. INTRODUCTION

Low frequency fluctuations in magnetically confined plasma have been investigated for many years and have been proposed as explanations of anomalous heat and particle losses, and the relaxation phenomena observed in several toroidal experimental devices, i.e. tokamaks and reversed field pinches (RFP). Understanding the dynamical processes associated with this low frequency turbulence is most important to the goal of achieving controlled nuclear fusion, and is very important for describing relaxation phenomena in astrophysical plasma, as well. Due to the complicated nature of this nonlinear problem and the number of different instability mechanisms (free-energy sources), it is almost impossible to formulate a general theory covering many different characteristics and aspects of low frequency turbulence in confined plasma. However, there have been many successful investigations with many different approaches toward modeling nonlinear plasma processes and explaining the resultant anomalous transport, associated with specific instability. Although the dynamics of these diverse nonlinear phenomena are widely different, the most successful methods for theoretical analysis of these nonlinear phenomena are statistical approaches based on renormalized turbulence theory.

This dissertation is devoted to two specific studies of low frequency turbulence, which pertain to ion-temperature-gradient-driven turbulence in tokamak plasmas and current-gradient driven tearing mode turbulence in RFP plasma. Although it contains two relatively independent works dealing with different driving mechanisms and magnetic configurations, these works

employ similar methods for theoretical analysis of the nonlinear processes. Each disscussion is self-contained.

The first study pertains to the development of an analytic theory of ion-temperature-gradient-driven turbulence in tokamaks. This research on low frequency electrostatic turbulence driven by ion drift instability is motivated by recent experimental observations from the Alcator-C tokamak. These results indicate anomalous energy loss through the ion conduction channel during deeply saturated, high density operation. This observation, and results of pellet injection experiments suggest the strong correlation between the ratio of density and ion temperature scale-lengths and observed ion thermal conduction, and the relationship between particle and energy confinement, in general. This trend appears to extend to auxiliary heated tokamak plasma regimes. In particular, recent charge exchange recombination spectroscopy experiment on the D-III tokamak during neutral beam injection have resulted in direct measurement of the magnitude and radial profile of the ion thermal conductivity. This result indicates a substantial departure from the neoclassical theory prediction which has long been considered adequate for calculating ion thermal conduction.

In Chapter II, a set of fluid equations is derived and the necessary analytic methods for the nonlinear calculation are developed. First, a heuristic description of ion-temperature-gradient-driven turbulence is presented using 'mixing-length' theory based on one-point renormalized equations, in order to identify the saturation mechanism. For a quantitative estimate of the saturation level and resultant ion thermal diffusivity, energy-conserving, renormalized spectrum energy equations are derived and solved using a spatial representation technique. From this solution of the energy mode-coupling equation, the wavenumber spectra of stationary ion-temperature-gradient-driven turbulence

is obtained and the resulting anomalous ion thermal diffusivity is calculated and is shown to result in 'Reynolds number' dependent corrections to the previously calculaed 'mixing-length' estimation. The understanding of dynamics underlying this electrostatic turbulence allows us to apply theoretical predictions to several experimentally observable (measurable) quantities. The theoretically predicted ion thermal diffusivity is compared to the experimentally-deduced one and is found to be consistent. The associated electron thermal diffusivity, particle and heat-pinch velocities are also calculated. The effects of impurity gradient on saturated ion-temperature-gradient-driven turbulence are discussed and a related explanation of density profile steepening during 'Z-mode' operation on the ISX-B tokamak is presented.

The second study is devoted to the role of multiple-helicity nonlinear interaction of tearing modes and the dynamics of magnetic relaxation and 'dynamo' activity in a high temperature, current-carrying plasma. This study of low frequency electromagnetic turbulence driven by current-gradients is motivated by recent experimental results which indicated the correlation between observed macroscopic magnetic fluctuations in RFP plasmas and the anomalous thermal transport and maintenance of the magnetic configration. These issues are discussed in the context of a larger RFP experiment capable of high-temperature, high-current operation.

In Chapter III, a set of fluid equations for tearing modes in the semicollisional regime is derived and a previous resistive MHD study of tearing mode turbulence is extended to high temperature regimes. This study utilizes renormalized turbulence theory, which is developed in Chapter II. Noting the direct connection between fluctuation evolution and configuration evolution, a generalized nonlinear theory of the turbulent dynamo and magnetic relaxation is proposed and two-point $\left\langle (\nabla_\perp \tilde{p})\tilde{\psi} \right\rangle$-correlation evolution is determined by

calculating the relaxation time τ_{cl}. This calculated relaxation time is shown to serve as the phase shift between $\tilde{v}_r$ and $\tilde{\psi}$, and hence controls magnetic energy relaxation and dynamo processes. Careful study of the two seperated regions of kink-tearing modes, i.e. the resonant region and the exterior region, reveals the direct relationship between the equilibrium magnetic energy relaxation and average magnetic flux evolution. Thus a theoretical interpretation of the observed correlation between magnetic fluctuations and maintenance of field reversal is provided.

Finally, the effects of diamagnetic corrections to the MHD turbulence theory are discussed and saturated magnetic fluctuation level is estimated. The result shows that the saturation level is independent or very weakly dependent on the magnetic Reynolds number S. The implications of this result for anomalous thermal transport and dynamo activity in high temperature RFP experiments are discussed.

CHAPTER 2. THEORY OF ION-TEMPERATURE-GRADIENT DRIVEN TURBULENCE IN TOKAMAKS

2.1 Introduction

The search for an adequate understanding of energy confinement in tokamaks has motivated theoretical and experimental research in plasma physics for a long time. Most of this research effort has been oriented toward explaining observed anomalies in electron thermal energy confinement, while neoclassical transport theory has long been considered adequate for calculating ion thermal conduction. However, experimental results now suggest that significant anomalous ion thermal transport may also occur.

In particular, recent experiments on the Alcator-C tokamak[1,2] indicate that when the plasma density is large enough so that the electron-ion thermal equilibration time $(\tau_{ei} \sim 1/n^2)$ approaches (from above) the neo-Alcator electron thermal energy confinement time $(\tau_{E_e} \sim n)$, significant anomalous energy loss can occur through the ion conduction channel. The onset of this loss process occurs while τ_{E_e} begins to saturate. Furthermore, it was also observed that the injection of large pellets and the subsequent steepening of the plasma density gradient resulted in decreased ion thermal conduction. Electron energy confinement remained in the deeply saturated phase. This interesting result suggests that peaked density profiles may be favorable to reduced ion thermal conduction, and that an important relationship between particle and energy confinement exists, in general.

This trend appears to extend into auxiliary heating regimes, in spite of numerous complications in data analysis and interpretation. In particular, neutral beam injection (which directly heats ions) is nearly always accompanied by a degradation in overall energy confinement and a weakening of the density dependence of the energy confinement time τ_E, as it departs from that predicted by neo-Alcator ohmic regime scaling. Furthermore, recent charge exchange recombination spectroscopy experiments on the D-III tokamak[3] during neutral beam injection have resulted in direct measurements of the magnitude and radial profile of the ion thermal conductivity $\chi_i(r)$. Substantial departures, in both magnitude and profile shape, from the neoclassical χ_i prediction are indicated. Finally, the observed density profile broadening, particle confinement time (τ_p) degradation, and density saturation (referred to as the "density clamp"), which frequently accompany the degradation of τ_E during cotangential injection, collectively reinforce the suspicion that ion thermal transport is closely linked to particle transport and confinement.

Ion-temperature-gradient-driven turbulence, which evolves from unstable ion-temperature-gradient modes (η_i-modes, where $\eta_i \equiv d\ln T_i/d\ln n$), has been proposed as a possible explanation of these results. Originally identified by Coppi, et al.,[4] the ion-temperature-gradient instability is an electrostatic sound wave driven unstable by an ion pressure gradient. For $\eta_i > \eta_{ic} \sim 1.5$, where η_{ic} denotes the critical value of η_i necessary for instability, the dynamics probably can be described using a simple fluid model where an adiabatic electron response is neutralized by an ion response determined by pressure ($\tilde{p}_i$), parallel velocity ($\tilde{v}_{\|i}$), and vorticity equations. A growth rate $\gamma \sim \left[\left(1+\eta_i\right)/\tau\right]^{1/2} k_y \rho_s c_s/L_s$ and a radial mode width $\lambda_r = \left[\left(1+\eta_i\right)/\tau\right]^{1/2} \rho_s$ are predicted. Approximate values of the pressure fluctuation level $\tilde{p}_i/p_0 \sim \lambda_r/L_p$ and the thermal diffusivity $\chi_i \sim \left[\left(1+\eta_i\right)/\tau\right]^2 \rho_s^2 c_s/L_s$ can then be trivially de-

duced using familiar mixing-length "rules." The qualitative consistency of the predicted χ_i with experimentally determined ion thermal diffusivity values, the favorable scaling of χ_i with density gradient $\left(\eta_i \sim L_n/L_{Ti}\right)$, and the simplicity and comparative parametric insensitivity of the plasma model collectively establish the ion-temperature-gradient mode as a very promising candidate for explaining anomalous ion thermal transport in tokamaks. Furthermore, extension of the simple electrostatic sheared slab model to include the effects of toroidicity, inductive electric fields, and nonadiabatic electron dynamics probably does not lead to conclusions which differ substantively from those discussed above. Finally, it has been observed that ion-temperature-gradient instability may be enhanced by inverted impurity profiles and may drive an anomalous inward particle flow.[24]

A quantitative understanding of the experimental observations requires a theory of saturated ion-temperature-gradient-driven turbulence. The frequently invoked mixing-length "rules" (i.e., $\tilde{p}_i/p_0 \sim 1/k_x L_p$, $D \sim \gamma/k_x^2$) are neither quantitatively accurate nor necessarily even qualitatively correct (i.e., see Ref. 5), and thus more careful analysis is required. Previous investigations of ion-temperature-gradient-driven turbulence have been primarily devoted to such mixing-length estimates or simple extensions thereof. In particular, in Ref. 6 the anomalous ion thermal diffusivity and inward particle flow velocity were calculated using a mixing-length estimate $\left(e\tilde{\phi}/T_e \sim 1/k_x L_n\right)$ of the electrostatic fluctuation level. However, both intuitive arguments and detailed theoretical analysis indicate that an estimate of the form $\tilde{p}_i/p_0 \sim 1/k_x L_p$ (i.e., pressure, rather than potential, "mixes") is more appropriate. Since $\tilde{p}_i/p_0 = \tilde{n}/n_0 + \tilde{T}_i/T_0 \neq e\tilde{\phi}/T_e$, the predictions of Ref. 6 differ, both qualitatively and quantitatively, from those presented here. The results of the first detailed nonlinear theory of ion-temperature-gradient-driven turbulence are dis-

cussed in Ref. 7. In that investigation, which dealt with a local model of the three-dimensional η_i-mode system, a perturbation expansion was used to obtain coupling equations. Solution of these equations yielded the saturation amplitude, which agreed with the simple mixing-length result. Several difficulties are apparent in this work. First, Eqs. (14)–(16) of Ref. 7 contain no dissipation effects, and thus cannot actually yield a stationary solution for $\eta_i > \eta_{ic}$. This difficulty is also manifested in the exact agreement of the mode-coupling result with the mixing-length estimate. In contrast, while the result of this investigation is similar to the mixing-length estimate, additional detailed functional dependencies, which are related to the nonlinear coupling of the fluctuations to the dissipative energy sink (ion Landau damping), also appear in the result. A second difficulty is the questionable treatment of incoherent mode coupling in Ref. 7. As a result, the consistency of the results with energy conservation constraints is dubious. Finally, it is worthwhile to note that the reason that none of the difficulties discussed here are manifested by the computational investigations described in Ref. 8 is because in that work, heating effects are omitted and the ion pressure gradient flattens. Thus, the results are representative of a quasilinear, rather than a nonlinear, saturation.

In this chapter, a renormalized theory of ion-temperature-gradient-driven turbulence is presented. For $\eta_i > \eta_{ic}$, ion-temperature-gradient-driven turbulence is described by hydrodynamic equations for density, parallel velocity, and pressure

$$\frac{\partial n_i}{\partial t} + \nabla \cdot (n_i \vec{v}_{\perp i}) + \nabla_{\parallel} \left(n_i \tilde{v}_{\parallel i} \right) = 0,$$

$$m_i n_i \left(\frac{\partial \tilde{v}_{\parallel i}}{\partial t} + \vec{v}_E \cdot \nabla_{\parallel} \tilde{v}_{\parallel i} \right) = -e n_i \nabla_{\parallel} \Phi - \nabla_{\parallel} P_i + \mu_{\parallel} \nabla_{\parallel}^2 \tilde{v}_{\parallel i},$$

$$\frac{\partial P_i}{\partial t} + \vec{v}_E \cdot \nabla P_i + \Gamma P_i \nabla_{\parallel} \tilde{v}_{\parallel i} = 0.$$

Three energy-like quadratic integrals $E^W = \frac{1}{2}\int d^3x \left(|\Phi|^2 + |\nabla_\perp \Phi|^2\right)$, $E^K = \frac{1}{2}\int d^3x \left|\tilde{v}_{\|i}\right|^2$ and $E^I = \frac{1}{2}\frac{1}{\Gamma}\int d^3x \left|\tilde{P}_i\right|^2$, which are useful in describing the nonlinear fluctuation dynamics, can be straightforwardly identified. The evolution of the fluctuation energies E^W, E^K, and E^I is governed by the two-point correlation equations

$$\frac{\partial}{\partial t}E^W = -\int d^3x \left[\Phi \nabla_\| \tilde{v}_{\|i} - \left\langle \Phi \hat{b} \times \nabla\Phi \cdot \nabla_\perp \left(\nabla_\perp^2 \Phi\right)\right\rangle\right]$$

$$\frac{\partial}{\partial t}E^K = -\int d^3x \left[\tilde{v}_{\|i}\nabla_\|\Phi + \tilde{v}_{\|i}\nabla_\|\tilde{P}_i + \mu_\| \left\langle \left(\nabla_\| \tilde{v}_{\|i}\right)^2\right\rangle + \left\langle \tilde{v}_{\|i}\hat{b}\times\nabla\Phi\cdot\nabla\tilde{v}_{\|i}\right\rangle\right]$$

$$\frac{\partial}{\partial t}E^I = -\int d^3x \left[\tilde{P}_i\nabla_\|\tilde{v}_{\|i} - \frac{1}{\Gamma}\left\langle \tilde{v}_r\tilde{P}_i\right\rangle \frac{d\langle P_0\rangle}{dr} + \frac{1}{\Gamma}\left\langle \tilde{P}_i\hat{b}\times\nabla\Phi\cdot\nabla\tilde{P}_i\right\rangle\right].$$

The various terms of the two-point correlation equations can be classified in three categories. The first, which includes the terms $\Phi\nabla_\|\tilde{v}_{\|i}$, $\tilde{v}_{\|i}\nabla_\|\tilde{P}_i$, and $\tilde{P}_i\nabla_\|\tilde{v}_{\|i}$ accounts for *linear* energy coupling (equipartitioning) due to sound wave propagation. The second category, which includes the terms $\left\langle \Phi\hat{b}\times\nabla\Phi\cdot\nabla_\perp\left(\nabla_\perp^2\Phi\right)\right\rangle$, $\left\langle \tilde{v}_{\|i}\hat{b}\times\nabla\Phi\cdot\nabla\tilde{v}_{\|i}\right\rangle$, and $\left\langle \tilde{P}_i\hat{b}\times\nabla\Phi\cdot\nabla\tilde{P}_i\right\rangle$ is related to *nonlinear* energy transfer resulting from turbulent $(c/B_0)\left(\tilde{E}\times\hat{b}\right)$ velocity shear stress. The third category includes the source term $(1/\Gamma)\left\langle \tilde{v}_r\tilde{P}_i\right\rangle d\langle P_0\rangle/dr$, proportional to the gradient of the average pressure, and the energy sink $-\mu_\|\left\langle\left(\nabla_\|\tilde{v}_{\|i}\right)^2\right\rangle$, proportional to the parallel viscosity. This shear stress induced energy transfer nonlinearly couples the long wavelength energy sources with the short wavelength energy sink, resulting in saturated, stationary turbulence.

In order to quantitatively describe saturated ion-temperature-gradient-driven turbulence, it is necessary to construct and solve three coupled, renormalized (i.e. closed) energy spectrum evolution equations. In order

to render this rather involved calculation analytically tractable, it is useful to identify the basic nonlinear spatial and temporal scales which characterize saturated ion-temperature-gradient-driven turbulence. The basic spatial scale (radial mixing-length) scale is $\Delta_{\vec{k}} = \left[D_{\vec{k}}/k'_{\|}\right]^{1/4}$, and is obtained by the asymptotic balance of the ion sound term with the vorticity convection term, where the $\tilde{E} \times \vec{B}$ nonlinearities have been renormalized $\left(\left(c/B_0\right)\left(\tilde{E} \times \hat{b}\right) \cdot \nabla \rightarrow D_{\vec{k}}/\Delta_{\vec{k}}^2\right)$ and $D_{\vec{k}}$ refers to turbulent radial diffusion. The basic temporal scales are the nonlinear coherence (correlation) time $\tau_{c,\vec{k}} = \Delta\omega_{\vec{k}}^{-1} = \left[D_{\vec{k}}/\Delta_{\vec{k}}^2\right]^{-1}$, the dissipation time $\tau_{d,\vec{k}} = \left[\mu_{\|} \int dx \left\langle \left(\nabla_{\|}\tilde{v}_{\|}\right)^2 \right\rangle_{\vec{k}} / E_{\vec{k}}^K\right]^{-1}$, and the energy equipartitioning time $\tau_{\mathrm{eq},\vec{k}} = \left[\int dx \left\langle \tilde{p}\nabla_{\|}\tilde{v}_{\|}\right\rangle_{\vec{k}} / E_{\vec{k}}^I\right]^{-1}$. In addition, it is useful to define a "Reynolds number" $\mathrm{Re} \equiv \tau_{d,\vec{k}}/\tau_{c,\vec{k}}$ which parameterizes the relative importance of nonlinear decorrelation in comparison to dissipative processes. At saturation, the level of turbulence must be sufficient so that nonlinear transfer of fluctuation energy to dissipation balances fluctuation growth. Therefore, $\Delta\omega_{\vec{k}} \sim \left[\left(1+\eta_i\right)/\tau\right]^2 k'_{\|}\Delta_{\vec{k}}^2/\Delta\omega_{\vec{k}}$ and $D_{\vec{k}} = \left[\left(1+\eta_i\right)/\tau\right]^{1/2} k'_{\|}\Delta_{\vec{k}}^3$, so that in turn $D_{\vec{k}} = \left[\left(1+\eta_i\right)/\tau\right]^2 \left(k_y\rho_s\right)\rho_s^2 c_s/L_s$ and $\Delta_{\vec{k}} = \left[\left(1+\eta_i\right)/\tau\right]^{1/2}\rho_s$. Hence, the basic time scales are given by $\tau_{\mathrm{eq},\vec{k}}^{-1} = 2(\Gamma/\tau)\left[\left(1+\eta_i\right)/\tau\right]\left(k_y\rho_s c_s/L_s\right)$, $\tau_{c,\vec{k}}^{-1} = \left[\left(1+\eta_i\right)/\tau\right]\left(k_y\rho_s c_s/L_s\right)$ and $\tau_{d,\vec{k}}^{-1} = \left[\mu_{\|}k_y^2/\left(k_{ox}^2 L_s^2\right)\right] \simeq (2/\tau)\left(k_y\rho_s c_s/L_s\right)$, so that $\tau_{\mathrm{eq},\vec{k}} < \tau_{c,\vec{k}} < \tau_{d,\vec{k}}$. The effective "Reynolds number" is given by $\mathrm{Re} = \left[k_{ox}^4 L_s^2 D_{\vec{k}}/\mu_{\|}k_{oy}^2\right] \simeq \left(1+\eta_i\right)$ for $\eta_i > \eta_{ic}$.

The problem of determining the saturation level of ion-temperature-gradient-driven turbulence can be simplified by exploiting the ordering $\tau_{\mathrm{eq},\vec{k}} < \tau_{c,\vec{k}} < \tau_{d,\vec{k}}$. In particular, $\tau_{\mathrm{eq},\vec{k}} < \tau_{c,\vec{k}}$ implies that energy "equipartitioning" among $E_{\vec{k}}^W$, $E_{\vec{k}}^K$ and $E_{\vec{k}}^I$ on a time scale faster than the nonlinear energy transfer time. Thus, $E_{\vec{k}}^W \simeq E_{\vec{k}}^K \simeq E_{\vec{k}}^I$, and the fluctuation energy

evolution equations may be added yielding

$$\frac{\partial}{\partial t}\left\langle \mathcal{E}_{12}\right\rangle_{\vec{k}} + \left\langle S_{12}^{I}\right\rangle + T_{12} = \left\langle S_{12}^{0}\right\rangle,$$

where $\left\langle \mathcal{E}_{12}\right\rangle_{\vec{k}}$ refers to the total fluctuation energy for the mode $\vec{k}$. The $\left\langle \mathcal{E}_{12}\right\rangle_{\vec{k}}$ equation states that the fluctuation energy in the mode $\vec{k}$ is determined by the balance of energy input due to pressure gradient relaxation $\left(\left\langle S_{12}^{0}\right\rangle = (1/\Gamma)\left\langle \tilde{P}_i(2)\nabla_{y_1}\tilde{\phi}(1)\right\rangle\left(d\left\langle P_0\right\rangle/dr\right) + \langle 1 \leftrightarrow 2\rangle\right)$ with the nonlinear transfer $\left(T_{12} = \left\langle \hat{b}\times\nabla_1\tilde{\phi}(1)\cdot\nabla_1\tilde{v}(1)\tilde{v}(2)\right\rangle + (1/\Gamma)\left\langle \hat{b}\times\nabla_1\tilde{\phi}(1)\cdot\nabla_1\tilde{P}_i(1)\tilde{P}_i(2)\right\rangle + \langle 1 \leftrightarrow 2\rangle\right)$ of energy to viscous dissipation $\left(\mu_{\parallel}\nabla_{\parallel}^2\right)$. The fluctuation spectrum can then be obtained by solution of the $\left\langle \mathcal{E}_{12}\right\rangle_{\vec{k}}$ equation. In particular, for $\mathrm{Re} \gg 1$, $\left\langle \mathcal{E}_{12}\right\rangle_{\vec{k}} \sim k_y^{-5/2}$. The spectrum is cut off at $k_d = \sqrt{\mathrm{Re}}\, k_{oy}$, where $k_{oy}\rho_s = 0.4$ is obtained from the calculated spectrum.

Once the fluctuation spectrum has been determined, it is straightforward to calculate the ion thermal diffusivity and other transport coefficients. In particular,

$$\chi_i = [C(\mathrm{Re})]^2\left((1+\eta_i)/\tau\right)^2\left(k_{oy}\rho_s\right)\left(\rho_s^2 c_s/L_s\right)$$

where $C(\mathrm{Re}) \simeq (\pi/2)\ln(1+\eta_i)$ and $k_{oy}\rho_s = 0.4$. It is interesting to note that $\chi_i = F(\mathrm{Re})\chi_i^{\mathrm{Mixing-Length}}$ so that the thermal diffusivity is given by the mixing-length estimate multiplied by a dimensionless function of the "Reynolds number," determined from the calculated fluctuation spectrum. This functional form is characteristic of large "Reynolds number" turbulence. Note that no undetermined parameters remain in the expression for χ_i. Finally, other transport coefficients can be calculated in a similar fashion.

In this chapter, the theory of ion-temperature-gradient-driven turbulence is presented. The principal results are:

(i) The fluctuation energy correlation function and fluctuation wavenumber spectra are calculated by solution of energy-conserving mode-coupling equations. The calculated wavenumber spectrum of ion pressure fluctuations has the form $\left\langle \tilde{P}_i^2 \right\rangle_{k_\theta} \sim k_\theta^{-5/2}$, where $\left(\tilde{P}_i/P_{oi}\right)_{\rm rms} \simeq 5.7\left[\left(1+\eta_i\right)/\tau\right]^{3/2}\rho_s/L_n$. Similarly, the rms fluctuating radial velocity is $\left(\tilde{v}_r\right)_{\rm rms} \simeq 2.3\left[\left(1+\eta_i\right)/\tau\right]^{3/2}\rho_s c_s/L_s$ and fluctuating density is $\left(\tilde{n}/n_0\right) = \left(e\tilde{\Phi}/T_e\right) \simeq 5.7\left[\left(1+\eta_i\right)/\tau\right]^{3/2}\rho_s/L_s$. Note that the predicted density fluctuation levels are quite similar to the usual drift-wave turbulence level $\tilde{n}/n_0 \approx 3\rho_s/L_n$. Hence, it may be difficult to experimentally distinguish η_i-mode induced density fluctuations from more commonplace low frequency, drift-wave turbulence. While the parameter scalings of these results are qualitatively consistent with mixing-length estimates, they have been derived using the calculated fluctuation spectra. In particular, no assumptions such as $k_y\rho_s \sim \mathcal{O}(1)$, etc. were used to obtain the numerical coefficients.

(ii) For $\eta_i > \eta_{ic}$, the ion thermal diffusivity χ_i is given by $\chi_i = \left[C(\mathrm{Re})\right]^2\left(\left(1+\eta_i\right)/\tau\right)^2\left(k_{oy}\rho_s\right)\left(\rho_s^2 c_s/L_s\right)$ where $C(\mathrm{Re}) \simeq (\pi/2)\ln\left(1+\eta_i\right)$. The numerical value of the ion thermal diffusivity is consistent with the experimentally measured χ_i for the Alcator-C tokamak (for which $k_{oy}\rho_s \simeq 0.4$).

(iii) For dissipative trapped electron dynamics (i.e., $\nu_* < 1$, $\nu_{\rm eff} > \bar{\omega}_{De}$), the electron heat conductivity due to ion-temperature-gradient-driven turbulence is given by:

$$\chi_e \simeq 15\sqrt{2}\epsilon^{3/2}\left[\frac{\pi}{2}\ln\left(1+\eta_i\right)\right]^4\left(\frac{1+\eta_i}{\tau}\right)^3\frac{c_s^2\rho_s^2}{\nu_e L_s^2}\left(k_{oy}^2\rho_s^2\right).$$

Here ϵ is the inverse aspect ratio.

Note that in general, $\chi_e \neq \chi_i$.

(iv) For collisional electron dynamics (i.e., $k_{||}v_{th,e} < \nu_{ei}$), the electron response to the ion-temperature-gradient-driven turbulence results in a particle flux:

$$\Gamma_r \simeq 2n_0[C(\mathrm{Re})]^4\left[\hat{\chi}_e+(1+\alpha_T)^2\right]\left[1-\frac{\eta_e}{\eta_e^c}\right] \cdot\left(\frac{m_e}{m_i}\right)\frac{0.51}{\hat{\chi}_e}\frac{\nu_e}{L_n}\left(\frac{1+\eta_i}{\tau}\right)^2\rho_s^2$$

where

$$\eta_e^c \simeq \left[\frac{\hat{\chi}_e+(1+\alpha_T)^2}{3/2\,(1+\alpha_T)}\right] \simeq 1.77.$$

Note that for $\eta_e > 1.77$, the flux is inward. For Alcator-C parameter, $\langle V_r\rangle = \Gamma_r/n_0 \simeq 1000$ cm/sec. Similarly, the electron thermal flux Q_r^e can be derived For $\eta_e > 2.65$, the electron thermal flux is inward and corresponds to a "heat-pinch."

(v) The effects of impurity gradients on ion-temperature-gradient driven turbulence have been investigated. For impurity density n_{oI} with scale length $|L_{nI}|$, $\chi_i \rightarrow \chi_i\Lambda^2$ and $\Gamma_r \rightarrow \Gamma_r\Lambda^3$ where $\Lambda = \left[1+Z\left(n_{oI}/n_{oi}\right)\left(L_{ni}/L_{nI}\right)\right]^{-1}$. Thus impurity distributions peaked on axis heal η_i-mode turbulence while distributions peaked at the edge enhance it. In particular, the enhancement

of Γ_r may underlie the density profile steepening observed during the "Z-mode" of the ISX-B tokamak.

After the completion and presentation[14] of the results of this investigation, an alternative derivation of χ_i for ion-temperature-gradient-driven turbulence was proposed by Connor.[19] In that work, based on dimensional analysis of the ion fluid equations, a χ_i similar to that obtained using "mixing-length rules" was derived. Several difficulties are apparent in this work. First, no dissipation effects (such as $\mu_{||}$) are included in the basic equations, which consequently do not even possess a stationary solution. Second, the dimensional analysis is actually performed on approximate ion fluid equations which omit parallel compressibility effects and thus do not conserve energy. Finally, as a consequence of the first difficulty, the χ_i actually derived has *no* functional dependence on $\mu_{||}$ or Reynolds number. Such dependence must be present in a theory which correctly accounts for the energy sink and dissipation range (at large k_θ) of the fluctuation spectrum.

The remainder of this chapter is organized as follows. In Sec. 2.2, the basic model and linear theory of the ion-temperature-gradient mode is reviewed. In Sec. 2.3, a heuristic description of η_i-mode turbulence is developed using "mixing-length" theory based on one-point renormalized equations. The renormalized two-point equation for the fluctuation energy correlation function is then derived. The energy mode-coupling equation is solved using a spatial representation technique, and the wavenumber spectrum is calculated. In Sec. 2.4, the detailed predictions of the theory for η_i-mode turbulence in tokamaks are presented. The ion and electron thermal diffusivities, anomalous particle fluxes, and impurity effects are discussed. Section 2.5 includes the summary and conclusions.

2.2 Basic Model and Linear Theory

An all-inclusive description of the ion-temperature-gradient-driven instability (η_i-mode) requires the use of kinetic theory to treat the detailed linear properties such as threshold values of η_i, associated with ion-wave interaction (Landau damping), and finite Larmor radius corrections.[4,9] However, a comparison of the Vlasov dispersion relation with the dispersion relation obtained from fluid equations suggests that the fluid model adequately describes the essential physics of η_i-mode in the phase velocity regime $v_{th,i} \lesssim |\omega/k_\parallel| < v_{th,e}$. That is, while fluid equations may obscure certain details of the linear stability theory and are not applicable to the case of flat density profile $(\eta_i > L_s/L_T)$, they adequately describe the nonlinear dynamics in the range $\eta_{ic} < \eta_i < L_s/L_T$. Hence, the use of a fluid model is justified for parameter regimes appropriate to the confinement region of many tokamak plasmas.

Here, we derive the fluid equations to describe the evolution of the ion-temperature-gradient-driven turbulence. To simplify the analysis and construct an analytically tractable model of the nonlinear evolution of the η_i-mode, we consider a simple radially inhomogeneous sheared slab of plasma. The magnetic field is given by $\vec{B} = B\left(\hat{z} + \left(x/L_s\right)\hat{y}\right)$ where $L_s^{-1} = B_y'(x)/B_0$ is the shear length. The parallel wavenumber thus varies with x and is given by

$$k_\parallel(x) \simeq \left(x - x_{\vec{k}}\right)\frac{k_y}{L_s} \tag{1}$$

in the neighborhood of the mode-rational surface $x_{\vec{k}}$, where $\vec{k}\cdot\vec{B}_0\left(x_{\vec{k}}\right) = 0$. In this geometry, low frequency $(\omega \ll \omega_{ci})$ perturbations have the form

$$\tilde{f}(x)\exp\left(-i\omega t + ik_y y + ik_\parallel z\right).$$

To describe ion dynamics, the basic fluid model consists of the coupled equations for the ion density $\tilde{n}_i(\vec{x},t)$, parallel ion velocity $\tilde{v}_{\|i}(\vec{x},t)$, and ion pressure $\tilde{P}_i(\vec{x},t)$.[10] Quasineutrality with adiabatic electron response ($\tilde{n}_e = \tilde{n}_i = e\tilde{\Phi}/T_e$, since $|\omega/k_\|| \ll v_{th,e}$) and electrostatic dynamics are assumed. Thus, the continuity equation for the ion density is given by

$$\frac{\partial n_i}{\partial t} + \vec{\nabla}\cdot(n_i\vec{v}_{\perp i}) + \nabla_\|\left(n_i\tilde{v}_{\|i}\right) = 0. \tag{2}$$

The perpendicular ion dynamics are due to $\vec{E}\times\vec{B}$ and ion diamagnetic-drifts, so that to the first order in $\mathcal{O}(\omega/\omega_{ci})$:

$$\vec{v}_{\perp i,1} = \vec{v}_E + \vec{v}_{Di}, \tag{3}$$

where

$$\vec{v}_E = \frac{c}{B}\hat{b}\times\vec{\nabla}\Phi$$

and

$$\vec{v}_{Di} = \frac{c}{eBn_i}\hat{b}\times\vec{\nabla}P_i$$

with

$$\hat{b} = \vec{B}/|\vec{B}|.$$

To the next order, the generalized ion polarization-drift is given by

$$\vec{v}_p = -\frac{c^2 m_i}{eB^2}\left[\frac{\partial}{\partial t} + \vec{v}_{\perp i,1}\cdot\vec{\nabla}_\perp\right]\vec{\nabla}_\perp\Phi.$$

Similarly, the equation of parallel motion is given by

$$m_i n_i\left(\frac{\partial\tilde{v}_{\|i}}{\partial t} + \vec{v}_E\cdot\vec{\nabla}\tilde{v}_{\|i}\right) = -en_i\nabla_\|\Phi - \nabla_\|\tilde{P}_i + \mu_\|\nabla_\|^2\tilde{v}_{\|i}. \tag{4}$$

It is important to note that the parallel flow is advected only by $\vec{v}_E$.[11] In Eq. (4) the parallel ion viscous diffusion term is retained. The parallel viscosity term

models either collisionless Landau damping $\left(\mu_{\|} \sim v_{th,i}^2/|\omega|\right)$ or collisional parallel viscosity $\left(\mu_{\|} \sim v_{th,i}^2/\nu_{ii}\right)$. This parallel viscosity is a sink of energy in the large-k (i.e. dissipation) region of the wavenumber spectrum and is especially important in the nonlinear theory. Finally, the evolution equation for ion pressure is

$$\frac{\partial P_i}{\partial t} + \vec{v}_E \cdot \nabla P_i + \Gamma P_i \nabla_{\|} \tilde{v}_{\|i} = 0, \tag{5}$$

where Γ is the ratio of the specific heats. The adiabatic compression term, $\Gamma \nabla_{\|} \tilde{v}_{\|i}$, must be retained to account for energy exchange between pressure fluctuations and parallel velocity fluctuations in the nonlinear theory. However, this term has little effect on linear stability and the basic scales associated with the η_i-modes.

To exploit the basic spatial and temporal scales characteristic of ion-drift modes (i.e., sound speed c_s and $\rho_s = c_s/\omega_{ci}$), we introduce a dimensionless form of the evolution equations where spatial scales are in units of ρ_s and the temporal scales are in units of ω_{ci}^{-1}. The dimensionless fields are defined in terms of the natural units T_e, c_s and P_i, so that the electrostatic potential is $\tilde{\phi} \equiv e\Phi/T_e$, the parallel ion momentum is $\tilde{v}_{\|} \equiv \tilde{v}_{\|i}/c_s$, and the ion pressure is $\tilde{p} \equiv \left[\tilde{p}_i/\langle P_{io}\rangle\right]\left(T_i/T_e\right)$, where $P_i = \langle P_{io}\rangle + \tilde{p}_i$ and $n_i = n_o + \tilde{n}_i$. We thus obtain the basic set of equations which describes ion-temperature-gradient-driven turbulence from Eqs. (2)–(5), which yield:

$$\frac{\partial}{\partial t}\left(1 - \nabla_{\perp}^2\right)\tilde{\phi} + v_D\left\{1 + \left(\frac{1+\eta_i}{\tau}\right)\nabla_{\perp}^2\right\}\nabla_y\tilde{\phi} - \hat{b} \times \nabla\tilde{\phi} \cdot \nabla_{\perp}\left(\nabla_{\perp}^2\tilde{\phi}\right) + \nabla_{\|}\tilde{v}_{\|} = 0 \tag{6}$$

$$\frac{\partial}{\partial t}\tilde{v}_{\|} + \hat{b} \times \nabla\tilde{\phi} \cdot \nabla\tilde{v}_{\|} - \mu\nabla_{\|}^2\tilde{v}_{\|} = -\nabla_{\|}\tilde{\phi} - \nabla_{\|}\tilde{p} \tag{7}$$

$$\frac{\partial}{\partial t}\tilde{p} + v_D\left(\frac{1+\eta_i}{\tau}\right)\nabla_y\tilde{\phi} + \hat{b} \times \nabla\tilde{\phi} \cdot \nabla\tilde{p} = -\Upsilon\nabla_{\|}\tilde{v}_{\|}, \tag{8}$$

where

$$v_D \equiv -\frac{cT_e}{eB}\frac{d\left(\ln n_o\right)}{dx}, \qquad \tau \equiv \frac{T_e}{T_i}, \qquad \eta_i = \frac{d\left(\ln T_i\right)}{d\left(\ln n_o\right)},$$

$$\Upsilon \equiv \frac{\Gamma}{\tau} \quad \text{and} \quad \mu \equiv \frac{\mu_{\|}\omega_{ci}}{c_s^2}.$$

In writing Eqs. (6)–(8), we retain only the dominant nonlinearities due to $\vec{E}\times\vec{B}$-convection. In order to understand the nonlinear dynamics of ion-temperature-gradient-driven turbulence, it is essential to consider the energetics of the system. The energy flows and energy balance can be elucidated by consideration of energy-like integrals quadratic in the fluctuating field amplitudes. These energy-like integrals are defined by the sum of the electrostatic energy (electron internal energy) and (ion) perpendicular kinetic energy

$$E^W \equiv \frac{1}{2}\int d^3x \left(|\tilde{\phi}|^2 + \left|\nabla_\perp\tilde{\phi}\right|^2\right), \tag{9}$$

the parallel ion kinetic energy

$$E^K \equiv \frac{1}{2}\int d^3x \left|\tilde{v}_{\|}\right|^2, \tag{10}$$

and the ion thermal energy

$$E^I \equiv \frac{1}{2}\frac{1}{\Upsilon}\int d^3x|\tilde{p}|^2. \tag{11}$$

Using the evolution equations for density, ion parallel velocity, and ion pressure, these energy-like integrals can readily be shown to satisfy certain relations by use of the conservation property of convective nonlinearities (i.e., $\int d^3x\tilde{A}\nabla\tilde{\phi}\times\hat{b}\cdot\nabla\tilde{A}=0$ for any $\tilde{A}$). It follows that

$$\frac{\partial}{\partial t}E^W = -\int d^3x\tilde{\phi}\nabla_{\|}\tilde{v}_{\|} \tag{12}$$

$$\frac{\partial}{\partial t}E^K = -\int d^3x\left[\tilde{v}_{\|}\nabla_{\|}\tilde{\phi} + \tilde{v}_{\|}\nabla_{\|}\tilde{p} + \mu\left|\nabla_{\|}\tilde{v}_{\|}\right|^2\right] \tag{13}$$

$$\frac{\partial}{\partial t}E^I = -\int d^3x \left[\tilde{p}\nabla_\parallel \tilde{v}_\parallel + \frac{1}{\Upsilon}\left(\frac{1+\eta_i}{\tau}\right) v_D \left\langle \tilde{p}\nabla_y \tilde{\phi}\right\rangle\right]. \tag{14}$$

Hence, the total energy of the system evolves according to

$$\frac{\partial}{\partial t}E = -\int d^3x \left[\frac{1}{\Upsilon}\left(\frac{1+\eta_i}{\tau}\right) v_D \left\langle \tilde{p}\nabla_y \tilde{\phi}\right\rangle + \mu \left|\nabla_\parallel \tilde{v}_\parallel\right|^2\right]. \tag{15}$$

These evolution equations state that the coupling terms $\tilde{\phi}\nabla_\parallel \tilde{v}_\parallel$ and $\tilde{p}\nabla_\parallel \tilde{v}_\parallel$ account for transfer of fluctuation energy between fields. Hence, the sum is conserved up to the difference of drive by ion-temperature-gradient source and dissipation by ion parallel viscous diffusion. In the saturated state, nonlinear processes dynamically regulate the balance of input from the ion-temperature-gradient free-energy source with the linear dissipation due to $\mu_\parallel$ (sink). Naturally, a stationarity of total energy evolution is a necessary condition for saturation.

The linear theory of the ion-temperature-gradient-driven instability has been investigated by many authors,[4,6,7,9,12] using both kinetic and fluid models in slab and toroidal geometry. Here, we do not attempt to address all details, nor undertake a review of the linear theories. However, it is instructive to review aspects of the linear theory from the viewpoint of developing a nonlinear theory. Within the framework of our model equations, the linear eigenmode equation can be derived in a straightforward manner by assuming a space-time variation of the form $\tilde{f}(x)\exp\left(-i\omega t + i\int k_x(x)\,dx + ik_y y\right)$ and $k_\perp \rho_s < 1$, so that we obtain the eigenmode equation

$$\frac{d^2}{dx^2}\tilde{\phi}_{\vec{k}} + Q(x,\Omega)\tilde{\phi}_{\vec{k}} = 0, \tag{16}$$

where the potential function is given by

$$Q(x,\Omega) = \left\{ -k_y^2 + \frac{[1-\Omega]}{\left[\Omega + \left((1+\eta_i)/\tau\right)\right]} + \frac{\left(L_n/L_s\right)^2 x^2}{\Omega^2\left[1 - \frac{\Gamma}{\tau}\left(L_n/L_s\right)^2 x^2/\Omega^2\right]}\right\} \tag{17}$$

with

$$\Omega \equiv \frac{\omega}{\omega_{*e}} = \frac{\omega}{(k_y v_D)}.$$

From this linear eigenmode equation, we can determine basic spatial and temporal scales of the η_i-mode such as the mode width, the growth rate, and the real frequency. In Eq. (16), we neglect the effects associated with Landau damping and finite Larmor radius corrections. This is appropriate for the fluid ion regime which describes the low-$k_\perp$ region of the wavenumber spectrum. This is an especially good model for high-shear regions of tokamak plasmas (i.e., $\hat{s} = rq'/q \geq 1$), where toroidicity corrections are probably insignificant.

The WKB eigenvalue condition for the Weber equation gives the following dispersion relation

$$\Omega^2\left(1+k_y^2\right) + \Omega\left[k_y^2\left(\frac{1+\eta_i}{\tau}\right) + i(2n+1)\frac{L_n}{L_s} - 1\right] + i(2n+1)\frac{(1+\eta_i)}{\tau}\frac{L_n}{L_s} = 0, \tag{18}$$

where $n = 0, 1, \ldots$ are radial wavenumbers. For small wavenumbers, $k_y^2 \ll \left(\tau/\left(1+\eta_i\right)\right) < 1$, the growth rate and mode width for the unstable ion-drift mode are given by $\Omega \simeq i\left(1+\eta_i/\tau\right)L_n/L_s$ and $\lambda_r \simeq \left(\left(1+\eta_i\right)/\tau\right)^{1/2}$, respectively. It is important to notice that the η_i-mode in this wavenumber regime is almost purely growing, with growth rate scaling inversely with the shear length. For the wavenumber regime of $k_y^2 \simeq \left(\tau/\left(1+\eta_i\right)\right) < 1$, the restoring force along $\vec{B}$ is stronger and the η_i-mode has a real frequency which is comparable to the growth rate. The complex eigenfrequency is given by

$$\Omega = \omega_r + i\gamma \simeq \left(\frac{-1+i}{\sqrt{2}}\right)\left[\frac{\left(\left(1+\eta_i\right)/\tau\right)L_n/L_s}{\left(1+k_y^2\right)}\right]^{1/2}.$$

The mode width does not vary significantly from the value for smaller k_y, provided the inequality $|\gamma| > |\omega_r|$ is satisfied. Throughout the range of wavenum-

bers (i.e., $k_y^2 \simeq \left(\tau/\left(1+\eta_i\right)\right) < 1$), the potential-well structure is found to persist and the growth rate is larger than the real frequency.

Detailed numerical (shooting code) solutions of the linear eigenmode equation, including kinetic effects, have been obtained by Waltz et al.[13] These numerical studies indicate that the most unstable mode is located in the low-k_y region of the wavenumber spectrum $\left(k_y^2 < 1\right)$ and the effective potential in this regime is found to be a well structure which can be adequately described by the potential function of Eq. (17). Hence, the eigenfunction has the character of a radially localized normal mode [Fig. 2.1]. These unstable modes are the principal free-energy source for the turbulence. For higher-k_y $\left(k_y^2 \gtrsim 1\right)$, ω_r/γ progressively increases and exceeds unity. The potential-well structure disappears and turns into a potential-hill. Hence, the eigenmode takes on the character of a propagating wave [Fig. 2.2]

The wave energy is then susceptible to absorption by shear damping, which results in parallel ion heating at the large-$k_{||}$ region of the eigenmode. These higher-k_y damped modes are a sink of fluctuation energy. Hence, a possible saturation mechanism is nonlinear energy transfer from low-k_y unstable modes into the high-k_y damped modes. In order to incorporate the important stabilizing effect associated with shear damping into the fluid theory, the sink of fluctuation energy is modeled by a parallel ion viscosity with coefficient $\mu_{||}$, which represents the damping of the high-k_y modes. It should be noted that the effect of the parallel viscosity on the low-k_y modes is weak, and the detailed nonlinear study shows that the saturated state has a weak dependence upon the value of the viscosity coefficient $\mu_{||}$ within the range of η_i-values where the fluid theory is applicable.

Finally, it is necessary to point out that for the two limiting cases associated with $\eta_i \sim \eta_{ic}$ and flat density, the fluid ion approximation is not

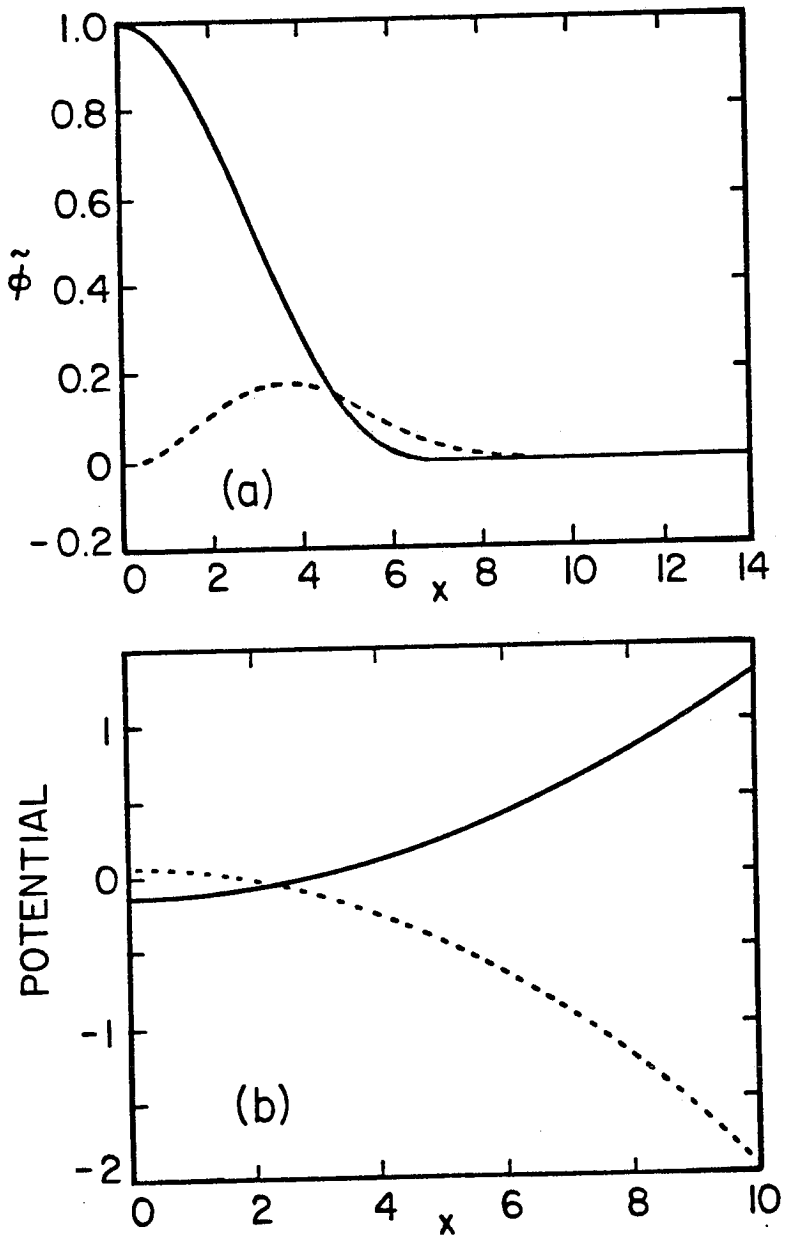

Fig. 2.1 Complex eigenmode (a), and potential function (b) for $k_y\rho_s = 0.3$, $\eta_i = 4.$, $T_e/T_i = 1.$, and $L_n/L_s = 1/20$.

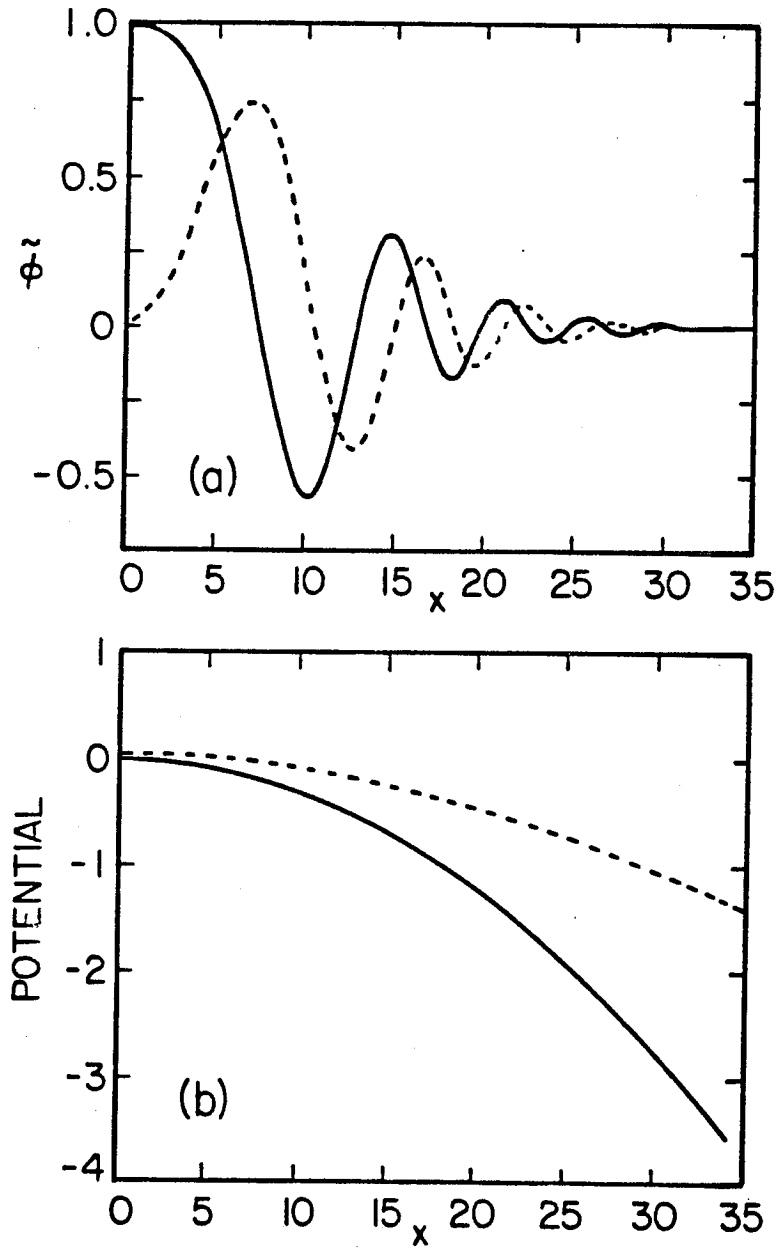

Fig. 2.2 Complex eigenmode (a), and potential function (b) for $k_y\rho_s = 0.7$, $\eta_i = 4.$, $T_e/T_i = 1.$, and $L_n/L_s = 1/20$.

valid. These two limiting cases have been previously discussed in studies of linear stability[6,12] and we will not repeat the results in this chapter. However, it should be noted that the range of η_i-values where the fluid theory is applicable $\left(\eta_{ic} < \eta_i < L_s/L_T\right)$ seems to correspond to most parameter regimes of experimental interest.[14]

2.3 Nonlinear Theory

In this section, the analytic theory of the nonlinear evolution and saturation of ion-temperature-gradient-driven turbulence is presented. The fluctuation levels, spectra, and the thermal diffusivity at saturation are calculated. The implications of these results for predictions of heat and particle transport in tokamak plasma are then discussed in Section 2.4.

Before proceeding with our discussions of the dynamics of nonlinear evolution and saturation of ion-temperature-gradient-driven turbulence, we pause to consider the question of whether quasi-linear flattening of the average ion-temperature-gradient or turbulent stabilization via nonlinear coupling to dissipation is the relevant saturation mechanism. In the case of η_i-mode turbulence in tokamaks, the average ion-temperature-gradient is driven by the balance of power input, through ohmic or neutral beam heating, with thermal transport. Furthermore, the density profile is determined by particle transport dynamics. Thus the η_i-profile is determined by external drive. Although η_i-mode induced heat loss can be substantial, it is not catastrophic, since predicted χ_i values are consistent with experimental observations. As marginal stability scenarios usually are based on the notion that violation of the marginal stability condition results in catastrophic transport (i.e., much larger than that

actually observed), an *a priori* assertion that the η_i-profile is determined by marginal stability considerations seems unreasonable. Thus, quasi-linear mechanisms alone are not adequate for the description of η_i-mode saturation, and nonlinear mechanisms must be considered.

The organization of this section is as follows: we begin with a heuristic description of η_i-mode turbulence using renormalized one-point theory and mixing-length estimates to outline the physics of the saturation mechanism and the energy dynamics of the system. We identify the important basic temporal and spatial scales and the "Reynolds" number of the η_i-mode system, and estimate the level of fluctuations and the thermal diffusion coefficient at saturation. We proceed to develop a more detailed nonlinear theory, utilizing a spatial representation of the two-point spectral energy equation to quantitatively calculate the wavenumber spectrum and the fluctuation level. Finally, a brief review of the nonlinear theory and a summary of results are presented.

A. Heuristic Description

Nonlinear theories based on heuristic ambient-gradient or mixing-length estimates (i.e., $\left|e\Phi/T_e\right| \sim 1/k_\perp L_{T_i}$, $D \sim \gamma/k_\perp^2$) do not necessarily account for the dynamics of nonlinear evolution and saturation of η_i-mode turbulence. Furthermore, since the mode width is a function of the linear growth rate, the meaning of the mixing-length estimate of saturation is unclear when growth rates vanish. Thus, it is necessary to determine spatial and temporal scales associated with saturated η_i-mode turbulence. Also, it is necessary to derive and solve a spectrum equation which properly accounts for energy flow from source to sink via nonlinear coupling.

Now, we consider the nonlinear evolution of η_i-mode turbulence using the equations derived previously. This set of nonlinear equations can be

analyzed by renormalizing the nonlinearities using iterative substitution techniques, and considering the nonlinear evolution of a linearly unstable η_i-mode in a background spectrum of multiple-helicity turbulence. The relevant nonlinear spatial and temporal scales can thus be identified. Renormalized two-point equations are then used to calculate the fluctuation levels and spectra.

Fourier transforming Eqs. (6)–(8) in the y and z directions, the nonlinear evolution equations for the test mode $(\vec{k})$ can be written as

$$\begin{aligned}
&\frac{\partial}{\partial t}(1-\nabla_\perp^2)\tilde{\phi}_{\vec{k}} + i\left(1+\frac{(1+\eta_i)}{\tau}\nabla_\perp^2\right)\omega_{*e}\tilde{\phi}_{\vec{k}} + ik_\parallel \tilde{v}_{\parallel\vec{k}} \\
&+\left\{\left[\frac{\partial}{\partial x}\left(\sum_{\vec{k}'}\left(-ik_y'\right)\tilde{\phi}_{-\vec{k}'}\nabla_\perp^2\tilde{\phi}_{\vec{k}''}\right) - ik_y\sum_{\vec{k}'}\frac{\partial\tilde{\phi}_{-\vec{k}'}}{\partial x'}\nabla_\perp^2\tilde{\phi}_{\vec{k}''}\right]\right. \\
&\left.-\left[\frac{\partial}{\partial x}\left(\sum_{\vec{k}'}\left(-ik_y'\right)\left(\nabla_\perp^2\tilde{\phi}_{-\vec{k}'}\right)\tilde{\phi}_{\vec{k}''}\right) - ik_y\sum_{\vec{k}'}\frac{\partial\left(\nabla_\perp^2\tilde{\phi}_{-\vec{k}'}\right)}{\partial x'}\tilde{\phi}_{\vec{k}''}\right]\right\} \\
&= 0
\end{aligned} \tag{19}$$

$$\begin{aligned}
&\frac{\partial}{\partial t}\tilde{v}_{\parallel\vec{k}} + ik_\parallel\tilde{\phi}_{\vec{k}} + ik_\parallel\tilde{p}_i + \mu k_\parallel^2\tilde{v}_{\parallel\vec{k}} \\
&-\left\{\left[\frac{\partial}{\partial x}\left(\sum_{\vec{k}'}\left(-ik_y'\right)\tilde{\phi}_{-\vec{k}'}\tilde{v}_{\parallel\vec{k}''}\right) - ik_y\sum_{\vec{k}'}\frac{\partial\tilde{\phi}_{-\vec{k}'}}{\partial x'}\tilde{v}_{\parallel\vec{k}''}\right]\right. \\
&\left.-\left[\frac{\partial}{\partial x}\left(\sum_{\vec{k}'}\left(-ik_y'\right)\tilde{v}_{\parallel-\vec{k}'}\tilde{\phi}_{\vec{k}''}\right) - ik_y\sum_{\vec{k}'}\frac{\partial\tilde{v}_{\parallel-\vec{k}'}}{\partial x'}\tilde{\phi}_{\vec{k}''}\right]\right\} = 0
\end{aligned} \tag{20}$$

$$\frac{\partial}{\partial t}\tilde{p}_{\vec{k}} + i\frac{(1+\eta_i)}{\tau}\omega_{*e}\tilde{\phi}_{\vec{k}} + ik_{\|}\Upsilon\tilde{v}_{\|\vec{k}}$$
$$-\left\{\left[\frac{\partial}{\partial x}\left(\sum_{\vec{k}'}\left(-ik'_y\right)\tilde{\phi}_{-\vec{k}'}\tilde{p}_{\vec{k}''}\right) - ik_y\sum_{\vec{k}'}\frac{\partial\tilde{\phi}_{-\vec{k}'}}{\partial x'}\tilde{p}_{\vec{k}''}\right]\right.$$
$$\left.-\left[\frac{\partial}{\partial x}\left(\sum_{\vec{k}'}\left(-ik'_y\right)\tilde{p}_{-\vec{k}'}\tilde{\phi}_{\vec{k}''}\right) - ik_y\sum_{\vec{k}'}\frac{\partial\tilde{p}_{-\vec{k}'}}{\partial x'}\tilde{\phi}_{\vec{k}''}\right]\right\} = 0, \qquad (21)$$

where $\vec{k} = (k_y, k_z)$, and the "driven" mode is $\vec{k}'' = \vec{k} + \vec{k}'$ with $\vec{k}'$ as the "background" mode and $\vec{k}$ as the "test" mode. To obtain renormalized equations, a standard weak coupling closure approximation[15] is used to renormalize the (convective) nonlinearities by iteratively substituting the nonlinearly driven fields $\tilde{\phi}^{(2)}_{\vec{k}''}$, $\left(\nabla^2_\perp\tilde{\phi}_{\vec{k}''}\right)^{(2)}$, $\tilde{v}^{(2)}_{\|\vec{k}''}$ and $\tilde{p}^{(2)}_{\vec{k}''}$ for $\tilde{\phi}_{\vec{k}''}$, $\nabla^2_\perp\tilde{\phi}_{\vec{k}''}$, $\tilde{v}_{\|\vec{k}''}$, and $\tilde{p}_{\vec{k}''}$, respectively. Here, $\tilde{\phi}^{(2)}_{\vec{k}''}$, $\left(\nabla^2_\perp\tilde{\phi}_{\vec{k}''}\right)^{(2)}$, $\tilde{v}^{(2)}_{\|\vec{k}''}$ and $\tilde{p}^{(2)}_{\vec{k}''}$ are nonlinearly driven by the direct beating of the test $(\vec{k})$ and background $(\vec{k}')$ modes. These driven fields satisfy the equations

$$\Delta\omega_{\vec{k}''}\left(1-\nabla^2_\perp\right)\tilde{\phi}^{(2)}_{\vec{k}''} + i\omega''_{*e}\left(1+\frac{(1+\eta_i)}{\tau}\nabla^2_\perp\right)\tilde{\phi}^{(2)}_{\vec{k}''} + ik''_{\|}\tilde{v}^{(2)}_{\|\vec{k}''} = S_\phi \qquad (22)$$

$$\Delta\omega_{\vec{k}''}\tilde{v}^{(2)}_{\|\vec{k}''} + ik''_{\|}\tilde{\phi}^{(2)}_{\vec{k}''} + ik''_{\|}\tilde{p}^{(2)}_{\vec{k}''} = S_v \qquad (23)$$

$$\Delta\omega_{\vec{k}''}\tilde{p}^{(2)}_{\vec{k}''} + i\left(\frac{1+\eta_i}{\tau}\right)\omega''_{*e}\tilde{\phi}^{(2)}_{\vec{k}''} + ik''_{\|}\Upsilon\tilde{v}^{(2)}_{\|\vec{k}''} = S_p, \qquad (24)$$

where S_ϕ, S_v, and S_p are the sources for the driven mode $(\vec{k}'')$ and are given by

$$S_\phi = \left\{ik'_y\tilde{\phi}_{\vec{k}'}\frac{\partial}{\partial x}\left(\nabla^2_\perp\tilde{\phi}_{\vec{k}}\right) - ik_y\frac{\partial\tilde{\phi}_{\vec{k}'}}{\partial x'}\left(\nabla^2_\perp\tilde{\phi}_{\vec{k}}\right)\right.$$
$$\left.+ik_y\tilde{\phi}_{\vec{k}}\frac{\partial}{\partial x'}\left(\nabla^2_\perp\tilde{\phi}_{\vec{k}'}\right) - ik'_y\frac{\partial\tilde{\phi}_{\vec{k}}}{\partial x}\left(\nabla^2_\perp\tilde{\phi}_{\vec{k}'}\right)\right\} \qquad (25)$$

$$S_v = \left\{ ik'_y \tilde{\phi}_{\vec{k}'} \frac{\partial \tilde{v}_{\|\vec{k}}}{\partial x} - ik_y \frac{\partial \tilde{\phi}_{\vec{k}'}}{\partial x'} \tilde{v}_{\|\vec{k}} + ik_y \tilde{\phi}_{\vec{k}} \frac{\partial \tilde{v}_{\|\vec{k}'}}{\partial x'} - ik'_y \frac{\partial \tilde{\phi}_{\vec{k}}}{\partial x} \tilde{v}_{\|\vec{k}'} \right\} \tag{26}$$

$$S_p = \left\{ ik'_y \tilde{\phi}_{\vec{k}'} \frac{\partial \tilde{p}_{\vec{k}}}{\partial x} - ik_y \frac{\partial \tilde{\phi}_{\vec{k}'}}{\partial x'} \tilde{p}_{\vec{k}} + ik_y \tilde{\phi}_{\vec{k}} \frac{\partial \tilde{p}_{\vec{k}'}}{\partial x'} - ik'_y \frac{\partial \tilde{\phi}_{\vec{k}}}{\partial x} \tilde{p}_{\vec{k}'} \right\}. \tag{27}$$

$\Delta\omega_{\vec{k}''}$ is the decorrelation rate for test ($\vec{k}$) and background ($\vec{k}'$) modes, and thus serves to limit the time scale of nonlinear interaction. The solutions of the driven mode equations can be obtained by convolving an integral transformation of the source functions with the global propagator for the field $\tilde{\phi}_{\vec{k}}$. However, a simple, approximate solution is sufficient to understand the basic dynamics of the nonlinear processes which we intend to discuss in this section. In particular, the turbulence is characterized by a single radial scale. Thus, the large-x asymptotic balance which determines the effective radial scale is dominated by the direct term contributions and, for this purpose, the $\tilde{\phi}^{(2)}_{\vec{k}''}$ terms (which contribute integral operators) can be ignored. With these approximations, driven fields are given approximately by

$$\left(\nabla^2_\perp \tilde{\phi}_{\vec{k}''}\right)^{(2)} \simeq S_\phi / \left[\Delta\omega_{\vec{k}''}\right] \tag{28}$$

$$\tilde{v}^{(2)}_{\|\vec{k}''} \simeq S_v / \left[\Delta\omega_{\vec{k}''}\right] \tag{29}$$

$$\tilde{p}^{(2)}_{\vec{k}''} \simeq S_p / \left[\Delta\omega_{\vec{k}''}\right]. \tag{30}$$

Note that the neglect of $\tilde{\phi}^{(2)}_{\vec{k}''}$ is consistent with the conservation law symmetry properties of the $\tilde{v}_\|$, $\tilde{p}$ and $\left\langle \tilde{v}^2_\| \right\rangle$, $\langle \tilde{p}^2 \rangle$ equations. The symmetry properties of the vorticity equation can be preserved by noting, for localized modes,

$$\frac{\partial}{\partial x} \sum_{\vec{k}'} -ik_y \left\{ \tilde{\phi}_{-\vec{k}'} \left(\nabla^2_\perp \tilde{\phi}_{\vec{k}''}\right) - \left(\nabla^2_\perp \tilde{\phi}_{-\vec{k}'}\right) \tilde{\phi}_{\vec{k}''} \right\}$$

$$= \frac{\partial}{\partial x} \sum_{\vec{k}} \left(-ik_y \frac{k_y^2}{k_y''^2} \right) \left\{ \tilde{\phi}_{-\vec{k}'} \left(\nabla^2_\perp \tilde{\phi}_{\vec{k}''}\right) \right\}$$

where an integration by parts has been performed. Substituting the driven-field solutions into the nonlinear coupling terms in Eqs. (19)–(21) (noting the radial parity of the fields) yields the renormalized equations which govern the evolution of the test mode ($\vec{k}$):

$$\begin{aligned}&\frac{\partial}{\partial t}(1-\nabla_\perp^2)\tilde{\phi}_{\vec{k}}+i\omega_{*e}\left(1+\frac{(1+\eta_i)}{\tau}\nabla_\perp^2\right)\tilde{\phi}_{\vec{k}}\\&+\frac{\partial}{\partial x}\left[D_{\vec{k}}\frac{\partial}{\partial x}\left(\nabla_\perp^2\tilde{\phi}_{\vec{k}}\right)\right]-C_{\vec{k}}k_y^2\tilde{\phi}_{\vec{k}}=-ik_\parallel\tilde{v}_{\parallel\vec{k}}\end{aligned}\tag{31}$$

$$\frac{\partial}{\partial t}\tilde{v}_{\parallel\vec{k}}-\frac{\partial}{\partial x}\left[D_{\vec{k}}\frac{\partial}{\partial x}\tilde{v}_{\parallel\vec{k}}\right]+C_{\vec{k}}k_y^2\tilde{v}_{\parallel\vec{k}}+\mu k_\parallel^2\tilde{v}_{\parallel\vec{k}}=-ik_\parallel\tilde{\phi}_{\vec{k}}-ik_\parallel\tilde{p}_{\vec{k}}\tag{32}$$

$$\frac{\partial}{\partial t}\tilde{p}_{\vec{k}}-\frac{\partial}{\partial x}\left[D_{\vec{k}}\frac{\partial}{\partial x}\tilde{p}_{\vec{k}}\right]+C_{\vec{k}}k_y^2\tilde{p}_{\vec{k}}=-i\frac{(1+\eta_i)}{\tau}\omega_{*e}\tilde{\phi}_{\vec{k}}-ik_\parallel\Upsilon\tilde{v}_{\parallel\vec{k}},\tag{33}$$

where

$$D_{\vec{k}}\equiv\sum_{\vec{k}'}\frac{\left(k_y'\right)^2\left|\tilde{\phi}_{\vec{k}'}\right|^2}{\Delta\omega_{\vec{k}+\vec{k}'}}$$

and

$$C_{\vec{k}}\equiv\sum_{\vec{k}'}\frac{\left|\partial\tilde{\phi}_{\vec{k}'}/\partial x'\right|^2}{\Delta\omega_{\vec{k}+\vec{k}'}}.$$

Here, the diffusion coefficients, $D_{\vec{k}}$ and $C_{\vec{k}}$, account for the principal nonlinear process, which is random convection of fluid elements by electrostatic turbulence. Note that only diffusive effects have been retained in the renormalized vorticity equation. This is because the diffusion terms dominate the large-x asymptotic balance, which in turn determines the basic scales of the turbulence. Obviously, more terms[18] must be retained in a complete, energy-conserving renormalization.

Having derived the renormalized equations for η_i-mode turbulence, we now discuss the saturation mechanism associated with turbulent

damping of unstable sound-wave propagation and the general properties of the saturated state of η_i-mode turbulence in a simple heuristic manner. Since η_i-mode turbulence is a driven system with (linear) viscous dissipation damping the smallest scales, it is necessary to delineate the different spatial scales associated with "inertial" or "dissipation" ranges. Thus, it is necessary to parameterize the relative importance of $\vec{E} \times \vec{B}$ turbulent convection and linear viscous diffusion. Hence, it is useful to define, in the usual fashion, a "Reynolds" number as the ratio of the nonlinear term to the linear dissipation term in the dynamical equation for $\tilde{v}_{\|}$. Thus, the Reynolds number for the η_i-mode system is defined by

$$\mathrm{Re} \equiv \frac{\left[D_{\vec{k}}/\Delta_{\vec{k}}^2\right]}{\left[\mu k_{oy}^2 \frac{\Delta_{\vec{k}}^2}{L_s^2}\right]} = \frac{\tau_{d,\vec{k}}}{\tau_{c,\vec{k}}}, \tag{34}$$

where $\tau_{d,\vec{k}}$ refers to the linear dissipation time associated with ion parallel viscosity and $\tau_{c,\vec{k}}$ refers to the coherence time (eddy-turnover time) associated with nonlinear scrambling by $\vec{E} \times \vec{B}$-convection. Here, $\Delta_{\vec{k}}$ is the poloidal wavenumber dependent radial correlation length and k_{oy} is the rms poloidal wavevector. Upon estimation of $\Delta_{\vec{k}}$ to be discussed below, it follows that for long wavelengths $\mathrm{Re} \sim \eta_i$. Hence, this system has a finite width "inertial" range spectrum for the parameter regime of experimental interest. Here, "inertial" range means $\tau_c \ll \tau_d$, but allows for fluctuation growth due to η_i relaxation. Thus, our definition is different from that used in Navier-Stokes turbulence. Finally, note that the fluid model is especially well-suited for large Re regimes. For high Reynolds numbers, the basic picture of saturation is constructed and the basic nonlinear spatial and temporal scales can be obtained by using a "mixing-length" theory based on the assumption of maximal turbulent energy transfer, which ignores the details of the energy sink. This information is then used in a

more complete and quantitative calculation of the fluctuation spectra. In particular, such calculations properly account for the role of the dissipative energy sink in determining the saturation level of the turbulence.

To describe the saturated state, it is natural to specify the saturation condition as $\partial/\partial t \left(E^W + E^K + E^I\right) = 0$, namely that total fluctuation energy must be stationary in time. When this criterion is satisfied (ignoring localized quasi-linear profile flattening) the energy evolution equations, Eqs. (12)–(15), state that drive by $d\langle P_{oi}\rangle/dx$ relaxation balances energy exchange (equipartitioning) by the linear coupling term $\tilde{\phi}\nabla_{\|}\tilde{v}_{\|}$, and that viscous parallel dissipation balances the sound-wave coupling destabilization term in Eq. (13). Then saturation can be achieved by energy flow from ion-temperature-gradient energy source to ion parallel dissipation (i.e., $\mu\int d^3x\left|\nabla_{\|}\tilde{v}_{\|}\right|^2 = \frac{1}{T}\int d^3x\left\langle\tilde{p}\nabla_y\tilde{\phi}\right\rangle\left(d\langle P_{oi}\rangle/dx\right)$). This transfer is dynamically regulated by the nonlinear coupling and by the linear equipartitioning terms. That is, the unstable fluctuations are excited primarily at low-k_y (large-scales) by tapping the ion-temperature-gradient free-energy source. Interactions among these large-scale unstable modes remove wave energy by transferring energy to smaller scales and ultimately to stable fluctuations. This nonlinear scrambling process is accounted for in the renormalized equations by turbulent diffusion. Therefore, for large Re, mixing-length theory based on maximal turbulent transfer can be used to qualitatively (but not quantitatively) describe the saturated state.

It is important to notice that the familiar Hasegawa-Mima[16] vorticity equation nonlinearity due to nonlinear polarization-drift does not play as important a role in this case as in the quasi-two-dimensional case of drift-wave turbulence. This is because the η_i-mode is fundamentally a three-dimensional sound wave with dynamics determined by the pressure and velocity field evolu-

tion. Indeed, in local theory the polarization-drift can be ignored. Nonlocally, it serves primarily to set the radial eigenmode scale.

Setting the temporal derivative equal to zero and using the nonlinear radial scale $\Delta_{\vec{k}}$ from the renormalized ion pressure equation (Eq. (33)), we can relate the pressure response, $\tilde{p}_{\vec{k}}$, to the electrostatic potential fluctuation $\tilde{\phi}_{\vec{k}}$ by asymptotically balancing turbulent $\vec{E}\times\vec{B}$ mixing of a localized pressure fluctuation over a nonlinear mode width with the ion-temperature-gradient driving term, thus obtaining

$$\tilde{p}_{\vec{k}} \simeq i\left(\frac{1+\eta_i}{\tau}\right)\omega_{*e}\tilde{\phi}_{\vec{k}}/\Delta\omega_{\vec{k}}\,, \tag{35}$$

where $\Delta\omega_{\vec{k}} = D_{\vec{k}}/\Delta_{\vec{k}}^2$ is the decorrelation rate associated with $\vec{E}\times\vec{B}$ turbulent convection. Substituting this relation into the ion parallel momentum balance equation (Eq. (32)), and balancing turbulent diffusion of ion parallel momentum (which couples to the destabilizing $\tilde{p}$-fluctuation) with the potential fluctuation, and then solving for $D_{\vec{k}}$ yields the diffusion rate required for mixing-length saturation. This diffusivity is given by

$$D_{\vec{k}} \simeq \left(\frac{1+\eta_i}{\tau}\right)^{1/2} k_{\|}'\Delta_{\vec{k}}^3, \tag{36}$$

where $k_{\|}' \equiv k_y/L_s$ in a sheared slab.

The dissipation mechanism for η_i-mode turbulence can be clearly seen by rewriting the ion parallel momentum balance equation using a heuristic balance argument as above. This yields

$$\left[\Delta\omega_{\vec{k}} + \mu k_{\|}^2 + \frac{k_{\|}^2}{\Delta\omega_{\vec{k}}}\left(\frac{1+\eta_i}{\tau}\right)\right]\tilde{v}_{\|\vec{k}} \simeq S_{\vec{k}}^0, \tag{37}$$

where the source of ion parallel momentum is given by $S_{\vec{k}}^0 \simeq \Upsilon\left(k_{\|}^2/\Delta\omega_{\vec{k}}\right)\tilde{v}_{\|\vec{k}}$. This equation states that the ion parallel momentum fluctuation is driven by

the transfer of pressure fluctuation energy, which taps the ion-temperature-gradient source through the compressional coupling term, and is damped by turbulent $\vec{E} \times \vec{B}$-convection to parallel viscous dissipation. That is, for the most unstable low-k_y modes, the parallel viscosity due to ion Landau damping is too weak to stabilize the fluctuation, but draining of energy by a cascade process effectively couples to larger parallel viscosity at larger k_y. This in turn cuts off the unstable propagating sound waves and saturates the turbulence. It should be noted that although a mixing-length theory was used to estimate the level of diffusion in the saturated state in this heuristic section, the picture of saturation is different from that of previously proposed theories which either invoked naive "mixing-length rules" or relied on an analogy to the Hasegawa-Mima type nonlinear vorticity equation system to achieve saturation. Theories which use naive "mixing-length rules" to estimate the saturation amplitude of the fluctuations describe the process of saturation by turbulent mixing of a pressure fluctuation over a linear eigenmode within one linear growth time. The other theory[7] relies on an analogy to the Hasegawa-Mima equation in order to redistribute fluctuation energy throughout $k_\perp$-space by mode-coupling processes, thus coupling to perpendicular viscosity in higher-$k_\perp$ modes which are the ultimate sink of energy. A linear ion parallel momentum balance equation is assumed and hence the important effect of turbulent transport of ion parallel momentum is neglected. These theories fail to discuss the important saturation mechanism associated with the cut-off of unstable sound-wave propagation by turbulent convection of ion parallel momentum to dissipation. They thus lead to spurious physical pictures of saturation which are not consistent with energy conservation or which do not include sound-wave dynamics or properly treat the effects of dissipation.

To complete our discussion of the saturated state, the nonlinear

radial scale must be determined in order to estimate the diffusion coefficient. The nonlinear radial scale can be estimated from the continuity equation by balancing vorticity diffusion with destabilizing sound-wave coupling. Thus, the turbulent mixing-length scale is given by

$$\Delta_{\vec{k}} \simeq \left[D_{\vec{k}} \Big/ k'_{\|} \right]^{1/4}. \tag{38}$$

Using the estimated diffusion level $D_{\vec{k}}$ in Eq. (36), which is necessary to maintain dynamical balance of turbulent transfer of energy with ion-temperature-gradient drive, it follows that saturation occurs for mixing-lengths

$$\Delta_{\vec{k}} \simeq \left(\frac{1+\eta_i}{\tau} \right)^{1/2} \tag{39}$$

with diffusion of the order of

$$D_{\vec{k}} \simeq \left(\frac{1+\eta_i}{\tau} \right)^2 \frac{k_y}{L_s}. \tag{40}$$

A more quantitative calculation of diffusion level at saturation will be presented in the following discussion of the formal nonlinear theory. With these two conditions Eqs. (39)–(40), the nonlinear evolution of η_i-modes can be described in the following way. Before reaching saturation, the spectrum gains energy from the ion-temperature-gradient free-energy source. The diffusion $D_{\vec{k}}$, and therefore the nonlinear radial scale $\Delta_{\vec{k}}$, increase. This process continues until energy drain by nonlinear coupling (of order diffusion) is sufficient to balance the driving force. A qualitative but not quantitative estimate of the fluctuation level at which this balance occurs is given by the "mixing-length" limit. At this point the perturbation is saturated and a stationary state is achieved.

Having elucidated the basic saturation mechanism and calculated the diffusion level at saturation, it is now possible to estimate a number of

relevant quantities and scales that characterize saturated η_i-mode turbulence. These include the mean-square radial velocity, the rms-value of potential fluctuations, and the level of pressure fluctuation, as well as the nonlinear coherence time, equipartitioning time and dissipation time scales. Using the definition of $D_{\vec{k}}$ and making a Markovian approximation, the level of diffusion at saturation, Eq. (40), can be rewritten as

$$\begin{aligned} D &= \sum_{\vec{k}'} \frac{\left(k_y'\right)^2 \left|\tilde{\phi}_{\vec{k}'}\right|^2}{\Delta\omega_{\vec{k}'}} \\ &= \sum_{\vec{k}'} \frac{E_{\vec{k}'}}{\Delta\omega_{\vec{k}'}} \simeq \left(\frac{1+\eta_i}{\tau}\right)^2 \frac{\left(k_y\right)_{\rm rms}}{L_s}, \end{aligned} \tag{41}$$

where $E_{\vec{k}'} = \left(k_y'\right)^2 \left|\tilde{\phi}_{\vec{k}'}\right|^2$ is the radial velocity squared. Then the rms radial velocity can be estimated as

$$\left(\tilde{v}_r\right)_{\rm rms} \simeq \left(\frac{1+\eta_i}{\tau}\right)^{3/2} \frac{\left(k_y\right)_{\rm rms}}{L_s} \tag{42}$$

and the rms-value of the electrostatic potential fluctuation level is

$$\left(\tilde{n}\right)_{\rm rms} = \left(\tilde{\phi}\right)_{\rm rms} \simeq \left(\frac{1+\eta_i}{\tau}\right)^{3/2} \frac{1}{L_s}.$$

In a similar fashion, the rms-value of pressure fluctuation level can be estimated by using the stationarity relation of $\tilde{p}$ and $\tilde{\phi}$ at saturation. It follows that

$$\left(\tilde{p}\right)_{\rm rms} \simeq \left(\frac{1+\eta_i}{\tau}\right)^{3/2} \frac{1}{L_n}.$$

Because of the $\left(k_y\right)_{\rm rms}$-dependence in various estimated quantities, it is necessary to calculate $\left(k_y\right)_{\rm rms}$ at saturation. This is possible only with the knowledge of the spectrum of fluctuations. Hence, we will calculate this value after the spectrum calculation, presented in the next section.

In addition to the quantities estimated above, the basic temporal scales associated with the nonlinear processes are also important, in order to address questions of energy flow. First of all, the basic nonlinear scrambling time can be defined by the eddy-turnover time associated with $\vec{E} \times \vec{B}$ turbulent convection, and is given by

$$\tau_{c,\vec{k}}^{-1} \equiv \left[D_{\vec{k}} / \Delta_{\vec{k}}^2 \right] \simeq \left(\frac{1+\eta_i}{\tau} \right) \frac{k_y}{L_s}.$$

Second, the dissipation time can be defined by using ion Landau damping as an effective parallel dissipation mechanism (here, $\mu \simeq v_{th,i}^2/|\omega|$ models the parallel viscosity due to ion Landau damping), and is given by

$$\tau_{d,\vec{k}}^{-1} \equiv \frac{\mu \int dx \left\langle \left| \nabla_{\|} \tilde{v}_{\|} \right|^2 \right\rangle_{\vec{k}}}{E_{\vec{k}}^K} \simeq 2 \left(\frac{k_y}{\tau L_s} \right).$$

Note here $\Delta_{\vec{k}}$ is used for x in $k_{\|}$. Recall that using these two time scales, the Reynolds number for η_i-mode turbulence (defined previously) can be estimated to be

$$\mathrm{Re} \equiv \frac{\tau_{d,\vec{k}}}{\tau_{c,\vec{k}}} \simeq (1+\eta_i)$$

when η_i must be large enough to use the fluid model. It is also important to define the equipartitioning time between $E_{\vec{k}}^W$, $E_{\vec{k}}^K$, and $E_{\vec{k}}^I$ through the linear energy exchange process,

$$\tau_{\mathrm{eq},\vec{k}}^{-1} \equiv \frac{\int dx \left\langle \tilde{p} \nabla_{\|} \tilde{v}_{\|} \right\rangle_{\vec{k}}}{E_{\vec{k}}^I}.$$

By using the stationarity relation, the equipartitioning time can be estimated as

$$\tau_{\mathrm{eq},\vec{k}}^{-1} \simeq 2\Upsilon \left(\frac{1+\eta_i}{\tau} \right) \left(\frac{k_y}{L_s} \right).$$

For the large but finite value of η_i, it is important to notice that the hierarchy of these time scales is given by

$$\tau_{\rm eq} \lesssim \tau_c < \tau_d.$$

The importance of this hierarchy will be addressed in the following section.

B. Formal Nonlinear Theory

In the preceding section, the dynamics of the saturated state have been discussed, and fluctuation saturation levels and the basic scales associated with ion-temperature-gradient-driven turbulence have been estimated using one-point renormalized equations. Although this information is important for a basic physical understanding of η_i-mode turbulence and the resulting confinement scaling of tokamak experiments, a quantitative description of the wavenumber spectrum of the fluctuations requires construction and solution of energy spectra evolution equations. For example, the average wavenumber $(k_y)_{\rm rms}$ cannot be determined from one-point theory and can be obtained only by use of energy spectral equations.

Before considering the dynamics of energy evolution, it is necessary to discuss energy conservation and energy flow in wavenumber space. The wavenumber space evolution equations for the energy-like integrals (with triplets renormalized) are given by

$$\frac{\partial}{\partial t} E^W = -\sum_{\vec{k}} \int dx \tilde{\phi}_{-\vec{k}} k_\parallel \tilde{v}_{\parallel \vec{k}}$$

$$+ \sum_{\vec{k}} \int dx \left\{ \sum_{\vec{k}'} \frac{\left(k_y'\right)^2 \left|\tilde{\phi}_{\vec{k}'}\right|^2}{\Delta\omega_{\vec{k}''}} \left\langle \frac{\partial \tilde{\phi}_{-\vec{k}}}{\partial x} \cdot \frac{\partial}{\partial x} \left(\nabla_\perp^2 \tilde{\phi}_{\vec{k}} \right) \right\rangle \right.$$

$$- \sum_{\vec{k}'} \frac{\left\langle \frac{\partial \tilde{\phi}_{-\vec{k}'}}{\partial x'} \cdot \frac{\partial}{\partial x'} \left(\nabla_\perp^2 \tilde{\phi}_{\vec{k}'} \right) \right\rangle}{\Delta\omega_{\vec{k}''}} k_y^2 \left| \tilde{\phi}_{\vec{k}} \right|^2 \Bigg\} \tag{43}$$

$$\begin{aligned}
\frac{\partial}{\partial t} E^K = & -i \sum_{\vec{k}} \int dx \left[\tilde{v}_{\|-\vec{k}} k_\| \tilde{\phi}_{\vec{k}} + \tilde{v}_{\|-\vec{k}} k_\| \tilde{p}_{\vec{k}} \right] \\
& -\mu \sum_{\vec{k}} \int dx k_\|^2 \left\langle \tilde{v}_{\|-\vec{k}} \tilde{v}_{\|\vec{k}} \right\rangle \\
& - \sum_{\vec{k}} \int dx \left\{ \sum_{\vec{k}'} \frac{\left(k_y'\right)^2 \left| \tilde{\phi}_{\vec{k}'} \right|^2}{\Delta\omega_{\vec{k}''}} \left| \frac{\partial \tilde{v}_{\|\vec{k}}}{\partial x} \right|^2 + \sum_{\vec{k}'} \frac{\left| \partial \tilde{\phi}_{\vec{k}'} / \partial x' \right|^2}{\Delta\omega_{\vec{k}''}} k_y^2 \left| \tilde{v}_{\|\vec{k}} \right|^2 \right\} \\
& + \sum_{\vec{k}} \int dx \sum_{\vec{p}+\vec{q}=\vec{k}} \left\{ \frac{p_y^2 \left| \tilde{\phi}_{\vec{q}} \right|^2}{\Delta\omega_{-\vec{p}-\vec{q}}} \left| \frac{\partial \tilde{v}_{\|\vec{q}}}{\partial x} \right|^2 + \frac{q_y^2 \left| \partial \tilde{\phi}_{\vec{p}} / \partial x \right|^2}{\Delta\omega_{-\vec{p}-\vec{q}}} \left| \tilde{v}_{\|\vec{q}} \right|^2 \right\}
\end{aligned} \tag{44}$$

$$\begin{aligned}
\frac{\partial}{\partial t} E^I = & -i \sum_{\vec{k}} \int dx \tilde{p}_{-\vec{k}} k_\| \tilde{v}_{\|\vec{k}} \\
& + \frac{i}{\Upsilon} \sum_{\vec{k}} \int dx \left\langle \tilde{p}_{-\vec{k}} k_y \tilde{\phi}_{\vec{k}} \right\rangle \left[\frac{d \left\langle P_{oi} \right\rangle}{dx} \right] \\
& - \frac{1}{\Upsilon} \sum_{\vec{k}} \int dx \left\{ \sum_{\vec{k}'} \frac{\left(k_y'\right)^2 \left| \tilde{\phi}_{\vec{k}'} \right|^2}{\Delta\omega_{\vec{k}''}} \left| \frac{\partial \tilde{p}_{\vec{k}}}{\partial x} \right|^2 + \sum_{\vec{k}'} \frac{\left| \partial \tilde{\phi}_{\vec{k}'} / \partial x \right|^2}{\Delta\omega_{\vec{k}''}} k_y^2 \left| \tilde{p}_{\vec{k}} \right|^2 \right\} \\
& + \frac{1}{\Upsilon} \sum_{\vec{k}} \int dx \sum_{\vec{p}+\vec{q}=\vec{k}} \left\{ \frac{p_y^2 \left| \tilde{\phi}_{\vec{p}} \right|^2}{\Delta\omega_{-\vec{p}-\vec{q}}} \left| \frac{\partial \tilde{p}_{\vec{k}}}{\partial x} \right|^2 + \frac{q_y^2 \left| \partial \tilde{\phi}_{\vec{p}} / \partial x \right|^2}{\Delta\omega_{-\vec{p}-\vec{q}}} \left| \tilde{p}_{\vec{q}} \right|^2 \right\}.
\end{aligned} \tag{45}$$

In Section 2.2, we discussed energy flow and conservation of energy in configuration space, and identified compressional and sound-wave coupling terms which transfer energy between fields. In mixing-length theory, saturation of low-k_y modes (Re$>$ 1) can be estimated by invoking turbulent mixing, represented

as a diffusion process, as a vehicle for draining energy from the low-k_y modes. Since the one-point theory does not conserve energy, saturation levels can at best be qualitatively estimated using mixing-length theory. However, spectral energy equations conserve energy. Thus, they are the natural tool for a spectrum calculation which is consistent with the basic conservation properties of the system.

Except for the vorticity nonlinearity, the renormalized convective nonlinearities have the common structure that the coherent part of the turbulent response drains energy, and the incoherent part refurnishes energy by emission. This competition results in an energy cascade. We can also identify an energy transfer mechanism from source to sink by noting the role of the compressional coupling term. The coupling term, $\int dx \tilde{p} \nabla_{||} \tilde{v}_{||}$, transfers pressure fluctuation energy to parallel momentum fluctuation energy through equipartitioning. Hence, ion-temperature-gradient-driven internal energy in $\langle \tilde{p}^2 \rangle$ can be transferred to parallel kinetic energy in $\left\langle \tilde{v}_{||}^2 \right\rangle$ and ultimately dissipated through parallel viscosity at the high-$\vec{k}$ sink. It should also be noted that the hierarchy of time scales associated with these important processes (i.e., $\tau_{\text{eq}} < \tau_c \ll \tau_d$) shows that equipartitioning can take place on a nonlinear time scale which is shorter than a correlation time and much shorter than a dissipation time. Even though equipartitioning takes place among all three fields, the most important dynamics of energy flow are controlled by the evolution of $\langle \tilde{p}^2 \rangle$ and $\left\langle \tilde{v}_{||}^2 \right\rangle$, which couple directly to the energy source and sink.

With these observations, a theory of energy evolution can be constructed by assuming equipartitioning of energy and by absorbing E^W into a total kinetic energy. The dynamics of nonlinear energy evolution can be described by two-point, one-time energy spectrum equations for $\langle \tilde{p}^2 \rangle$ and $\langle \tilde{v}^2 \rangle$, which retain incoherent emission as well as coherent diffusion. Two-point equa-

tions for the energy spectrum can be obtained straightforwardly from the one-point equations, Eqs. (6)–(8), by multiplying by the field at a second point and taking an ensemble average. After symmetrizing, the resulting equations are

$$\frac{\partial}{\partial t}\left\langle \tilde{v}(1)\tilde{v}(2)\right\rangle - \mu\left(\nabla_{\|1}^2+\nabla_{\|2}^2\right)\left\langle \tilde{v}(1)\tilde{v}(2)\right\rangle + T_{12}^v = -\left\langle \tilde{v}(2)\nabla_{\|1}\tilde{p}(1)\right\rangle - \left\langle \tilde{v}(1)\nabla_{\|2}\tilde{p}(2)\right\rangle \tag{46}$$

$$\frac{1}{\Upsilon}\frac{\partial}{\partial t}\left\langle \tilde{p}(1)\tilde{p}(2)\right\rangle + T_{12}^p = -\left\langle \tilde{p}(2)\nabla_{\|1}\tilde{v}(1)\right\rangle - \left\langle \tilde{p}(1)\nabla_{\|2}\tilde{v}(2)\right\rangle + \frac{1}{\Upsilon}\left\{\left\langle \tilde{p}(2)\nabla_{y_1}\tilde{\phi}(1)\right\rangle + \left\langle \tilde{p}(1)\nabla_{y_2}\tilde{\phi}(2)\right\rangle\right\}\left[\frac{d\left\langle P_{oi}\right\rangle}{dx}\right] \tag{47}$$

where T_{12}^v and T_{12}^p are triplets due to convective nonlinearities. The triplets are given by

$$T_{12}^v = \left\langle \hat{b}\times\nabla_1\tilde{\phi}(1)\cdot\nabla_1\tilde{v}(1)\tilde{v}(2)\right\rangle + \langle 1\leftrightarrow 2\rangle \tag{48}$$

$$T_{12}^p = \frac{1}{\Upsilon}\left\langle \hat{b}\times\nabla_1\tilde{\phi}(1)\cdot\nabla_1\tilde{p}(1)\tilde{p}(2)\right\rangle + \langle 1\leftrightarrow 2\rangle\,. \tag{49}$$

Here, the slow time-scale variations are described by the time derivative, and $\langle 1\leftrightarrow 2\rangle$ stands for term with indices 1 and 2 exchanged. The evolution equation for the total energy can be obtained by adding two equations and assuming equipartition of energy between fields. This resulting equation can be formally written as

$$\frac{\partial}{\partial t}\left\langle \mathcal{E}_{12}\right\rangle + \left\langle S_{12}^I\right\rangle + T_{12} = \left\langle S_{12}^0\right\rangle, \tag{50}$$

where

$$\left\langle \mathcal{E}_{12}\right\rangle \equiv \left\langle \tilde{v}(1)\tilde{v}(2)\right\rangle + \frac{1}{\Upsilon}\left\langle \tilde{p}(1)\tilde{p}(2)\right\rangle$$

represents the total energy correlation function,

$$\left\langle S_{12}^0\right\rangle \equiv \frac{1}{\Upsilon}\left\langle \tilde{p}(2)\nabla_{y_1}\tilde{\phi}(1)\right\rangle\left[\frac{d\left\langle P_{oi}\right\rangle}{dx}\right] + \langle 1\leftrightarrow 2\rangle$$

is the fluctuation source, proportional to the ion-temperature-gradient,

$$\langle S_{12}^I \rangle \simeq -\mu \left(\nabla_{\|1}^2 + \nabla_{\|2}^2 \right) \langle \tilde{v}(1) \tilde{v}(2) \rangle$$

is the sink, representing dissipation by parallel viscosity, and

$$T_{12} \equiv T_{12}^v + T_{12}^p$$

is the nonlinearity (mode coupling). Here, it is important to notice that the nonlinearities (triplets) vanish as the relative separation goes to zero, while the source and sink do not. Turbulent mixing, which is represented by the transfer term, destroys all but the smallest spatial scales on the time scale of a correlation time. Also note that the gradient source drives energy at all scales, and that the dissipative effects of parallel viscosity are also included in this system. Unlike the turbulent mixing process, these produce diffusion which stays finite as the relative separation goes to zero. This scale-independent decay mechanism destroys small-scale correlation in the "dissipation" region of spectrum. Hence, this two-point energy evolution equation incorporates the basic effects of dissipation, source, and turbulent transfer.

While the neglect of incoherent mode coupling (an approximation made in the one-point theory) does not significantly alter the predicted fluctuation levels and scalings, the spectrum is sensitive to the effects of incoherent mode coupling. Hence, for the large Reynolds regime case considered here, the steady-state two-point correlation is determined not by the balance of ion-temperature-gradient drive with parallel viscous dissipation, but by inhomogeneities in the transfer terms associated with mode coupling. In order to analytically solve the spectral energy equation, here we use a spatial representation which is an application of the methods of renormalized two-point theory (clump theory) to this fluid plasma system. The basic techniques utilized were

originally proposed in the context of phase space density turbulence.[17] In this case, transfer in wavenumber space is represented by spatially-inhomogeneous relative diffusion. By inverting the spatially-represented energy evolution operator, the structure of the wavenumber spectrum can be obtained. This inversion accounts for the spatially-inhomogeneous turbulent scattering process, as well as the coupling to the dissipation and turbulent diffusion which determines the decay of the correlation. This procedure enables us to obtain an approximate analytic solution of the mode-coupling equation. Furthermore, the inversion of the operator determines the spectrum balance (steady-state) condition which in turn determines the saturation level.

Now, we can find the evolution operator in the spatial representation.[18] We transform the evolution equation for the two-point (energy) correlation, Eq. (50), to a relative coordinate system $(\vec{x}_+, \vec{x}_-)$ where $\vec{x}_+ = \frac{1}{2}(\vec{x}_1 + \vec{x}_2)$ is the average position of the points 1 and 2, and $\vec{x}_- = \frac{1}{2}(\vec{x}_1 - \vec{x}_2)$ is the relative position between them. Here, it is necessary to renormalize the nonlinearities (triplets), which describe turbulent scattering of energy due to temporally and spatially-varying potential fluctuations. The weak coupling closure with standard iteration scheme used in the previous section is used to renormalize the triplets. Introducing Fourier expansions in the y and z directions, the triplets can be written as

$$
\begin{aligned}
T_{12} = \sum_{\vec{k}} \sum_{\vec{k}'} \sum_{\vec{k}''} \Bigg\langle & \exp\left(ik_y y_1 + ik_z z_1\right) \exp\left(ik'_y y_1 + ik'_z z_1\right) \exp\left(ik''_y y_2 + ik''_z z_2\right) \\
& \Bigg\{ \left[-ik_y \tilde{\phi}_{\vec{k}}(1) \frac{\partial \tilde{v}_{\vec{k}'}}{\partial x_1}(1) \tilde{v}_{\vec{k}''}(2) + ik'_y \frac{\partial \tilde{\phi}_{\vec{k}}}{\partial x_1}(1) \tilde{v}_{\vec{k}'}(1) \tilde{v}_{\vec{k}''}(2) \right] \\
& + \frac{1}{\Upsilon} \left[-ik_y \tilde{\phi}_{\vec{k}}(1) \frac{\partial \tilde{p}_{\vec{k}'}}{\partial x_1}(1) \tilde{p}_{\vec{k}''}(2) + ik'_y \frac{\partial \tilde{\phi}_{\vec{k}}}{\partial x_1}(1) \tilde{p}_{\vec{k}'}(1) \tilde{p}_{\vec{k}''}(2) \right] \Bigg\} \Bigg\rangle \\
& + \langle 1 \leftrightarrow 2 \rangle \,. \qquad (51)
\end{aligned}
$$

The average $\langle \cdots \rangle$ can be computed by integrating over the average position variables y_+ and z_+. After eliminating the trivial summation, the triplet can then be expressed in terms of test ($\vec{k}$), background ($\vec{k}'$) and driven beat ($\vec{k}'' = \vec{k} + \vec{k}'$) modes. The driven fluctuations are iteratively determined, using the solution for the driven fields given in Eqs. (28)–(30). As discussed in Section II, we neglect the driven potential fluctuation $\tilde{\phi}_{\vec{k}+\vec{k}'}$ and make a Markovian approximation $\left(\Delta\omega_{\vec{k}''} \sim \Delta\omega_{\vec{k}'}\right)$ in the driven propagator, thus obtaining the renormalized triplet

$$T_{12} = -\left(D_-^x \frac{\partial^2}{\partial x_-^2} + D_-^y \frac{\partial^2}{\partial y_-^2}\right) \langle \mathcal{E}_{12} \rangle \,, \tag{52}$$

where the relative diffusion coefficients are given by

$$D_-^x = 2D^x - D^{x(1,2)} - D^{x(2,1)} \tag{53}$$

and

$$D_-^y = 2D^y - D^{y(1,2)} - D^{y(2,1)} \tag{54}$$

with $D^x = D_{\vec{k}}$ and $D^y = C_{\vec{k}}$ in the expressions of Eqs. (31)–(33) and

$$\left(D^{x(1,2)} + D^{x(2,1)}\right) = 2\sum_{\vec{k}'} \cos\left(\vec{k}' \cdot \vec{x}_-\right) \frac{\left(k_y'\right)^2 \left\langle \tilde{\phi}_{\vec{k}'}(1)\tilde{\phi}_{\vec{k}'}(2)\right\rangle}{\Delta\omega_{\vec{k}'}}$$

$$\left(D^{y(1,2)} + D^{y(2,1)}\right) = 2\sum_{\vec{k}'} \cos\left(\vec{k}' \cdot \vec{x}_-\right) \frac{\left\langle \partial\tilde{\phi}_{-\vec{k}'}/\partial x_1(1) \cdot \partial\tilde{\phi}_{\vec{k}'}/\partial x_2(2)\right\rangle}{\Delta\omega_{\vec{k}'}}.$$

Here, the renormalized triplet approximates the $\vec{E} \times \vec{B}$ turbulent mixing and mode coupling as a relative diffusion across the magnetic field. The resulting relative diffusions, D_-^x and D_-^y, are inhomogeneous and are seen to consist of two parts, scale-independent diffusion, D^x and D^y, same as one-point case, and scale-dependent correlated diffusion, $D^{(2,1)}$ and $D^{(1,2)}$, which accounts for

incoherent mode coupling. These inhomogeneities of relative diffusion show that triplet behavior as $1 \rightarrow 2$ is correctly accounted for in the renormalization procedure. The inhomogeneity of relative diffusion with respect to relative separation is illustrated in Fig. 2.3.

The characteristic spatial scale is referred to as correlation scale for which $D^{(1,2)}$ and $D^{(2,1)}$ differ from zero. The correlation peaks when the relative separation is less than correlation scale. For relative separation less than the corresponding correlation scale, i.e., $\left|\vec{k}_0 \cdot \vec{x}_-\right| < 1$, where $\vec{k}_0$ is the spectrum-averaged wavenumber (i.e., typical wavenumber of fluctuations), the relative diffusion coefficients, D_-^x and D_-^y, can be approximated by expanding in the relative variables

$$D_-^{(x,y)} \simeq 2D^{(x,y)} \left(k_{ox}^2 x_-^2 + k_{oy}^2 y_-^2 + k_{oz}^2 z_-^2\right).$$

Having renormalized the triplet nonlinearity, we also need to express the parallel viscous diffusion term as a dissipation operator for energy correlation in the relative coordinate. Using the equipartitioning assumption, we first write the dissipation term as a Fourier expansion in the y and z directions at each radial position, i.e.,

$$\begin{aligned}\left\langle S_{12}^I \right\rangle =& \mu \left(\nabla_{\|1}^2 + \nabla_{\|2}^2\right) \langle \tilde{v}(1)\tilde{v}(2) \rangle \simeq \frac{\mu}{2} \left(\nabla_{\|1}^2 + \nabla_{\|2}^2\right) \langle \mathcal{E}_{12} \rangle \\ =& \frac{\mu}{2} \Bigg\langle \sum_{\vec{k}_1} \sum_{\vec{k}_2} \exp\left(ik_{y_1} y_1 + ik_{y_2} y_2\right) \exp\left(ik_{z_1} z_1 + ik_{z_2} z_2\right) \\ & \left\{ \frac{\left[x_1 - x_s\left(\vec{k}_1\right)\right]^2}{L_s^2} k_{y_1}^2 + \frac{\left[x_2 - x_s\left(\vec{k}_2\right)\right]^2}{L_s^2} k_{y_2}^2 \right\} \left(\mathcal{E}_{12}\right)_{\vec{k}_1, \vec{k}_2} \Bigg\rangle .\end{aligned} \tag{55}$$

To obtain this expression, recall that the wavenumbers corresponding to each position, k_{y_α} and $k_{z_\alpha} (\alpha = 1, 2)$, and $\nabla_{\|\alpha}$ vanish at the rational surface associ-

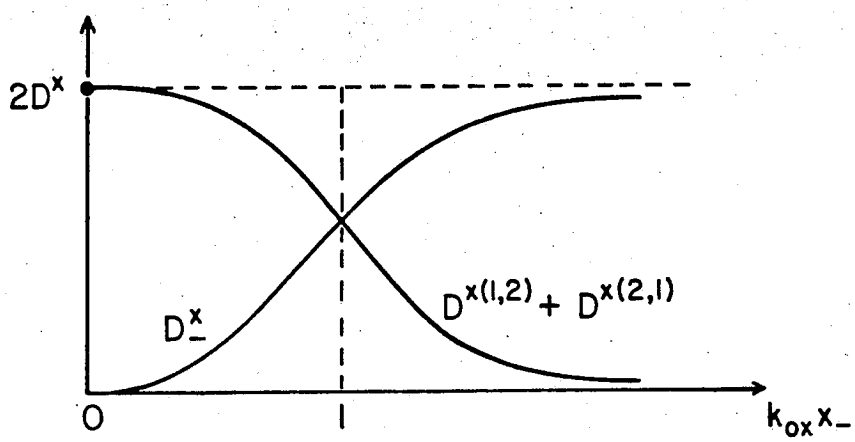

Fig. 2.3 Illustration for the inhomogeneity of relative diffusion coefficient to the normalized relative coordinate.

ated with that position $x_s\left(\vec{k}_\alpha\right)$, i.e.,

$$\frac{B_z}{B}k_{z_\alpha}+\frac{B_y\left(x_s\left(\vec{k}_\alpha\right)\right)}{B}k_{y_\alpha}=0. \tag{56}$$

As before, the average $\langle\cdots\rangle$ produces Kronecker deltas $\delta_{k_{y_1}+k_{y_2},0}$, $\delta_{k_{z_1}+k_{z_2},0}$ which relate the two wavevectors $\left(\vec{k}_1=-\vec{k}_2\right)$. As a result, the double Fourier expansion is reduced to one in the relative variable. Furthermore, using the reflection invariance ($\vec{k}\rightarrow-\vec{k}$) of Eq. (56), it can be seen that both positions are tied to a single rational surface defined by $\frac{B_z}{B}k_z+\frac{B_y(x_s)}{B}k_y=0$. Again, writing x_1 and x_2 in terms of the relative coordinates, the dissipation operator (in the spatial representation) is given by

$$\begin{aligned}\frac{\mu}{2}\left(\nabla_{\|1}^2+\nabla_{\|2}^2\right)\langle\mathcal{E}_{12}\rangle&=\frac{\mu}{4}\sum_{\vec{k}}e^{ik_yy_-+ik_zz_-}\left[\frac{\left(x_+-2x_s\right)^2+x_-^2}{L_s^2}\right]k_y^2\langle\mathcal{E}_{12}\rangle_{\vec{k}}\\&\simeq\frac{\mu}{4}\left[\frac{\left(x_+-2x_s\right)^2+x_-^2}{L_s^2}\right]\frac{\partial^2}{\partial y_-^2}\langle\mathcal{E}_{12}\rangle.\end{aligned} \tag{57}$$

Thus, the renormalized two-point equation is given by

$$\left\{\frac{\partial}{\partial t}-\frac{\mu}{4}\left[\frac{\left(x_+-2x_s\right)^2}{L_s^2}+\frac{x_-^2}{L_s^2}\right]\frac{\partial^2}{\partial y_-^2}-\left(D_-^x\frac{\partial^2}{\partial x_-^2}+D_-^y\frac{\partial^2}{\partial y_-^2}\right)\right\}\langle\mathcal{E}_{12}\rangle=\left\langle S_{12}^0\right\rangle \tag{58}$$

where $\left\langle S_{12}^0\right\rangle$, the source term which accounts for fluctuation energy growth through average ion-pressure-gradient relaxation, is given by Eq. (50). Note that here, $(x_+-2x_s)\approx\Delta_{\vec{k}}$, the turbulent correlation length.

In order to determine the steady-state spectrum, it is necessary to find the steady-state solution of Eq. (58). This requires inversion of the evolution operator

$$\mathcal{L}=\frac{\partial}{\partial t}-\frac{\mu}{4}\left[\frac{\left(x_+^2-2x_s\right)^2}{L_s^2}+\frac{x_-^2}{L_s^2}\right]\frac{\partial^2}{\partial y_-^2}-\left(D_-^x\frac{\partial^2}{\partial x_-^2}+D_-^y\frac{\partial^2}{\partial y_-^2}\right) \tag{59}$$

which describes the decay of correlation by relative diffusion due to $\vec{E} \times \vec{B}$ shear stress, and by parallel ion viscous dissipation. Formally, we can invert the evolution operator $\mathcal{L}$, and obtain the steady-state solution of Eq. (58) as

$$\langle \mathcal{E}_{12} \rangle = \tau_{\rm cl}(x_-, y_-) \left\langle S^0_{12} \right\rangle , \tag{60}$$

where the inverse operator $\tau_{\rm cl}(x_-, y_-) = \mathcal{L}^{-1}$. The operator $\tau_{\rm cl}(x_-, y_-)$ describes characteristic time associated with the evolution of two-point correlation, and depends on the relative separation of the two points.

A solution for $\tau_{\rm cl}$ may be obtained using the Green's function g, satisfying the homogeneous equation

$$\mathcal{L} g \left(\vec{x}_- \mid \vec{x}'_- \right) = 0, \tag{61}$$

so that

$$\langle \mathcal{E}_{12} \rangle = \int d\vec{x}'_- g \left(\vec{x}_- \mid \vec{x}'_- \right) \left\langle S^0_{12} \left(\vec{x}'_- \right) \right\rangle .$$

Although obtaining an exact expression for the Green's function g is possible, it is usually very complicated. Hence, it is sufficient for our purposes to determine the characteristic time $\tau_{\rm cl}$ associated with the evolution operator $\mathcal{L}$. This approximate correlation time, $\tau_{\rm cl}$, can be determined by calculating the moments of the Green's function, which are defined by

$$\langle A \rangle \equiv \int d^3x'_- A \left(\vec{x}'_- \right) g \left(\vec{x}_- \mid \vec{x}'_- \right) .$$

A set of relative coordinate moment evolution equations can be obtained by taking the second moments of the Green's function and using the relation

$$\frac{\partial}{\partial t} g = \left\{ \frac{\mu}{4} \left[\frac{\left(x_+ - 2x_s \right)^2}{L_s^2} + \frac{x_-^2}{L_s^2} \right] \frac{\partial^2}{\partial y_-^2} + \left(D_-^x \frac{\partial^2}{\partial x_-^2} + D_-^y \frac{\partial^2}{\partial y_-^2} \right) \right\} g$$

and integrating by parts. The resulting moment equations are

$$\frac{\partial}{\partial t}\left(k_{ox}^2\left\langle x_-^2\right\rangle\right) = 4D_{\vec{k}}k_{ox}^2\left[k_{ox}^2\left\langle x_-^2\right\rangle + k_{oy}^2\left\langle y_-^2\right\rangle + k_{oz}^2\left\langle z_-^2\right\rangle\right] \tag{62}$$

$$\begin{aligned}\frac{\partial}{\partial t}\left(k_{oy}^2\left\langle y_-^2\right\rangle\right) = {} & \frac{\mu k_{oy}^2}{2L_s^2}\left[\left(x_+ - 2x_s\right)^2 + \left\langle x_-^2\right\rangle\right] \\ & + 4C_{\vec{k}}k_{oy}^2\left[k_{ox}^2\left\langle x_-^2\right\rangle + k_{oy}^2\left\langle y_-^2\right\rangle + k_{oz}^2\left\langle z_-^2\right\rangle\right]\end{aligned} \tag{63}$$

$$\frac{\partial}{\partial t}\left(k_{oz}^2\left\langle z_-^2\right\rangle\right) = 0. \tag{64}$$

By defining a relative separation normalized with correlation scale

$$R_-^2(t) \equiv k_{ox}^2 x_-^2(t) + k_{oy}^2 y_-^2(t) + k_{oz}^2 z_-^2(t) \tag{65}$$

and its moments

$$\left\langle R_-^2(t)\right\rangle = k_{ox}^2\left\langle x_-^2\right\rangle + k_{oy}^2\left\langle y_-^2\right\rangle + k_{oz}^2\left\langle z_-^2\right\rangle,$$

the resulting evolution equation of relative separation is

$$\frac{\partial^2}{\partial t^2}\left\langle R_-^2\right\rangle - 4\left(D_{\vec{k}}k_{ox}^2 + C_{\vec{k}}k_{oy}^2\right)\frac{\partial}{\partial t}\left\langle R_-^2\right\rangle - \frac{2\mu k_{oy}^2}{L_s^2 k_{ox}^2}\left(D_{\vec{k}}k_{ox}^2\right)\left\langle R_-^2\right\rangle = 0. \tag{66}$$

It is desirable to define a Reynolds number and other relevant parameters using the correlation scale $\vec{k}_0$. Therefore, let the Reynolds number be defined as

$$\mathrm{Re} \equiv \frac{\left[D_{\vec{k}}k_{ox}^2\right]}{\left[\mu k_{oy}^2/\left(L_s^2 k_{ox}^2\right)\right]} = \frac{\tau_{d,\vec{k}}}{\tau_{c,\vec{k}}},$$

where $D_{\vec{k}}$ is the scale-independent radial diffusion coefficient, and τ_c is the coherent (one-point) relaxation time, and is given by $\tau_{c,\vec{k}}^{-1} = \left[D_{\vec{k}}k_{ox}^2\right]$ in the high Reynolds number limit. τ_d is the parallel dissipation time and is given by

$\tau_{d,\vec{k}}^{-1} = \left[\mu k_{oy}^2 / \left(L_s^2 k_{ox}^2\right)\right]$. By parameterizing the ratio between scale-independent diffusions in the x and y directions as $\delta \equiv \left(C_{\vec{k}} k_{oy}^2 / D_{\vec{k}} k_{ox}^2\right)$, the evolution equation, Eq. (66), can be rewritten as

$$\frac{\partial^2}{\partial t^2}\left\langle R_-^2 \right\rangle - \frac{4(1+\delta)}{\tau_c}\frac{\partial}{\partial t}\left\langle R_-^2 \right\rangle - \frac{2}{\tau_d \tau_c}\left\langle R_-^2 \right\rangle = 0. \tag{67}$$

Equation (67) describes the divergence of neighboring fluid elements by the turbulent scattering at high Reynolds numbers. At the small scales, however, scattering is damped by parallel dissipation.

The solution of the evolution equation is obtained as an initial value problem in which the initial separation is given by the second moments, i.e.,

$$\left\{\left\langle x_-^2 \right\rangle, \left\langle y_-^2 \right\rangle, \left\langle z_-^2 \right\rangle\right\}\Big|_{t=0} = \left\{x_-^2, y_-^2, z_-^2\right\}, \tag{68}$$

and hence, $\left\langle R_-^2 \right\rangle\Big|_{t=0} = R_-^2$ determines the first and second derivatives of $\left\langle R_-^2 \right\rangle$ at the initial time:

$$\frac{\partial}{\partial t}\left\langle R_-^2(t) \right\rangle\Big|_{t=0} = \frac{4(1+\delta)}{\tau_c} R_-^2 + \frac{k_{ox}^2}{2\tau_d}\left[\left(x_+ - 2x_s\right)^2 - x_-^2\right] \tag{69}$$

and

$$\frac{\partial^2}{\partial t^2}\left\langle R_-^2(t) \right\rangle\Big|_{t=0} = \left\{\frac{16(1+\delta)^2}{\tau_c^2} + \frac{2}{\tau_c \tau_d}\right\} R_-^2 + \frac{2(1+\delta)}{\tau_c \tau_d} k_{ox}^2 \left[\left(x_+ - 2x_s\right)^2 + x_-^2\right]. \tag{70}$$

Then, the solution of Eq. (67) is given by

$$\left\langle R_-^2(t) \right\rangle = A e^{u+t} + B e^{u-t}, \tag{71}$$

where $u_\pm$ are the two roots of the characteristic equation generated by the trial solution e^{ut}:

$$u^2 - \frac{4(1+\delta)}{\tau_c} u - \frac{2}{\tau_c \tau_d} = 0. \tag{72}$$

The two roots are given by

$$u_{\pm} = \frac{2(1+\delta)}{\tau_c}\left\{1 \pm \sqrt{1+\frac{\mathrm{Re}^{-1}}{2(1+\delta)^2}}\right\}.$$

The coefficients, A and B, are determined by requiring that Eq. (67) satisfies the initial conditions Eqs. (68)–(70). Thus,

$$A = (u_+ - u_-)^{-1}\left[\left(\frac{1}{u_+}\right)\frac{\partial^2}{\partial t^2}\left\langle R_-^2\right\rangle\Big|_{t=0} - \left(\frac{u_-}{u_+}\right)\frac{\partial}{\partial t}\left\langle R_-^2\right\rangle\Big|_{t=0}\right], \quad (73)$$

$$B = (u_+ - u_-)^{-1}\left[\left(\frac{u_+}{u_-}\right)\frac{\partial}{\partial t}\left\langle R_-^2\right\rangle\Big|_{t=0} - \left(\frac{1}{u_-}\right)\frac{\partial^2}{\partial t^2}\left\langle R_-^2\right\rangle\Big|_{t=0}\right]. \quad (74)$$

For initial separations which are much smaller than the correlation scale, $\left|\vec{k}_0 \cdot \vec{x}_-\right| \ll 1$, the time t will become large before relative separation reaches the correlation scale, i.e., $\left|\vec{k}_0 \cdot \vec{x}_-\right| \simeq 1$. Then we may approximate the solution with the time-asymptotically dominant piece, which is (noting that $u_- < 0$),

$$\left\langle R_-^2(t)\right\rangle \simeq A e^{u+t}. \quad (75)$$

Here, the coefficient A can be calculated straightforwardly using Eq. (73), which yields

$$A = \frac{\left[(1+\varepsilon/2)+\sqrt{1+\varepsilon}\right]}{\sqrt{1+\varepsilon}\left(1+\sqrt{1+\varepsilon}\right)}\left\{\alpha k_{ox}^2\left(x_+ - 2x_s\right)^2 + (1+\alpha)k_{ox}^2 x_-^2 + k_{oy}^2 y_-^2 + k_{oz}^2 z_-^2\right\} \quad (76)$$

where $\varepsilon = \mathrm{Re}^{-1}/\left(2(1+\delta)^2\right) \to 0$ as $\mathrm{Re} \to \infty$, and $\alpha = \varepsilon(1+\delta)\left(1+\sqrt{1+\varepsilon}\right)/4\left[(1+\varepsilon/2)+\sqrt{1+\varepsilon}\right] \to 0$ as $\mathrm{Re} \to \infty$. When time t is of the order of the correlation time τ_{cl}, the relative separation reaches the correlation scale, i.e., $\left\langle R_-^2(t)\right\rangle\Big|_{t=\tau_{cl}} \simeq 1$. Using this condition, the two-point

correlation lifetime can be determined by solving for t in Eq. (75), thus yielding

$$\tau_{\rm cl} = \frac{-\tau_c}{2(1+\delta)\left[1+\sqrt{1+\varepsilon}\right]} \ln\left\{C\left[\alpha k_{ox}^2 \left(x_+ - 2x_s\right)^2 + (1+\alpha)k_{ox}^2 x_-^2 + k_{oy}^2 y_-^2 + k_{oz}^2 z_-^2\right]\right\} \tag{77}$$

where $C = \left[(1+\varepsilon/2)+\sqrt{1+\varepsilon}\right]/\sqrt{1+\varepsilon}\left(1+\sqrt{1+\varepsilon}\right) \to 1$ as $\mathrm{Re} \to \infty$. The factor multiplying the logarithm in the expression of $\tau_{\rm cl}$ represents the large separation coherence time, retaining finite Reynolds number effects.

For Reynolds number exceeding order unity, the logarithmic function yields peaked correlation functions for small initial separations. The peaking becomes increasingly pronounced as the Reynolds number increases. The correlation scales are determined by the coefficients of the relative coordinate in the logarithm. The radial scale of correlation is then

$$\Delta_x \simeq (1+\alpha)^{-1/2} C^{-1/2} k_{ox}^{-1},$$

where k_{ox}^{-1} is the (nonlinear) radial mode width (mixing-length). This radial scale incorporates finite Reynolds number corrections to the mixing-length estimate through the parameters α and C, which are functions of Reynolds number. The result of the mixing-length theory can be recovered for $\mathrm{Re} \to \infty$ limit, i.e., $\Delta_x \simeq k_{ox}^{-1} = \Delta_{\bar{k}}$ as $\mathrm{Re} \to \infty$. The correlation scale in the y direction is k_{oy}^{-1}, which corresponds to a typical wavelength in the fluctuation spectrum. It is also important to notice that the one-point response correctly reduced to the coherent turbulent response in the limit of large Reynolds number. This limit is assumed in the mixing-length "theory." The "inertial" range corresponds to scales for which $\mathrm{Re} \gg 1$, and represents regime where the nonlinear effect dominates the dissipation in the two-point equation, and for which the dynamics is conservative. Also in this limit, the parameter α approaches zero and the correlation is singular at zero initial separation. For finite Reynolds number regimes,

the correlation function is finite even with zero initial separation, because parallel dissipation contributes through the $\alpha k_{ox}^2 \left(x_+ - 2x_s\right)^2$ term. The "dissipation" range k_y-spectrum can be estimated using the definition of Reynolds number and setting $\mathrm{Re} \sim 1$ for the dissipation range wavenumber, that is, in the dissipation range the linear parallel dissipation is comparable to nonlinear effects. This yields $\left(k_y\right)_d \simeq \sqrt{\mathrm{Re}}\, k_{oy}$, where $\left(k_y\right)_d$ is the dissipation range wavenumber.

It is worthwhile to note here that the correlation boundary can be defined by

$$C\left\{\alpha k_{ox}^2 \left(x_+ - 2x_s\right)^2 + (1+\alpha) k_{ox}^2 x_-^2 + k_{oy}^2 y_-^2 + k_{oz}^2 z_-^2\right\} = 1. \qquad (78)$$

In the normalized relative coordinates, this forms an ellipsoidal surface for finite Reynolds number. For the case of infinite Reynolds number, this correlation boundary is a spherical surface with radius unity in normalized relative coordinates.

Using τ_{cl} given in Eq. (77), we can obtain the stationary spectrum equation from the steady-state solution of the two-point energy correlation equation,

$$\left\langle \mathcal{E}_{12} \right\rangle \simeq \tau_{\mathrm{cl}} \left\langle S_{12}^0 \right\rangle .$$

In order to calculate the steady-state wavenumber spectrum from the stationary spectrum equation, it is necessary to express the source $\left\langle S_{12}^0 \right\rangle$ in terms of $\left\langle \mathcal{E}_{12} \right\rangle$ by using the steady-state condition of Eq. (35) and the equipartitioning assumption. This yields

$$\left\langle S_{12}^0 \right\rangle \simeq \sum_{\vec{k}} \left(\frac{1+\eta_i}{\tau}\right) \frac{|k_y|}{L_s} \left\langle \mathcal{E}_{12}(x_-) \right\rangle_{\vec{k}} e^{ik_y y_-} e^{ik_z z_-}. \qquad (79)$$

Since two-points are well correlated only if the relative separation is small compared to correlation scales, i.e., $\left|\vec{k}_0 \cdot \vec{x}_-\right| \ll 1$, the approximation

$\exp(ik_y y_- + ik_z z_-) \simeq 1$ is employed and the x_--dependence in $\langle \mathcal{E}_{12}(x_-) \rangle_{\vec{k}'}$ is also neglected in the source term for the high Reynolds number regime. Thus, we can rewrite the stationary spectrum equation as

$$\langle \mathcal{E}_{12}(x_-, y_-, z_-) \rangle \simeq \tau_{\rm cl}(x_-, y_-, z_-) \langle S^0 \rangle , \tag{80}$$

where $\langle S^0 \rangle$ is the source term evaluated with these approximations.

Since $\langle S^0 \rangle$ is now independent of the relative coordinate $\vec{x}_-$, the wavenumber spectrum of the energy correlation can be determined by the Fourier transform of $\tau_{\rm cl}(x_-, y_-, z_-)$. After Fourier transforming both sides of Eq. (80) in the y and z directions, and taking an x_--average over radial correlation length Δ_x, we obtain

$$\langle \mathcal{E}_{12} \rangle_{\vec{k}} = \left(\frac{1}{4\pi \Delta_x} \right) \int_{-\Delta_x}^{\Delta_x} dx_- \int dy_- \int dz_- \bar{\tau}_{\rm cl}(x_-, y_-, z_-) \langle S^0 \rangle e^{-ik_y y_-} e^{-ik_z z_-} \tag{81}$$

where

$$\bar{\tau}_{\rm cl}(x_-, y_-, z_-) = \tau_{\rm cl}(x_+, x_-, y_-, z_-) \Big|_{(x_+ - 2x_s) = \Delta_x} .$$

Since the expression for $\tau_{\rm cl}$ loses its meaning and validity when the argument of the logarithm is larger than unity, it is necessary to restrict the range of integration to within the correlation boundary, as given by Eq. (78). The integration can be performed using a Fourier-Bessel expansion and the summation theorem of Bessel functions. This yields

$$\begin{aligned} (\bar{\tau}_{\rm cl})_{\vec{k}} &\equiv \frac{1}{2\Delta_x} \int_{-\Delta_x}^{\Delta_x} dx_- \int dy_- \int dz_- \bar{\tau}_{\rm cl}(x_-, y_-, z_-) e^{-ik_y y_-} e^{-ik_z z_-} \\ &= \frac{\tau_c}{2(1+\delta)\left(1+\sqrt{1+\varepsilon}\right)} F(k_y, k_z) , \end{aligned} \tag{82}$$

where

$$F(k_y,k_z) = -\frac{1}{\Delta_x}\int_0^{\Delta_x} dx_- \int dy_- \int dz_-\, e^{-ik_y y_-}\, e^{-ik_z z_-}$$
$$\ln\left\{\left(\frac{\alpha}{\alpha+1}\right) + C\left[(1+\alpha)k_{ox}^2 x_-^2 + k_{oy}^2 y_-^2 + k_{oz}^2 z_-^2\right]\right\}$$
$$= \frac{4\pi}{Ck_{oy}k_{oz}}\int_0^{\xi}\left[\sqrt{\xi^2-\rho^2} - \sqrt{1+\rho^2-\xi^2}\cos^{-1}\sqrt{1+\rho^2-\xi^2}\right]\rho J_0\left(\frac{\beta\rho}{\sqrt{C}}\right)d\rho \quad (83)$$

with $\xi = \sqrt{1/(1+\alpha)}$ and $\beta = \sqrt{(k_y/k_{oy})^2 + (k_z/k_{oz})^2}$. Details of these integrations are given in the Appendix A. Hence, the inertial range energy k_y-spectrum can be calculated by taking the $\mathrm{Re} \to \infty$ limit and summing over k_z, yielding

$$\langle \mathcal{E}_{12}\rangle_{k_y} \simeq 2\int_0^{\infty} dk_z \langle \mathcal{E}_{12}\rangle_{\vec{k}} = \frac{2\pi k_{oy}}{k_y^2}\left(1 - J_0\left(\frac{k_y}{k_{oy}}\right)\right)\langle S^0\rangle . \quad (84)$$

The wavenumber dependence of the energy spectrum fits a power law of the form

$$\langle \mathcal{E}_{12}\rangle_{k_y} \sim k_y^{-5/2}$$

in the first decade of decay from its peak value.

Numerical evaluations of the k_y-wavenumber spectrum of energy correlation for the two cases ($\mathrm{Re} = 5$ and $\mathrm{Re} \to \infty$) are plotted in Fig. 2.4.

In the low-k_y region of the spectrum, $\langle \mathcal{E}_{12}\rangle_{k_y} \sim k_y^0$ and exhibits an energy-containing range structure. In the $k_y \simeq k_{oy}$ range, the spectrum falls off according to the power law and exhibits an inertial range structure. Finally, for $k_y \gtrsim 6k_{oy}$, $\langle \mathcal{E}_{12}\rangle_{k_y}$ is oscillatory due to the approximation used to cutoff τ_{c1} at the correlation boundary. This oscillation indicates a breakdown of the approximations at high-k_y. However, the energy content of the spectrum in this range is negligible, and this region falls in the dissipation range $k_y > (k_y)_d$. Therefore, these oscillations are of no consequence.

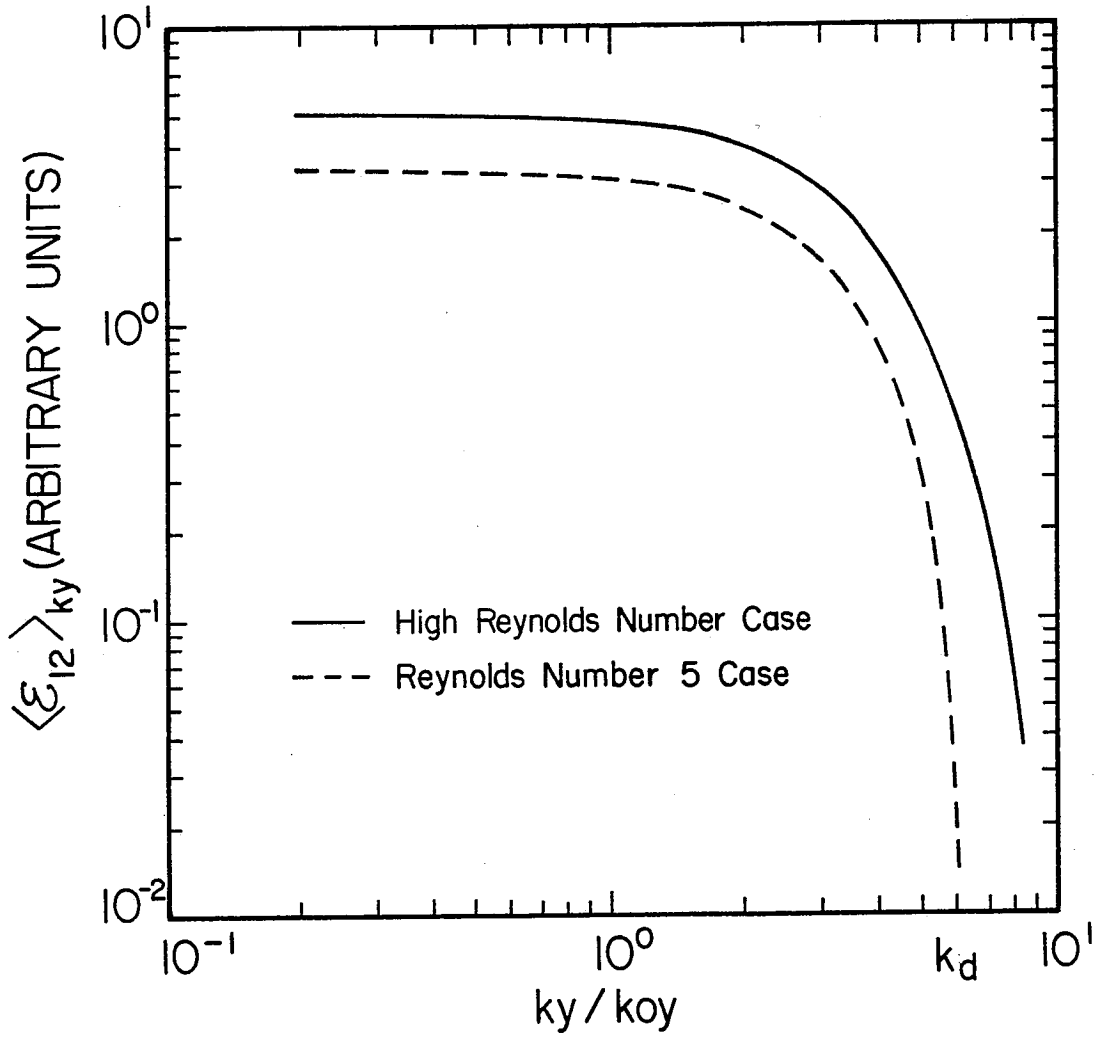

Fig. 2.4 Wavenumber spectrum of energy correlation for the high Reynolds number and Re= 5 cases.

Now, we can compare the results of the two-point theory with predictions of one-point mixing-length theory. Noting the source can be written as

$$\langle S^0 \rangle \simeq \sum_{\vec{k}'} \left(\frac{1+\eta_i}{\tau} \right) \frac{|k'_y|}{L_s} \langle \mathcal{E}_{12} \rangle_{\vec{k}'}$$

and multiplying by (k_y/k_{oy}), and integrating both sides of Eq. (81) over k_y and k_z, and solving for D^x yields

$$D^x \simeq \left\{ \frac{\pi^2}{4(1+\delta)^2} \left[\ln(1+\eta_i) \right]^2 \right\} \left(\frac{k_{oy}}{L_s} \right) \left(\frac{1+\eta_i}{\tau} \right)^2 . \tag{85}$$

This result has identical scalings to the results of one-point theory, but contains an additional numerical multiplier given in brackets, which depends on Reynolds number (i.e., $\mathrm{Re} = \left[D_{\vec{k}} k_{ox}^2 \right] \Big/ \left[\mu k_{oy}^2 / \left(L_s^2 k_{ox}^2 \right) \right] \simeq (1+\eta_i)$). Even though the additional multiplier is order unity and a weak function of Reynolds number ($\mathrm{Re} \sim \eta_i$), it is very important to notice that this multiplier is crucial for a description of steady state turbulence because it depends on dissipation through the definition of Reynolds number. Because the transport coefficients, such as diffusivity and conductivity, depend on spectral sum of fluctuation amplitudes, it is necessary to determine the integration range of the spectrum (i.e., dissipation range wavenumber) even for high Reynolds number turbulence. The theories based only on the inertial range structure of high Reynolds number turbulence, such as the mixing-length theory and the scale transformation technique,[19] may estimate transport scalings. However, those theories fail to represent the crucial property of the steady-state condition associated with dissipation.

Having derived the wavenumber spectrum of fluctuations, one can evaluate the spectrum-averaged wavenumber of η_i-mode turbulence (i.e.,

$(k_y)_{\rm rms} = k_{oy}$) by taking the rms-value of the k_y-wavenumber, i.e.,

$$(k_y)_{\rm rms} \equiv \left[\frac{\sum_{k_y} k_y^2 \langle \mathcal{E}_{12} \rangle_{k_y}}{\sum_{k_y} \langle \mathcal{E}_{12} \rangle_{k_y}} \right]^{1/2} . \tag{86}$$

The integration of Eq. (86) shows that $(k_y)_{\rm rms}$ is a weak function of Reynolds number and has a numerical value of 0.4 (in ρ_s^{-1} unit) for the η_i-value to which the fluid model is applicable. This typical wavenumber can only be calculated by using two-point theory. The other theories based on one-point renormalization or on scale transformation effectively treat this wavenumber as a free parameter.

Using the predicted diffusion level, Eq. (85), and the rms wavenumber, the mean-squared radial velocity can be estimated as

$$(\tilde{v}_r)_{\rm rms} \equiv \sqrt{\bar{E}_{\vec{k}}} \simeq \left\{ \frac{\pi^2}{4(1+\delta)^2} \left[\ln (1+\eta_i) \right]^2 \right\} \left(\frac{k_{oy}}{L_s} \right) \left(\frac{1+\eta_i}{\tau} \right)^{3/2} . \tag{87}$$

The principal results of this section are the calculations of the two-point energy correlation function, the wavenumber spectrum of the ion pressure fluctuations, and the ion thermal diffusivity and average wavenumber. To summarize these results, the energy spectrum dependence on poloidal wavenumber is given by

$$\left\langle \tilde{P}_i^2 \right\rangle_{k_\theta} \sim k_\theta^{-5/2}$$

with the spectrum-averaged poloidal wavenumber being $(k_\theta \rho_s)_{\rm rms} \simeq 0.4$. The ion thermal diffusivity is given by

$$\chi_i \simeq \left[\frac{\pi^2}{4} \left(\ln (1+\eta_i) \right)^2 \right] \left(\frac{1+\eta_i}{\tau} \right)^2 \frac{(k_\theta \rho_s)_{\rm rms}}{L_s} \rho_s^2 c_s .$$

The predicted rms-values of fluctuating radial velocity, pressure and potential are

$$(\tilde{v}_r)_{\rm rms} \simeq \left[\frac{\pi^2}{4} \left(\ln (1+\eta_i) \right)^2 \right] \left(\frac{1+\eta_i}{\tau} \right)^{3/2} (k_\theta \rho_s)_{\rm rms} \frac{\rho_s c_s}{L_s} ,$$

and

$$\left(\tilde{P}_i/P_{oi}\right)_{\text{rms}} \simeq \left[\frac{\pi^2}{4}\left(\ln\left(1+\eta_i\right)\right)^2\right]\left(\frac{1+\eta_i}{\tau}\right)^{3/2}\frac{\rho_s}{L_n},$$

and

$$\left(\frac{\tilde{n}}{n_0}\right)_{\text{rms}} = \left(\frac{e\Phi}{T_e}\right)_{\text{rms}} \simeq \left[\frac{\pi^2}{4}\left(\ln\left(1+\eta_i\right)\right)^2\right]\left(\frac{1+\eta_i}{\tau}\right)^{3/2}\frac{\rho_s}{L_s},$$

respectively.

Having obtained the wavenumber spectrum and fluctuation levels at saturation, we now consider the effect of η_i-mode turbulence on heat and particle transport in tokamak experiments.

A. Ion and Electron Thermal Conduction

Recent experimental results from the Alcator-C tokamak[1,2] have indicated that in the high-density, saturated electron confinement regime of Ohmically-heated discharges, in which the electron energy confinement time $\tau_E \left(\propto n\right)$ approaches or exceeds the equilibration time between electrons and ions $\tau_{ei} \left(\propto 1/n^2\right)$, there is an anomalous ion heat loss which is apparently related to large η_i-values (i.e., $\eta_i > \eta_{ic}$ observed). This is also consistent with the observation that the injection of a large pellet and the subsequent density gradient steepening result in an improvement in energy confinement. There is also an indication of anomalous ion heat conductivity in neutral beam heated, density-clamped (L-mode) tokamak experiments (e.g., D-III tokamak[3]). In this case, beam injection directly heats the ions while simultaneously, particle confinement degrades. This results in an increase in η_i. For the L-phase of Doublet-III, the results of transport analyses with measured ion temperature profiles (determined by charge exchange recombination spectroscopy) indicate significant departure from neoclassical ion heat conductivity values χ_i^{Neo}.[20] Also, the radial dependence of χ_i is not related to χ_i^{Neo}.[3] It is plausible to explore an interpretation of this anomaly as η_i-mode turbulence driven ion conduction heat loss.

The anomalous ion thermal conductivity can be calculated in a

straightforward manner, by using the saturation level of fluctuations. The ion thermal flux $q(r)$ due to $\vec{E} \times \vec{B}$ turbulent convection of perturbed ion pressure is given in terms of the pressure-potential cross correlation by

$$\begin{aligned} q_i(r) &= -\left\langle \tilde{p}_i \nabla_y \tilde{\phi} \right\rangle \\ &= \sum_{k_y} (-ik_y) \left\langle \tilde{p}_i \tilde{\phi} \right\rangle_{k_y} . \end{aligned} \tag{88}$$

Using the stationarity relation Eq. (35), one can express the ion thermal flux in terms of the saturation level of electrostatic potential fluctuations

$$q_i(r) = \tau \sum_{k_y} \left(\frac{1+\eta_i}{\tau} \right) \frac{k_y^2}{L_n} \left| \tilde{\phi}_{\vec{k}} \right|^2 \Big/ \left[D^x \Big/ (\Delta_x)^2 \right]. \tag{89}$$

Using the decorrelation rate $\left[D^x / (\Delta_x)^2 \right]$ given in Eq. (85), the integrated radial velocity $\mathbf{b}E$ in Eq. (87), and the definition of ion thermal conductivity

$$\chi_i(r) \equiv -q_i(r) \Big/ \left[\frac{d \langle P_{oi} \rangle}{dr} \right], \tag{90}$$

we find the final form of the anomalous ion thermal conductivity to be (for $\eta_i > \eta_{ic} \sim 1.5$).

$$\chi_i \simeq \left[\frac{\pi^2}{4} \left(\ln (1+\eta_i) \right)^2 \right] \frac{(k_y)_{\text{rms}}}{L_s} \left(\frac{1+\eta_i}{\tau} \right)^2 . \tag{91}$$

In dimensional units, χ_i can be expressed as

$$\chi_i \simeq \left[\frac{\pi^2}{4} \left(\ln (1+\eta_i) \right)^2 \right] \frac{(k_y \rho_s)_{\text{rms}}}{L_s} \left(\frac{1+\eta_i}{\tau} \right)^2 \rho_s^2 c_s, \tag{92}$$

where the mean wavenumber $(k_y \rho_s)_{\text{rms}} \simeq 0.4$.

For the case of nearly flat density profiles observed in the ohmic saturation regime of the Alcator-C tokamak, ($\eta_i \simeq 4$, $T_i \simeq 700eV (T_i \simeq T_e)$ and $B_0 \simeq 9T$ for $r = a/2$) the ion thermal conductivity due to η_i-mode turbulence

is approximately $4.0 \times 10^3 \mathrm{cm}^2/\mathrm{sec}$. Also, note that the scaling $\chi_i \sim (1+\eta_i)^2$ implies that large values of η_i are unlikely and that L_{T_i} is a weak function of ion heating power P_I (i.e., thermal balance implies $L_{T_i} \sim P_I^{-1/3}$), so that $T_i(r)$ profiles remain comparatively similar. This is consistent with observed $\eta_i(r)$ profiles from the L-phase regime of the ASDEX tokamak, where $\eta_{ic} < \eta_i \lesssim 3$.[22]

Another application of η_i-mode turbulence driven anomalous ion heat loss has been proposed in the context of a high current RFP by An et al.[21] They studied a coupled system of resistive-interchange and ion-temperature-gradient-driven turbulence, and reported the possibility of significant ion thermal loss in a high current, high temperature RFP. This coupled system might also be relevant to the understanding of anomalous heat transport in stellarators.

In a tokamak plasma, in addition to (direct) ion heat loss, there is a possible electron thermal loss associated with the dissipative trapped electron response ($\nu_* < 1$) to η_i-mode turbulence. In the trapped-electron regime (i.e., $\nu_{*e} < 1$, $\nu_{*e} \equiv \nu_{\mathrm{eff},e}/\omega_{be}$) of tokamak plasmas, the presence of trapped electrons can result in a heat flux associated with background fluctuations driven by the η_i-mode turbulence. It is well known[23] that for $\nu_{*e} < 1$, the perturbed distribution for trapped electrons is

$$f_e^T = \frac{eF_{Me}}{T_e}\left[\bar{\Phi} - \frac{\omega - \omega_{*e}\left(1+\eta_e(E/T_e - 3/2)\right)}{\omega - \bar{\omega}_{De} + i\nu_{\mathrm{eff},e}}\bar{\Phi}\right] \tag{93}$$

with $\bar{\Phi} \equiv$ trapped-particle-orbit-averaged electrostatic potential. The anomalous electron heat flux can be estimated by using

$$(Q_r^e)^T \simeq \left\langle \left(\frac{1}{2}mv_e^2\right)\tilde{v}_{Er}\cdot\tilde{n}\right\rangle^T, \tag{94}$$

where $\langle \ldots \rangle^T$ represents the velocity-space average over trapped electrons. For a simple estimate of the trapped-electron contribution, the bounce average can

be ignored and the resulting heat flux is given by

$$\left(Q_r^e\right)^T \simeq -n_{oe}\left(15\sqrt{2}\right)\epsilon^{3/2}\left(k_y^2\rho_s^2\right)\frac{c_s^2}{\nu_e}\frac{dT_e}{dr}\left|\frac{e\Phi}{T_e}\right|^2 \tag{95}$$

in the high-collisionality limit of the banana regime where ω, $\bar{\omega}_{De} \ll \nu_{\mathrm{eff},e}$ and $\eta_i \simeq \eta_e \gg 1$. Using the saturation amplitude of the radial velocity of the η_i-mode turbulence given by Eq. (87), the electron heat conductivity is given by

$$\chi_e \simeq 15\sqrt{2}\epsilon^{3/2}\left[\frac{\pi}{2}\ln\left(1+\eta_i\right)\right]^4\left(\frac{1+\eta_i}{\tau}\right)^3\left(\frac{c_s^2\rho_s^2}{\nu_e L_s^2}\right)\left(k_y^2\rho_s^2\right)_{\mathrm{rms}} \tag{96}$$

where ϵ is the inverse aspect ratio and the mean wavenumber has been used to evaluate χ_e ($(k_y\rho_s)_{\mathrm{rms}} = 0.4$). Thus, ion-temperature-gradient-driven turbulence can also result in increased anomalous electron thermal conduction. However, while there is certainly a relation between the resulting χ_i and χ_e, they clearly scale quite differently and cannot be arbitrarily assumed to be comparable. In particular, for $\epsilon^{3/2}c_s/L_s\nu_e < 1$, $\chi_e < \chi_i$.

B. Particle Transport

1. Ion-Mixing Driven Particle Influx

As in the case of the high-density saturation regime of the Alcator-C tokamak experiment, there have been many gas-fueled tokamaks which exhibit an anomalous inward density pinch after puffing of neutral gas into the plasma chamber. Previously, the theory of the ion-mixing mode[24] has been proposed to explain this anomalous inward particle flux. The coupling of ion-temperature-gradient-driven modes to a collisional electron response is thought to be responsible for this anomaly. However, as discussed previously, the estimate of the saturation level used in Ref. 24 (invoking the heuristic ambient-

gradient type argument) is probably incorrect. Here, we re-examine the ion-mixing driven particle transport using the results of the η_i-mode turbulence calculation which has been presented in previous sections.

In the η_i-mode turbulence theory, the electron density response has been approximated as adiabatic. Because the density and radial velocity are 90° out-of-phase in the adiabatic approximation, no particle transport can result. However, when considering near-edge tokama plasma where the anomalous inward particle pinch is significant, finite electron parallel thermal conductivity due to collisions is not negligible. Thus, the nonadiabatic part of the electron density response should be retained. It can provide a phase difference between $\tilde{n}$ and $\tilde{\phi}$, thus giving rise to net particle transport.

For the wide range of collisionality regimes which are appropriate for near-edge tokamak parameters, the electron fluid equations[10] can be applied to calculate the (electron) density response. Also, by comparing the radial scale length of the collisional electron response $\Delta_{\vec{k}}^{c}$ [5] with the nonlinear η_i-mode radial mixing scale $\Delta_{\vec{k}}$, it can be shown that the linear electron response is an adequate approximation (i.e., $\Delta_{\vec{k}}^{c} < \Delta_{\vec{k}}$). A laborious but straightforward calculation shows that the electron density response is given by

$$\frac{\tilde{n}_e}{n_0} = A\left(\vec{k},\omega\right)\tilde{\phi}, \tag{97}$$

where

$$A\left(\vec{k},\omega\right) \equiv \frac{\left[\left(3/2\hat{\chi}_e\frac{\omega_{*e}}{\omega} - \frac{\omega_\chi^2}{\omega^2}\right) + i(3/2\frac{\omega_\chi}{\omega} + \left\{\hat{\chi}_e + (1+\alpha_T)^2 - 3/2\,(1+\alpha_T)\,\eta_e\right\}\frac{\omega_{*e}\omega_\chi}{\omega^2}\right)\right]}{\left[\left(3/2\hat{\chi}_e - \frac{\omega_\chi^2}{\omega^2}\right) + i\left(3/2 + \hat{\chi}_e + (1+\alpha_T)^2\right)\frac{\omega_\chi}{\omega}\right]} \tag{98}$$

and

$$\omega_\chi \equiv \frac{\hat{\chi}_e}{0.51}\frac{T_{eo}}{m_e\nu_e}k_\parallel^2 \tag{99}$$

with numerical factors of $\hat{\chi}_e = 1.61$ and $\alpha_T = 0.71$ for $k_\parallel v_{th,e} < \nu_e$. For the regime where

$$\left(\frac{\overline{\omega_\chi}}{\omega_{*e}}\right) = \left(\frac{\hat{\chi}_e}{0.51}\right)\left(\frac{m_i}{m_e}\right)\left(\frac{\overline{\omega_{*e}}}{\nu_e}\right)\left(\frac{L_n}{L_s}\right)^2\left(\frac{\overline{\Delta_r}}{\rho_s}\right)^2 \gg 1,$$

where the overbars indicate evaluation at a mean wavenumber and mean radial scale, the electron density response is almost adiabatic with a small nonadiabatic (imaginary) part due to electron thermal conductivity. Although the nonadiabatic part of electron density response is important for evaluating particle transport, it can be shown that this nonadiabatic electron response in the $(\omega_\chi/\omega_{*e}) \gg 1$ regime has little influence on the basic stability and the radial scale of the η_i-mode. Hence, the resulting particle flux can be quasilinearly calculated by using the saturated radial velocity level which has been determined in the context of η_i-mode turbulence.

Proceeding, the anomalous particle flux, Γ_r from $\vec{E}\times\vec{B}$ turbulent convection of the perturbed density is given in terms of the density-potential cross correlation by

$$\Gamma_r \simeq \langle \tilde{v}_{Er}\cdot\tilde{n}\rangle = -i\sum_{k_y} k_y \left\langle \tilde{\phi}\tilde{n}\right\rangle_{k_y}. \tag{100}$$

For the $\left(\overline{\omega_\chi/\omega_{*e}}\right) \gg 1$ regime, the particle flux is given by

$$\Gamma_r \simeq 2\left[\hat{\chi}_e + (1+\alpha_T)^2\right]\left[1-\frac{\eta_e}{\eta_e^c}\right]\sum_{k_y} k_y\left(\frac{\omega_{*e}}{\omega_\chi}\right)\left|\tilde{\phi}_{\vec{k}}\right|^2, \tag{101}$$

where

$$\eta_e^c \simeq \left[\frac{\hat{\chi}_e + (1+\alpha_T)^2}{3/2\,(1+\alpha_T)}\right] \simeq 1.77.$$

Using the rms-value of the radial velocity given in Eq. (87), the particle pinch

velocity can be calculated (in dimensional units) and is

$$\langle V_r \rangle \equiv \frac{\Gamma_r}{n_0}$$
$$\simeq \left[\frac{\pi^4}{8}\left(\ln\left(1+\eta_i\right)\right)^4\right]\left[\hat{\chi}_e + \left(1+\alpha_T\right)^2\right]\left[1-\frac{\eta_e}{\eta_e^c}\right]\left(\frac{m_e}{m_i}\right)\frac{0.51}{\hat{\chi}_e}\frac{\nu_e}{L_n}\left(\frac{1+\eta_i}{\tau}\right)^2\rho_s^2. \tag{102}$$

It should be noticed, however, that the assumptions $k_{\|}v_{th,e} < \nu_e$ and $\eta_e > \eta_e^c$ must be satisfied for consistency and applicability of the theory (also, $\eta_i > \eta_{ic}$ must be satisfied for instability). Because this inflow of particles is due to the off-diagonal element of flux-force transport relation, the critical value η_e^c represents competition between two opposing forces (namely dn/dr corresponding to particle diffusion, and dT/dr, which corresponds to the inward pinch).

For the case of near-edge parameters in the Alcator-C tokamak with $\eta_i \approx \eta_e \simeq 4$, $T_i \approx T_e \simeq 50eV$ and $B \simeq 9T$, the pinch velocity is approximately $\langle V_r \rangle \simeq 1000$ cm/sec.

For the collisional regime where $\left(\overline{\omega_\chi/\omega_{*e}}\right) > 1$, it is interesting to note that in addition to an inward flux of particles, there also exists a "heat-pinch" effect. Recently, the concept of a heat-pinch has been proposed in order to explain the disparity between thermal diffusivities obtained from heat pulse propagation studies and transport analysis. This flow of electron heat can be determined from the electron pressure-potential cross correlation

$$Q_r^e \simeq \left\langle \tilde{v}_{Er} \cdot \tilde{P}_e \right\rangle \tag{103}$$

where $\tilde{P}_e = \tilde{n}_e T_{eo} + n_0 \tilde{T}_e$. Thus

$$Q_r^e =$$
$$\left[\frac{\pi^4}{8}\left(\ln\left(1+\eta_i\right)\right)^4\right]\left[\hat{\chi}_e + \left(1+\alpha_T\right)^2\right]\left[1-\frac{\eta_e}{\eta_e^{\mathrm{HP}}}\right]\left(\frac{m_e}{m_i}\right)\frac{0.51}{\hat{\chi}_e}\frac{\nu_e}{L_n}\left(\frac{1+\eta_i}{\tau}\right)^2\rho_s^2. \tag{104}$$

Electron heat can flow inward ("Heat-Pinch") provided $\eta_e > \eta_e^{HP}$ with $\eta_e^{HP} = \frac{2}{3}\left[1 + \alpha_T + \hat{\chi}_e/\alpha_T\right] \simeq 2.65$. It should be noticed that the critical η_e-value for a heat-pinch is greater than the critical η_e-value for a particle-pinch because of the additional contribution from $\tilde{T}_e$.

For the central region of tokamaks which are characterized by low collisionality, the dissipative trapped-electron response[22] provides the necessary phase-shift between the density response and fluctuating electrostatic potential for net particle transport. This results in the conclusion that the resulting particle flux is directed outward rather than inward. However, experimental results indicate that anomalous particle pinch effects are only necessary in the near-edge region (rather than throughout the whole plasma cross-section) in order to explain the transport analysis results.[25,26]

2. Impurity Effects on Particle Transport

Recent experimental results from the ISX-B tokamak have indicated that in a neutral beam heated plasma contaminated with small quantities of a recycling low-Z impurity, it is possible to produce a "Z-mode" discharge[27] characterized by confinement properties which are improved in comparison to the "L-mode" discharge. The improved energy confinement is accompanied by and thought to be due to peaking of the density profile in the (energy) confinement zone. The global energy confinement time scaling is modified from "ISX-B scaling"[28,29] by introduction of a density dependence. Although transport analyses indicate improved particle confinement in "Z-mode" discharges, power balance shows that the improved energy confinement is due primarily to a reduction in electron thermal diffusivity χ_e.

In order to explain the improved energy confinement in "Z-mode" discharge, an extension of the Carreras-Diamond electron thermal

diffusivity[30,31] based on resistive ballooning turbulence, has been proposed for the regime where $\omega_{*e} > \gamma$, the linear growth rate. The effect of large-ω_* is to reduce the electron thermal diffusivity through diamagnetic modifications to the resistive ballooning mode. The χ_e prediction compares favorably with experimental results.[32] However, even though the proposed "large-ω_*" extension of the Carreras-Diamond χ_e is consistent with experimental results, it is also necessary to explain the improvement of particle confinement and the resulting steepening of the density gradient associated with the introduction of a recycling impurity into the "Z-mode" discharge.

Here, we propose a mechanism for an ion-mixing driven inward particle flow enhanced by an inverted edge impurity density profile due to (sustained) impurity puffing during "Z-mode" operation. The model of the L to Z-phase transition sequence can thus be described as follows:

i) For the near-edge region of a beam-heated, density-clamped plasma (characteristic of "L-mode" discharges), the η_i-mode can be destabilized by background ion-temperature-gradient free energy.

ii) With introduction of a small amount of low-Z impurity by puffing, background η_i-mode turbulence is amplified by the inverted impurity density profile, providing larger effective η_i-values.

iii) This impurity enhancement effect changes the saturation amplitude of the background η_i-mode turbulence, hence the ion-mixing driven inflow increases and the resulting ambient density profile steepens.

iv) With steepening of the density profile, the background resistive ballooning turbulence enters the $\omega_* > \gamma$ regime, which results in a reduced electron thermal diffusivity.

To describe the impurity effects on the η_i-mode,[33] equations for cold impurity ions are necessary. For simplicity, we assume that only one im-

purity species with charge Z and density n_I is present, and that the concentration of this impurity is small compared to that of background ions, i.e., $Zn_I \ll n_i \lesssim n_e$. For a long-wavelength η_i-mode with cold impurity ions (corresponding to the phase velocity regime $v_{th,I} \ll v_{th,i} \lesssim |\omega/k_\parallel| < v_{th,e}$), impurity dynamics equations[10,34] can be derived using equations for impurity ion density and parallel momentum, along with the quasineutrality condition

$$\tilde{n}_e = \tilde{n}_i + Z\tilde{n}_I.$$

Details of the equations are given in Appendix B.

As in the case of the η_i-mode, the energy flow and balance can be seen clearly by defining energy-like integrals

$$E^W \equiv \frac{1}{2}\int d^3x \left(|\tilde{\phi}|^2 + \frac{n_{oi}}{n_{oe}} \left| \nabla_\perp \tilde{\phi} \right|^2 \right) \tag{105}$$

$$E^K \equiv \frac{1}{2}\int d^3x \left(\frac{n_{oi}}{n_{oe}} \left| \tilde{v}_{\parallel i} \right|^2 \right) \tag{106}$$

$$E^Z \equiv \frac{1}{2}\int d^3x \left(\frac{n_{oI}}{n_{oe}} \frac{m_I}{m_i} \left| \tilde{v}_{\parallel I} \right|^2 \right) \tag{107}$$

$$E^I \equiv \frac{1}{2}\frac{1}{\Upsilon}\int d^3x \left(\frac{n_{oi}}{n_{oe}} |\tilde{p}_i|^2 \right). \tag{108}$$

Using the impurity equations, Eqs. (B1)–(B4), it follows that the total energy of the system evolves according to

$$\begin{aligned} \frac{\partial}{\partial t}E =& \frac{\partial}{\partial t}\left(E^W + E^K + E^Z + E^I\right) \\ =& -\int d^3x \left\{ \frac{1}{\Upsilon}\left(\frac{1+\eta_i}{\tau}\right) \frac{n_{oi}}{n_{oe}} \frac{1}{L_{ni}} \left\langle \tilde{p}_i \nabla_y \tilde{\phi} \right\rangle \right. \\ & \left. - \frac{n_{oi}}{n_{oe}} \mu_i \left| \nabla_\parallel \tilde{v}_{\parallel i} \right|^2 - \frac{n_{oI}}{n_{oe}} \frac{m_I}{m_i} \mu_I \left| \nabla_\parallel \tilde{v}_{\parallel I} \right|^2 \right\}. \end{aligned} \tag{109}$$

This shows that the structure of the energy balance is the same as in the η_i-mode case, except for an additional sink due to impurity ions. However, μ_I

for cold impurity ions is negligible. As described in Section III, the required diffusion and radial correlation length at saturation can be estimated and are given by

$$D_{\vec{k}}^{I} \simeq [C(\mathrm{Re})]^2 \left(\frac{1+\eta_i}{\tau}\right)^{1/2} \frac{k_y}{L_s} \left(\Delta_x^I\right)^3 A^{1/2}, \tag{110}$$

$$\Delta_{\vec{k}}^{I} \simeq \left[D_{\vec{k}}^{I} \Big/ k_{\|}'\right]^{1/4} \tag{111}$$

respectively, where the additional multiplier of Eq. (85) is included as $C(\mathrm{Re})$, and the enhancement factor is defined by

$$A \equiv \left[1 + Z\frac{n_{oI}}{n_{oi}}\frac{L_{ni}}{L_{nI}}\right]^{-1}. \tag{112}$$

Here, we assume an inverted impurity density gradient, i.e., $L_{ni}L_{nI} < 0$, and $\left|Z\left(n_{oI}/n_{oi}\right)\left(L_{ni}/L_{nI}\right)\right| < 1$. Basically, the ion-temperature-gradient drives fluctuations, and ion parallel viscous dissipation sinks the fluctuation energy, but impurity ions with an inverted density profile effectively enhance η_i, thus amplifying the resulting fluctuations. Similarly, impurity distributions peaked in the center effectively reduce η_i, resulting in lower fluctuation levels and less transport. The most important aspect of this enhancement effect is manifested in the inward particle pinch velocity. With average pinch velocity for the ion-mixing case Eq. (102), the impurity-enhanced pinch velocity can be estimated by

$$\langle V_r \rangle^I \simeq \langle V_r \rangle \cdot A^3. \tag{113}$$

This enhanced pinch velocity for the edge region of the "Z-mode" discharge may be responsible for the observed steepening of the density profile after impurity puffing.

2.5 Conclusions

For high density regimes of tokamaks in the ohmic "saturated" phase and in the presence of auxiliary ion heating such as neutral beam injection, the significant anomalous energy loss through the ion conduction channel has been observed. Since the ion-temperature-gradient is frequently steeper than the density gradient for such regimes of tokamak operation, ion-temperature-gradient-driven turbulence is a strong candidate for the explanation of anomalous ion heat loss in tokamak experiments. Here we have studied ion-temperature-gradient-driven turbulence using two-point equations for the energy correlation function and have calculated the wavenumber spectra of the ion pressure fluctuations. In the saturated state, we have obtained the stationary spectrum from the steady-state solution of the two-point energy correlation equation. Hence, we have calculated fluctuation levels and the resulting ion thermal diffusivity using the spectra. These analytical predictions have been compared with the observed ion thermal diffusivity in the Alcator-C tokamak and are in good agreement.

The principal results of this chapter are:

(i) The fluctuation energy correlation function and fluctuation wavenumber spectra are calculated by solution of energy-conserving mode-coupling equations. The calculated wavenumber spectrum of ion pressure fluctuations has the form $\left\langle \tilde{P}_i^2 \right\rangle_{k_\theta} \sim k_\theta^{-5/2}$, where $\left(\tilde{P}_i/P_{oi}\right)_{\rm rms} \simeq 5.7\left[\left(1+\eta_i\right)/\tau\right]^{3/2}\rho_s/L_n$. Similarly, the rms fluctuating radial velocity is $\left(\tilde{v}_r\right)_{\rm rms} \simeq 2.3\left[\left(1+\eta_i\right)/\tau\right]^{3/2}\rho_s c_s/L_s$ and fluctuating density is $\left(\tilde{n}/n_0\right) = \left(e\tilde{\Phi}/T_e\right) \simeq 5.7\left[\left(1+\eta_i\right)/\tau\right]^{3/2}\rho_s/L_s$. Note that the predicted

density fluctuation levels are quite similar to the usual drift-wave turbulence level $\tilde{n}/n_0 \approx 3\rho_s/L_n$. Hence, it may be difficult to experimentally distinguish η_i-mode induced density fluctuations from more commonplace low frequency, drift-wave turbulence. While the parameter scalings of these results are qualitatively consistent with mixing-length estimates, they have been derived using the calculated fluctuation spectra. In particular, no assumptions such as $k_y\rho_s \sim \mathcal{O}(1)$, etc. were used to obtain the numerical coefficients.

(ii) For $\eta_i > \eta_{ic}$, the ion thermal diffusivity χ_i is given by $\chi_i = [C(\mathrm{Re})]^2 \left((1+\eta_i)/\tau\right)^2 (k_{oy}\rho_s)\left(\rho_s^2 c_s/L_s\right)$ where $C(\mathrm{Re}) \simeq (\pi/2)\ln(1+\eta_i)$. The numerical value of the ion thermal diffusivity is consistent with the experimentally measured χ_i for the Alcator-C tokamak (for which $k_{oy}\rho_s \simeq 0.4$).

(iii) For dissipative trapped electron dynamics (i.e., $\nu_* < 1$, $\nu_{\mathrm{eff}} > \bar{\omega}_{De}$), the electron heat conductivity due to ion-temperature-gradient-driven turbulence is given by:

$$\chi_e \simeq 15\sqrt{2}\epsilon^{3/2}\left[\frac{\pi}{2}\ln(1+\eta_i)\right]^4\left(\frac{1+\eta_i}{\tau}\right)^3\frac{c_s^2\rho_s^2}{\nu_e L_s^2}\left(k_{oy}^2\rho_s^2\right).$$

Here ϵ is the inverse aspect ratio.

Note that in general, $\chi_e \neq \chi_i$.

(iv) For collisional electron dynamics (i.e., $k_\parallel v_{th,e} < \nu_{ei}$), the electron response to the ion-temperature-gradient-driven turbulence results in a particle flux:

$$\Gamma_r \simeq 2n_0[C(\mathrm{Re})]^4 \left[\hat{\chi}_e + (1+\alpha_T)^2\right] \left[1 - \frac{\eta_e}{\eta_e^c}\right] \cdot \left(\frac{m_e}{m_i}\right) \frac{0.51}{\hat{\chi}_e} \frac{\nu_e}{L_n} \left(\frac{1+\eta_i}{\tau}\right)^2 \rho_s^2$$

where

$$\eta_e^c \simeq \left[\frac{\hat{\chi}_e + (1+\alpha_T)^2}{3/2\,(1+\alpha_T)}\right] \simeq 1.77.$$

Note that for $\eta_e > 1.77$, the flux is inward. For Alcator-C parameter, $\langle V_r \rangle = \Gamma_r/n_0 \simeq 1000$ cm/sec. Similarly, the electron thermal flux Q_r^e can be derived. For $\eta_e > 2.65$, the electron thermal flux is inward and corresponds to a "heat-pinch."

(v) The effects of impurity gradients on ion-temperature-gradient driven turbulence have been investigated. For impurity density n_{oI} with scale length $|L_{nI}|$, $\chi_i \rightarrow \chi_i A^2$ and $\Gamma_r \rightarrow \Gamma_r A^3$ where $A = \left[1 + Z\left(n_{oI}/n_{oi}\right)\left(L_{ni}/L_{nI}\right)\right]^{-1}$. Thus impurity distributions peaked on axis heal η_i-mode turbulence while distributions peaked at the edge enhance it. In particular, the enhancement of Γ_r may underlie the density profile steepening observed during the "Z-mode" of the ISX-B tokamak.

In this chapter, a sheared slab model of ion-temperature-gradient-driven turbulence was used in order to elucidate the basic physics and phenomenological consequences in a simple and clear fashion. Although little change in the basic conclusions is to be expected, the theory can be applied to the toroidal branch of the η_i-mode using the large-n ballooning representation. This will be discussed in a future publication.

CHAPTER 3. DYNAMICS OF MAGNETIC RELAXATION IN CURRENT-CARRYING PLASMA

3.1 Introduction

Recent experimental results[35,36,37,38] from several Reversed Field Pinch (RFP) experiments have indicated the correlation of the observed structure and level of macroscopic magnetic fluctuations with anomalous thermal transport in the core region, and with field reversal maintenance (dynamo). Typically, the dominant observed magnetic fluctuations have poloidal mode number m=1, toroidal mode number $10 < n < 20$, with relatively broad frequency width $\Delta\omega \sim S^{-1/3}$($S = \tau_R/\tau_A$ is the magnetic Reynolds number). Because the magnetic field structure in RFP equilibrium is almost totally generated by plasma current and the safety factor $q(r)$ decreases monotonically in radius with the maximum value of 0.1 at the magnetic axis, it is widely believed that current-gradient driven modes, such as the kink-tearing mode, are responsible for driving magnetic fluctuations and the resulting anomalous thermal losses associated with magnetic turbulence.

Previous theoretical investigations,[39,40] either analytical or computational, have assumed that a spectrum of m=1 modes, with $10 < n < 20$ and resonant surfaces within the reversal surface (see Fig. 3.1), are due to tearing modes which are destabilized by resistive diffusion of the equilibrium magnetic configuration away from a minimum energy Taylor state.[41]

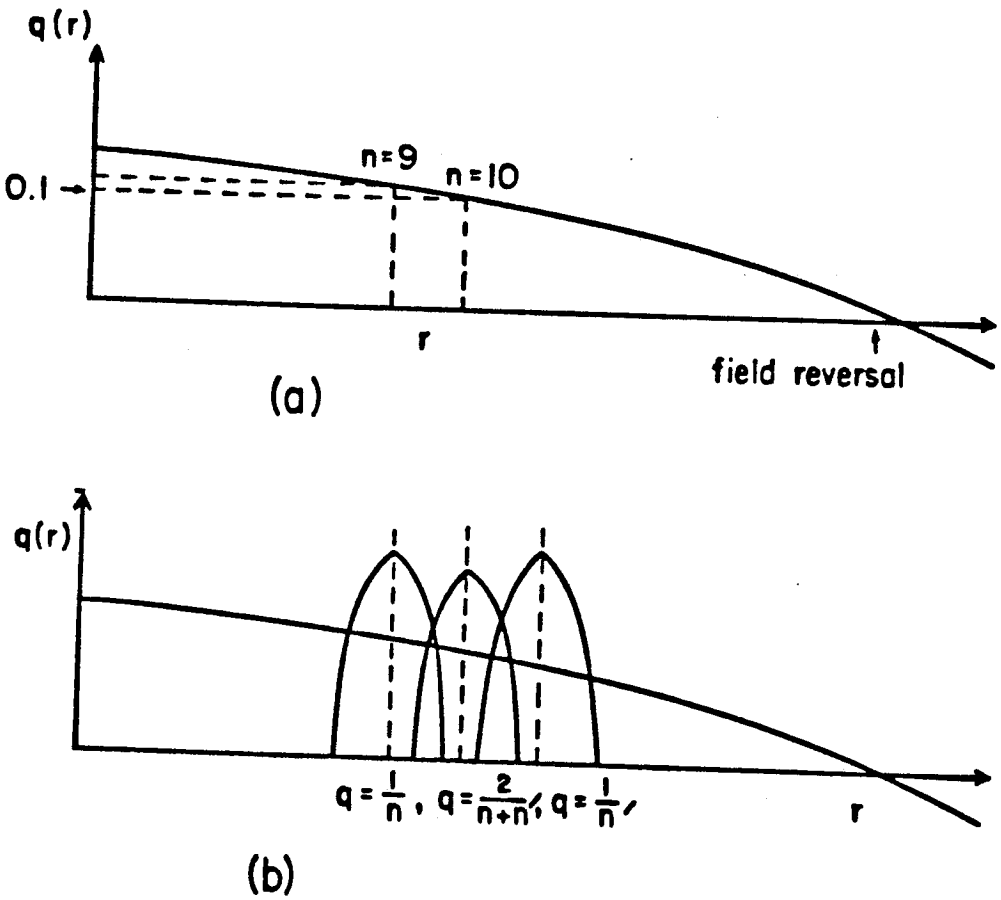

Fig. 3.1 (a) RFP q(r)-profile with location of resonances (not to scale). (b) Location of primary ($m = 1$) and nonlinearly driven ($m = 2$) modes (not to scale).

These investigations have studied m=1 tearing instabilities using the resistive magnetohydrodynamic (MHD) equations. The results of the nonlinear theory of resistive tearing mode turbulence are discussed in detail by An et al., in Ref. 40. In that investigation, reduced resistive MHD equations for RFP plasmas have been used to obtain Fourier mode coupling equations and renormalized turbulence theory was applied to derive spectral equations. Solution of these spectral equations yielded the saturation level of magnetic fluctuations $(\delta B_r/B_0)_{\rm rms} \sim S^{-1/3}$, which compared favorably with experimental observations. For the case of dynamo activity, the quasilinear theory has been used to estimate the average electric field $\left\langle \tilde{v} \times \tilde{B} \right\rangle$, induced by m=1 mode turbulence. The magnetic fluctuation level required to maintain field-reversal against resistive diffusion was calculated and has been shown to be consistent with the calculated saturation level of m=1 turbulence which has been previously been mentioned.

Although the resistive MHD study of m=1 tearing mode turbulence has been shown to be consistent with experimental observations, there several weak points in analyses using approximations involving use of linear growth-rate in estimation of the driving source and of the relaxation time sale of the average magnetic flux $\langle\psi\rangle$. This approximation is frequently dubious. Also, there is practical interest in checking the validity of the predicted scaling with the magnetic Reynolds number (S) for the proposed high temperature, high current experiment.

In this chapter, a generalized nonlinear theory of the turbulent dynamo and magnetic relaxation is proposed, using the plasma model of semi-collisional fluid equations. This model supports tearing modes, and has all basic features of the reduced MHD model.[42,43] The theory addresses the direct connection between configuration evolution and fluctuation evolution through

the flux transport term $\left\langle (\nabla_\perp \tilde{p})\tilde{\psi} \right\rangle$. For tearing modes in the semi-collisional regime, the fluid equations consist of Ohm's law for $\tilde{\psi}$, the equation of motion for vorticity $\nabla_\perp^2 \tilde{\phi}$ and the equation of state for $\tilde{p}_e$. Using this set of equations, the evolution equations for the three energy-like integrals $E^M = \frac{1}{2}\int d^3x \left|\nabla_\perp \tilde{\psi}\right|^2$, $E^K = \frac{1}{2}\int d^3x \left|\nabla_\perp \tilde{\psi}\right|^2$ and $E^I = \frac{1}{2\alpha}\int d^3x \left|\tilde{p}\right|^2$ are derived. Along with the steady-state condition for energy evolution, the renormalized one-point equation is used to identify saturation mechanisms, one of which is the stabilizing Alfvénic effect due to the stress that magnetic turbulence exerts on the fluid motion. A physical interpretation of the saturation mechanism is that the multiple helicity interaction of neighboring m=1's with stable ($\Delta' < 0$), driven m=2's generates a nonlinear $\vec{J} \times \vec{B}$ force which stabilizes the m=1 mode by opposing the growth of m=1 fluid motion. Note that this saturation mechanism is the same as in the resistive MHD study of Ref. 40.

In order to obtain a quantitative estimate of the saturation m=1 fluctuation levels, the renormalized spectral equations for semi-collisional regime are derived. Noting the direct relationship between the source of fluctuation with the flux transport process, the two-point theory is used to determine the relaxation time of $\left\langle (\nabla_\perp \tilde{p})\tilde{\psi} \right\rangle$ correlation by treating the $\tilde{\psi}$ and $\tilde{p}$ equations on an equal footing. This relaxation time τ_{cl} is shown to provide the crucial phase shift between $\tilde{v}_r$ and $\tilde{\psi}$ in the source of fluctuation energy. Hence, this approach enables us to formulate theory without depending on linear growth-rate for the phase-shift and the relaxation time.

To address the dynamics of magnetic configuration evolution, this approach connects the magnetic energy evolution with configuration evolution by the equilibrium magnetic energy evolution equation

$$\frac{\partial E^M_{eq}}{\partial t} = -\int dx \langle J_0 \rangle' \left\langle (\nabla_\perp \tilde{p})\tilde{\psi} \right\rangle$$

and the average magnetic flux equation

$$\frac{\partial \langle \psi \rangle}{\partial t} = -\frac{\partial}{\partial r} \left\langle (\nabla_\perp \tilde{p})\, \tilde{\psi} \right\rangle .$$

Hence, the evolution of the $\left\langle (\nabla_\perp \tilde{p})\tilde{\psi} \right\rangle$ correlation determines not only the source of fluctuations but the connection between magnetic energy relaxation and configuration evolution.

In this chapter, the theory of current-gradient-driven m=1 tearing mode turbulence is presented. The principal results are:

(i) A set of fluid equations for a tearing mode in the semi-collisional regime is derived and is used to investigate current gradient driven m=1 magnetic turbulence in RFP. Using a standard iterative closure scheme, the renormalized spectral equations are derived and the stabilizing Alfvénic effects associated with the progressive current filamentation process (cascade) are identified as the saturation mechanism.

(ii) In order to calculate the source of fluctuation energy in the spectral energy equation without approximating the driving term by the linear growth rate, the two-point correlation equation for $\left\langle (\nabla_\perp \tilde{p})\tilde{\psi} \right\rangle$ is derived and the characteristic time scale τ_{cl} is calculated. The relaxation time τ_{cl} is shown to approach the Alfvénic eddy turnover time, asymptotically.

(iii) Using the relaxation time τ_{cl} of the two-point $\left\langle (\nabla_\perp \tilde{p})\tilde{\psi} \right\rangle$-correlation for the phase-shift between $\tilde{v}_r$ and $\tilde{\psi}$ in the source function, the source of fluctuation is calculated and the direct relationship between fluctuation evolution and configuration evolution is identified. The dynamical processes in the two separate

regions of kink-tearing mode activity, i.e., the resonant region ($k_{||} \rightarrow 0$) and the exterior region ($\vec{B} \cdot \nabla J \rightarrow 0$), are explored and the calculated magnetic fluctuation level is shown to be independent of, or very weakly dependent on the magnetic Reynolds number S. Thus, dynamo related heat transport even in the high temperature regime, is predicted. However, this magnetic fluctuation will provide the dynamo mechanism for sustaining the stable magnetic configuration in future experiments.

The remainder of this chapter is organized as follows. In Sec. 3.2, the fluid model equations are derived and the energy flow and energy balance are discussed using the evolution of three energy-like integrals. In Sec. 3.3-A, a saturation mechanism is discussed using renormalized one-point equations. In Sec. 3.3-B, a generalized nonlinear theory of the turbulent dynamo and magnetic relaxation is proposed noting the relation between these two dynamical processes through the turbulent transport of magnetic flux. The resulting relaxation time τ_{cl} is calculated and the fluctuation level is estimated. Sec. 3.4 includes the summary and conclusions.

3.2 Model

In previous work, the behavior of current gradient driven instabilities in the reversed field pinch (RFP) was studied using the resistive MHD equations. Here, we derive the set of fluid equations for the evolution of the kink-tearing modes for a high temperature RFP. The understanding of the kink-tearing evolution can also be utilized for basic studies of magnetic relaxation of current-carrying plasma (e.g., dynamo).

Although the global magnetic configuration of an RFP plasma differs from that of a tokamak plasma, the core region of an RFP plasma, where the magnetic fluctuations due to kink-tearing modes are resonant, can be modeled as a locally straight and strong magnetic field (i.e., $\vec{B} = \nabla \tilde{A}_{\|} \times \hat{n}$), with exterior properties accounted for global constraint parameters, such as Δ', etc. To simplify the analysis by constructing an analytically tractable model of the nonlinear evolution of kink-tearing modes in an RFP, we consider reduced fluid equations which have been used to describe tokamak plasmas. These reduced fluid equations[44,45,46,47] have been derived by many authors in the context of various specific problems. Here, we introduce the fluid equations to describe the evolution of kink-tearing modes in the core of an RFP. Using conventional normalizations in the literature, we introduce a dimensionless form of the evolution equations where spatial scales are in units of a (the poloidal dimension) and temporal scales are in units of τ_A (the Alfvén time). We thus obtain the basic set of dimensionless equations from Ohm's law, the equation of motion (vorticity) and the equation of state (pressure), which yield:

$$\frac{\partial}{\partial t}\tilde{\psi} + \nabla_\perp(\tilde{\phi}+\tilde{p}) \times \hat{z} \cdot \nabla_\perp \tilde{\psi} + v_D \nabla_y \tilde{\psi} = -\nabla_{\|}^{(0)}(\tilde{\phi}+\tilde{p}) + \eta \nabla_\perp^2 \tilde{\psi} \qquad (114)$$

$$\begin{aligned}\frac{\partial}{\partial t}(\nabla_\perp^2 \tilde{\phi}) + \nabla_\perp(\tilde{\phi}-\tilde{p}) \times \hat{z} \cdot \nabla_\perp(\nabla_\perp^2 \tilde{\phi}) - v_D \nabla_y(\nabla_\perp^2 \tilde{\phi}) \\ = -\nabla_{\|}^{(0)} \tilde{J} + \nabla \tilde{\psi} \times \hat{z} \cdot \nabla \tilde{J} + \nabla_y \tilde{\psi} \langle J_0 \rangle' \end{aligned} \qquad (115)$$

$$\frac{\partial}{\partial t}\tilde{p} + \nabla_\perp \tilde{\phi} \times \hat{z} \cdot \nabla \tilde{p} - v_D \nabla_y \tilde{\phi} = \alpha \left(\nabla_{\|}^{(0)} \tilde{J} - \nabla_\perp \tilde{\psi} \times \hat{z} \cdot \nabla \tilde{J} - \nabla_y \tilde{\psi} \langle J_0 \rangle' \right) \qquad (116)$$

with Ampère's law

$$\tilde{J} = \nabla_\perp^2 \tilde{\psi}, \qquad (117)$$

where $\tau_A = a/v_A$, $\tau_R = (4\pi a^2/c^2\eta), v_D = \frac{d}{dr}\hat{P}_0$, $\eta = \frac{\tau_A}{\tau_R}, \alpha = \frac{\rho_s^2}{a^2}$, $\langle J_0\rangle' = \frac{d}{dr}\langle J_0\rangle$ and $\nabla_{\|}^{(0)} = \left\langle \hat{b} \right\rangle \cdot \vec{\nabla}$. Here $\tilde{\psi} = -A_z/(a\langle B\rangle)$ is the perturbed parallel vector potential, $\left\langle \vec{B} \right\rangle$ is the average magnetic field vector, $\tilde{\phi} = -c\Phi/(v_A a\langle B\rangle)$ is the electrostatic potential (the fluid stream function) and $\tilde{p} = \left(\frac{\beta}{2\Omega_{ci}\tau_A}\right)\tilde{n}(x)/\langle n_0\rangle$ is the perturbed electron pressure with $\beta = \frac{8\pi T_0 n_0}{\langle B\rangle^2}$. For simplicity, we only consider the case of isotropic, isothermal electron response with constant temperature (i.e., $T_e = T_0$), neglect parallel ion motion in Ohm's law and ignore ion pressure fluctuations. All fluctuating fields are expanded in toroidal (n) and poloidal (m) harmonics, so that

$$\vec{k}\cdot\left\langle \vec{B} \right\rangle = k_{\|} = (\langle B_\theta\rangle/r)(m - nq(r)) \simeq -(\langle B_\theta\rangle/r)(nq'x).$$

In order to understand the nonlinear process of magnetic relaxation, it is essential to examine the energetics of the system. The energy flow and energy balance can be elucidated by consideration of energy-like integrals quadratic in the fluctuating fields. These energy-like integrals are defined by the magnetic energy,

$$E^M = \frac{1}{2}\int d^3x \left|\nabla_\perp \tilde{\psi}\right|^2, \tag{118}$$

the kinetic energy

$$E^K = \frac{1}{2}\int d^3x \left|\nabla_\perp \tilde{\phi}\right|^2, \tag{119}$$

and the internal energy

$$E^I = \frac{1}{2\alpha}\int d^3x |\tilde{p}|^2. \tag{120}$$

Using the evolution equations, Eqs. (114)-(117), these energy-like integrals can readily be shown to satisfy the following relations

$$\frac{\partial}{\partial t}E^M = \int d^3x \left\{\tilde{J}\nabla_{\|}^{(0)}(\tilde{\phi}+\tilde{p}) - \eta|\tilde{J}|^2 + \left\langle \tilde{J}\nabla_\perp(\tilde{\phi}+\tilde{p})\times\hat{z}\cdot\nabla\tilde{\psi}\right\rangle\right\} \tag{121}$$

$$\frac{\partial}{\partial t}E^K = \int d^3x \left\{ \tilde{\phi}\nabla_{\parallel}^{(0)}\tilde{J} - \left\langle \tilde{\phi}\nabla_{\perp}\tilde{\psi} \times \hat{z}\cdot\nabla\tilde{J} \right\rangle - \left\langle \tilde{\phi}\nabla_y\tilde{\psi} \right\rangle \langle J_0\rangle' \right\} \tag{122}$$

$$\frac{\partial}{\partial t}E^I = \int d^3x \left\{ \tilde{p}\nabla_{\parallel}^{(0)}\tilde{J} - \left\langle \tilde{p}\nabla_{\perp}\tilde{\psi} \times \hat{z}\cdot\nabla\tilde{J} \right\rangle - \left\langle \tilde{p}\nabla_y\tilde{\psi} \right\rangle \langle J_0\rangle' + \frac{v_D}{\alpha}\left\langle \tilde{p}\nabla_y\tilde{\phi} \right\rangle \right\}. \tag{123}$$

Hence, the total energy of the system evolves according to

$$\frac{\partial}{\partial t}E = -\int d^3x \left[\left\langle (\tilde{\phi}+\tilde{p})\nabla_y\tilde{\psi} \right\rangle \langle J_0\rangle' - \frac{v_D}{\alpha}\left\langle \tilde{p}\nabla_y\tilde{\phi} \right\rangle + \eta|\tilde{J}|^2 \right]. \tag{124}$$

These evolution equations state that the coupling terms $\tilde{J}\nabla_{\parallel}^{(0)}\tilde{\phi}$ and $\tilde{J}\nabla_{\parallel}^{(0)}\tilde{p}$ account for transfer of fluctuation energy between fields. Hence the sum is conserved up to the difference of kink-drive by current-gradient ($\left\langle (\tilde{\phi}+\tilde{p})\nabla_y\tilde{\psi} \right\rangle \langle J_0\rangle'$) and resistive dissipation ($\eta|\tilde{J}|^2$). In the saturated state, nonlinear processes (i.e., $\left\langle \tilde{J}\nabla_{\perp}(\tilde{\phi}+\tilde{p}) \times \hat{z}\cdot\nabla\tilde{\psi} \right\rangle$ and $\left\langle (\tilde{\phi}+\tilde{p})\nabla_{\perp}\tilde{\psi} \times \hat{z}\cdot\nabla\tilde{J} \right\rangle$) dynamically regulate the balance of input from the current-gradient free-energy source with the resistive dissipation. Naturally, a stationarity of total energy is a necessary condition for saturation (i.e., $(\partial/\partial t)E = 0$). In the total-energy equation, there is one other source term from density-gradient (i.e., $v_D\left\langle \tilde{p}\nabla_y\tilde{\phi} \right\rangle$), however, for simplicity density gradient drive is ignored.

3.3 Dynamics of Magnetic Relaxation

In this section, the analytic theory of multiple-helicity nonlinear interaction of tearing modes in (spatially) densely-packed turbulence (i.e., the $\vec{k}\cdot\vec{B}_0 = 0$ surface falls in or near the small-$k''_{||}$ inertial interior region of the driven fluctuation), and a generalized nonlinear theory of the turbulent dynamo and energy dynamics in a high-temperature current-carrying plasma are presented.

A. Theory of multiple-helicity nonlinear interaction of tearing modes

In the RFP, where the safety factor $q(r)$ decreases monotonically with radius, a spectrum of m=1 tearing modes, with $10 < n < 20$ and resonant surfaces within the reversal surface, are destabilized by resistive diffusion of the magnetic configuration away from a Taylor minimum energy state. This results in the formation of magnetic islands. Due to the proximity of neighboring rational surfaces, where $q(r_1) = 1/n$ and $q(r_2) = 1/(n+1)$, respectively, the islands overlap for fluctuation levels of $(\delta B_r/B_0)_{m=1} \simeq \varepsilon/(n^2 r q') \sim \varepsilon^2$ where $\varepsilon = a/R$, the inverse aspect ratio. For the inverse aspect ratio $\varepsilon \sim 1/4$ of existing and proposed RFP-devices, island overlap occurs at fluctuation levels less than that which are observed. Thus, strong multiple-helicity nonlinear mode interactions, which generate turbulence and magnetic field line stochasticity, occur throughout the RFP core.

As a consequence of the nonlinear interaction of the islands formed at r_1 and r_2, an m=2, n'=2n+1 current sheet and island are resonantly driven. The m=2, n'=2n+1 mode is linearly stable ($\Delta'_{m=2} < 0$) and is further stabilized by flattening of the equilibrium current gradient by (global) m=1 modes. Thus, the driven (stable) m=2 modes nonlinearly absorb energy from the linearly unstable primary m=1 modes, which saturate when the rate of coupling of

energy to m=2 balances the rate of equilibrium magnetic energy release by m=1 modes. This progressive current filamentation process (cascade) continues with the generation of $m \geqq 3$, and eventually terminates when the driving energy (tapped through m=1 modes) is resistively dissipated at small scales and depleted by quasilinear profile modification.

These phenomena were previously analyzed theoretically using renormalized spectral equations based on resistive MHD equations. In these works, the conventional reduced resistive MHD equations were adopted by observing that the region of resonant tearing mode interactions can be modeled as locally strong straight magnetic fields (effectively, a sheared slab), with exterior properties accounted for by constraint parameters, such as Δ', etc. The renormalized turbulence theory based on resistive MHD predicted the rms m=1 magnetic fluctuation level at saturation to be $(\delta B/B_0)_{\rm rms} \simeq (\gamma_{m=1}\tau_A)/|\Delta'_{m=2}a|^{1/2}$ with $\gamma_{m=1}\tau_A \sim S^{-1/3}$, and the resulting electron thermal conductivity (collisionless) due to magnetic field line stochasticity $\chi_{E_e} \sim (0.01)v_{\rm th,e}aS^{-2/3}$ where $v_{\rm th,e}$ is the electron thermal velocity.[48] These results are in reasonable agreement with experimental observations of frequency widths $\Delta\omega \sim S^{-1/3}$ of m=1 modes and of temperature scaling with current.

In order to extend the renormalized turbulence theory into regimes of proposed high temperature, high current RFP plasmas, it is necessary to consider the roles diamagnetic effects and thermal force effects in the nonlinear evolution and saturation of m=1 tearing modes. The basic model equations, Eqs. (114)-(117), can be used to investigate these effects in the context of tearing modes. In this chapter, for further simplicity, we examine only the semi-collisional regime of tearing modes while neglecting electrostatic potential effects. For the linear evolution of semi-collisional drift-tearing modes $(k_\parallel^2 v_{\rm th,e}^2 > \omega\nu_{ei})$, the ion Larmor radius tends to be larger than the resistive

layer width $\left(\rho_s > \Delta_D \simeq |\omega\nu_{ei}|^{1/2} / \left(k'_{\|} v_{\mathrm{th,e}}\right)\right)$ and the electrostatic part of the parallel electric field can be ignored ($k_{\|}\tilde{\phi} \ll \omega\tilde{A}_{\|}$) in the region of large $\tilde{J}_{\|}$.[49] Even though the electrostatic potential effects on the nonlinear evolution of m=1 modes are not rigorously established as negligible, we will omit $\tilde{\phi}$ from our basic model in this investigation. The electrostatic potential effects will be discussed in a future publication.

With these assumptions, the dynamics of m=1 tearing modes in the semi-collisional regime can be most easily understood using the equations for parallel component of vector potential (Ohm's law) and perturbed pressure, which can be written as:

$$\frac{\partial}{\partial t}\tilde{\psi} + \nabla_{\perp}\tilde{p} \times \hat{z} \cdot \nabla\tilde{\psi} + v_D \nabla_y \tilde{\psi} = -\nabla_{\|}^{(0)}\tilde{p} + \eta\nabla_{\perp}^2\tilde{\psi} \tag{125}$$

$$\frac{\partial}{\partial t}\tilde{p} = \alpha\left(\nabla_{\|}^{(0)}\tilde{J} - \nabla_{\perp}\tilde{\psi} \times \hat{z} \cdot \nabla\tilde{J} - \nabla_y\tilde{\psi}\,\langle J_0\rangle'\right). \tag{126}$$

It is important to note that these model equations include all the basic conceptual features of incompressible MHD, while addressing high temperature effects. It is easy to show that m=1 modes in this model are unstable and driven by Δ' (magnetic free-energy) with growth rate $\gamma^{\ell} \sim S^{-1/3}$.[50] The evolution of energy-like integrals has the same structure as Eqs. (121)-(124) and total fluctuation energy is conserved up to the difference of kink-drive $\left(\left\langle\tilde{p}\nabla_y\tilde{\psi}\right\rangle\langle J_0\rangle'\right)$ and resistive dissipation ($\eta|\tilde{J}|^2$).

Now, we consider the nonlinear evolution of densely-packed, fully developed, multiple-helicity tearing mode turbulence using Eqs. (125)-(126). This set of nonlinear equations can be analyzed by renormalizing the nonlinearities using standard iterative substitution techniques.[51] Here, we present both the one-point theory (propagator calculation) and the accompanying physical picture of saturation, and the two-point theory of the spectra and quantitative estimation of saturated fluctuation levels.

Fourier transforming Eqs. (125)-(126) in the y and z directions, the nonlinear evolution equations for the test mode $(\vec{k})$ can be written as

$$\frac{\partial}{\partial t}\tilde{\psi}_{\vec{k}} + i\omega_*\tilde{\psi}_{\vec{k}} + \left\{\left[\frac{\partial}{\partial x}\left(\sum_{\vec{k}'}(-ik'y)\tilde{p}_{\vec{k}'}\tilde{\psi}_{\vec{k}''}\right) - ik_y\sum_{\vec{k}'}\frac{\partial\tilde{p}_{-\vec{k}'}}{\partial x'}\tilde{\psi}_{\vec{k}''}\right] - \left[\frac{\partial}{\partial x}\left(\sum_{\vec{k}'}(-ik'_y)\tilde{\psi}_{-\vec{k}'}\tilde{p}_{\vec{k}''}\right) - ik_y\sum_{\vec{k}'}\frac{\partial\tilde{\psi}_{-\vec{k}'}}{\partial x'}\tilde{p}_{\vec{k}''}\right]\right\} = -ik_\parallel\tilde{p}_{\vec{k}} + \eta\tilde{J}_{\vec{k}} \tag{127}$$

$$\frac{1}{\alpha}\frac{\partial}{\partial t}\tilde{p}_{\vec{k}} = -ik_\parallel\tilde{J}_{\vec{k}} - ik_y\langle J_0\rangle'\tilde{\psi}_{\vec{k}} - \left\{\left[\frac{\partial}{\partial x}\left(\sum_{\vec{k}'}(-ik'_y)\tilde{\psi}_{-\vec{k}'}\tilde{J}_{\vec{k}''}\right) - ik_y\sum_{\vec{k}'}\frac{\partial\tilde{\psi}_{-\vec{k}'}}{\partial x'}\tilde{J}_{\vec{k}''}\right] - \left[\frac{\partial}{\partial x}\left(\sum_{\vec{k}''}(-ik'_y)\tilde{J}_{\vec{k}'}\tilde{\psi}_{\vec{k}''}\right) - ik_y\sum_{\vec{k}'}\frac{\partial\tilde{J}_{\vec{k}'}}{\partial x'}\tilde{\psi}_{\vec{k}''}\right]\right\} \tag{128}$$

where $\vec{k} = (k_y, k_z)$ and the driven mode is $\vec{k}'' = \vec{k} + \vec{k}'$, with $\vec{k}'$ representing the background mode. To obtain renormalized equations, a standard weak coupling closure approximation is used to renormalize the nonlinearities by iteratively substituting the nonlinearly driven fields $\tilde{p}^{(2)}_{\vec{k}''}$, $\tilde{\psi}^{(2)}_{\vec{k}''}$ and $\tilde{J}^{(2)}_{\vec{k}''}$ for $\tilde{p}_{\vec{k}''}$, $\tilde{\psi}_{\vec{k}''}$ and $\tilde{J}_{\vec{k}''}$, respectively. Here $\tilde{p}^{(2)}_{\vec{k}''}$, $\tilde{\psi}^{(2)}_{\vec{k}''}$ and $\tilde{J}^{(2)}_{\vec{k}''}$ are nonlinearly driven by the direct beating of the test $(\vec{k})$ and background $(\vec{k}')$ modes. These driven fields satisfy the equations

$$\left(\Delta\omega_{\vec{k}''} + i\omega''_*\right)\tilde{\psi}^{(2)}_{\vec{k}''} + ik''_\parallel\tilde{p}^{(2)}_{\vec{k}''} - \eta\tilde{J}^{(2)}_{\vec{k}''} = S_\psi \tag{129}$$

$$\Delta\omega_{\vec{k}''}\tilde{p}^{(2)}_{\vec{k}''} - ik''_\parallel\alpha\tilde{J}^{(2)}_{\vec{k}''} + ik''_y\alpha\langle J_0\rangle'\tilde{\psi}^{(2)}_{\vec{k}''} = -\alpha S_J \tag{130}$$

where S_ψ and S_J are the sources for the driven mode ($\vec{k}''$) and are given by

$$S_\psi = -\left[ik_y\tilde{p}_{\vec{k}'}\frac{\partial\tilde{\psi}_{\vec{k}}}{\partial x} - ik_y\frac{\partial\tilde{p}_{\vec{k}'}}{\partial x'}\tilde{\psi}_{\vec{k}} + ik_y\tilde{p}_{\vec{k}}\frac{\partial\tilde{\psi}_{\vec{k}'}}{\partial x'} - ik_y'\frac{\partial\tilde{p}_{\vec{k}}}{\partial x}\tilde{\psi}_{\vec{k}'}\right] \tag{131}$$

$$S_J = \left[ik_y'\tilde{\psi}_{\vec{k}'}\frac{\partial\tilde{J}_{\vec{k}}}{\partial x} - ik_y\frac{\partial\tilde{\psi}_{\vec{k}'}}{\partial x'}\tilde{J}_{\vec{k}} + ik_y\tilde{\psi}_{\vec{k}}\frac{\partial\tilde{J}_{\vec{k}'}}{\partial x'} - ik_y'\frac{\partial\tilde{\psi}_{\vec{k}}}{\partial x}\tilde{J}_{\vec{k}'}\right] \tag{132}$$

where $\Delta\omega_{\vec{k}''}$ is the decorrelation rate for test and background modes, and thus serves to limit the time scale of nonlinear interaction. These driven, coupled equations can be solved for $\tilde{\psi}^{(2)}_{\vec{k}''}$ and $\tilde{p}^{(2)}_{\vec{k}''}$ in the case of densely packed, fully developed turbulence. The expression for driven current $\tilde{J}^{(2)}_{\vec{k}''}$ is given by

$$\tilde{J}^{(2)}_{\vec{k}''} = \sigma_*(x)\tilde{\psi}^{(2)}_{\vec{k}''} + S(x) \tag{133}$$

where the semi-collisional conductivity is

$$\sigma_*(x) = 1\Big/\left[\bar{x}_R^2\left(1+\frac{x^2}{W_c^2}\right)\right] \tag{134}$$

and the source function is

$$S(x) = \left[-\sigma_*(x)\left\{i\alpha\left[k_\parallel'\Big/\Delta\omega_{\vec{k}''}\left(\Delta\omega_{\vec{k}''}+i\omega_*''\right)\right]S_J + S_\psi\Big/\left(\Delta\omega_{\vec{k}''}+i\omega_*''\right)\right\}\right]. \tag{135}$$

Here, x refers to x'' (the distance from the $\vec{k}''\cdot\vec{B}_0 = 0$ surface), $\bar{x}_A^2 = \left[\Delta\omega_{\vec{k}''}\left(\Delta\omega_{\vec{k}''}+i\omega_*''\right)\Big/(k_y''/L_s)^2\right]$ (local shear-Alfvén width), $\bar{x}_R^2 = \eta/\left[\Delta\omega_{\vec{k}'}+i\omega_*''\right]$ (resistive skin-depth) and $W_c^2 = \left[\bar{x}_R^2\bar{x}_A^2\right]/\alpha$ (semi-collisional current channel width). A solution of Eq. (133) can be constructed from Ampère's law, Eq. (117), with the tearing ordering $k_x^2 > k_y^2$. Then, Eq. (133) can be rewritten as

$$\mathcal{L}\tilde{\psi}^{(2)}_{\vec{k}''} = S(x) \tag{136}$$

where the differential operator is given by

$$\mathcal{L} = \frac{d^2}{dx^2} - \sigma_*(x). \tag{137}$$

This equation is known as the Gegenbauer equation and has the associated Legendre function as a solution. The homogeneous solution is given by

$$\tilde{\psi}_h = a\left[zP_\nu(z) - P_{\nu-1}(z)\right] + b\left[zQ_\nu(z) - Q_{\nu-1}(z)\right] \tag{138}$$

where P_ν and Q_ν are Legendre functions in the complex plane with $z = i\,x/W_c$ and $\nu(\nu+1) = (\bar{x}_A^2/\alpha)$. The constants a and b can be determined by imposing the boundary condition that $\tilde{\psi}^{(2)}_{\vec{k}''}$ smoothly match the driven, exterior Newcomb solution (kink-mode) as x'' becomes large. This requires that, for $\partial^2\tilde{\psi}^{(2)}_{\vec{k}''}/\partial x^2 = \tilde{J}^{(2)}_{\vec{k}''}$,

$$\Delta'\psi_0 = \int_{-\infty}^{\infty} dx \tilde{J}^{(2)}_{\vec{k}''} \tag{139}$$

where ψ_0 is defined by the condition that for large x, $\psi \to \psi_0 + \psi'_{\pm}x$ with $\Delta' = (\psi'_+ - \psi'_-)/\psi_0$. In this problem, it will be shown that $\psi_0 = \psi(0)$. By imposition of these boundary conditions, it is tacitly assumed that the driven $\vec{k}''$ fluctuations have the basic structure of kink-tearing modes. With boundary condition, the general solution can be determined assuming the sources (S_ψ and S_J) are approximately constant in x within the inner layer, and by neglecting the term in the source which breaks the tearing-mode parity. Then, the general solution is given (approximately) by

$$\tilde{\psi}^{(2)}_{\vec{k}''} = \frac{S_\psi}{\left[\Delta\omega_{\vec{k}''} + i\omega''_*\right]}\left\{1 + \Delta'\frac{g(x)}{\pi W_c}\right\} \tag{140}$$

where

$$g(x) = \frac{\pi W_c}{2i}\left[zP_\nu(z) - P_{\nu-1}(z)\right]. \tag{141}$$

By recalling the definition of ψ_0, straightforward algebra yields:

$$\psi_0 = S_\psi / \left[\Delta\omega_{\vec{k}''} + i\omega''_*\right] \tag{142}$$

for $\left|\bar{x}_A^2/\alpha\right| \ll 1$. Hence, the driven flux $\tilde{\psi}_{\vec{k}''}^{(2)}$ satisfies the boundary condition of Eq. (139). Using Ampère's law, the localized driven current can be determined by

$$\tilde{J}_{\vec{k}''}^{(2)} \simeq \frac{S_\psi}{\left[\Delta\omega_{\vec{k}''} + i\omega_*''\right]} \frac{\left(\frac{\Delta'}{\bar{x}_R^2}\right)\left[\frac{g(x)}{\pi W_c}\right]}{\left[1 + \frac{x^2}{W_c^2}\right]}. \tag{143}$$

For small current-channel width, $W_c^2 \to 0$, it is straightforward to verify

$$\lim_{W_c \to 0} \frac{[g(x)/\pi W_c]}{\left[1 + \frac{x^2}{W_c^2}\right]} \simeq c\delta(x) \tag{144}$$

where c is a constant obtained from the function $g(x)$. Finally, substitution of $\tilde{\psi}_{\vec{k}''}^{(2)}$ and $\tilde{J}_{\vec{k}''}^{(2)}$ into Eq. (130) determines $\tilde{p}_{\vec{k}''}^{(2)}$, where

$$\tilde{p}_{\vec{k}''}^{(2)} \simeq \left(i\frac{S_\psi}{k_\parallel'}\right)\left(\frac{\Delta' g(x)}{W_c^2}\right) \frac{\left(\frac{1}{\pi W_c}\right) x}{\left[1 + \frac{x^2}{W_c^2}\right]}. \tag{145}$$

It is important to notice that the driven-density $\tilde{p}_{\vec{k}''}^{(2)}$ exists only within localized current-channel, i.e., $\lim_{W_c \to 0} \tilde{p}_{\vec{k}''}^{(2)} \sim x\delta(x)$. The physical reason behind this observation follows from the fact that $\vec{B} \cdot \nabla \tilde{J} \to 0$ for $\vec{k} \cdot \vec{B}_0 \neq 0$ in multiple-helicity interaction.

The results of the calculation of the nonlinearily driven fields in the densely packed turbulence model may be summarized as:

$$\tilde{\psi}_{\vec{k}''}^{(2)} = \frac{S_\psi}{\left[\Delta\omega_{\vec{k}''} + i\omega_*''\right]} \left\{1 + \Delta_{\vec{k}''}' \frac{g(x)}{\pi W_c}\right\} \tag{146}$$

$$\tilde{J}_{\vec{k}''}^{(2)} = \frac{S_\psi}{\left[\Delta\omega_{\vec{k}''} + i\omega_*''\right]} \left(\frac{\Delta_{\vec{k}''}'}{\bar{x}_R^2}\right) \frac{[g(x)/(\pi W_c)]}{\left[1 + \frac{x^2}{W_c^2}\right]} \tag{147}$$

and

$$\tilde{p}^{(2)}_{\vec{k}''} = i\left(\frac{S_\psi}{k'_\parallel}\right)\left(\frac{\Delta'_{\vec{k}''}g(x)}{W_c^2}\right)\frac{[x/(\pi W_c)]}{\left[1+\dfrac{x^2}{W_c^2}\right]} \approx 0 \tag{148}$$

where the Green's function $g(x)$ is given in Eq. (141). To derive these, terms which break the tearing parity of the test mode equation have been dropped. By examining the limit of small $\bar{x}_A$ and W_c, these driven mode solutions can be shown to match smoothly to the driven exterior solutions (kink). Even though this high temperature regime introduces one other spatial scale, namely the current-channel width W_c, the effects of driven modes on the test mode are similar to their resistive MHD counterparts which have been studied in Ref. 40.

The renormalized equations for semi-collisional modes are now constructed by substituting Eqs. (146)-(148) into Eqs. (127) and (128), requiring that the tearing parity of the test mode equation be maintained. Then, the renormalized equations with tearing mode ordering, $k_x > k_y$, are:

$$\frac{\partial}{\partial t}\tilde{\psi}_{\vec{k}} - \frac{\partial}{\partial x}D_{\vec{k}}\frac{\partial}{\partial x}\tilde{\psi}_{\vec{k}} + i\omega_*\tilde{\psi}_{\vec{k}} + ik_\parallel\tilde{p}_{\vec{k}} = \eta\tilde{J}_{\vec{k}} \tag{149}$$

and

$$\frac{1}{\alpha}\frac{\partial}{\partial t}\tilde{p}_{\vec{k}} + \frac{\partial}{\partial x}\mathcal{A}_{\vec{k}}\frac{\partial}{\partial x}\tilde{p}_{\vec{k}} = ik_\parallel\tilde{J}_{\vec{k}} - ik_y\left\langle J_0\right\rangle'\tilde{\psi}_{\vec{k}} \tag{150}$$

where

$$D_{\vec{k}} = \sum_{\vec{k}'}\frac{(k'_y)^2\left|\tilde{p}_{\vec{k}'}\right|^2}{\left[\Delta\omega_{\vec{k}''} + i\omega''_*\right]}\left[1+\Delta'_{\vec{k}''}\frac{g(x'')}{\pi W_c}\right] \tag{151}$$

$$\mathcal{A}_{\vec{k}} \cong \sum_{\vec{k}'}\frac{(k'_y)^2\left(1-\dfrac{n'^2}{n''^2}\right)\left|\tilde{\psi}_{\vec{k}'}\right|^2}{\left[\Delta\omega_{\vec{k}''} + i\omega''_*\right]}\left(\frac{\Delta'_{\vec{k}''}g(x'')}{\bar{x}_R^2}\right)\frac{[1/(\pi W_c)]}{\left[1+\dfrac{x^2}{W_c^2}\right]}. \tag{152}$$

Here, $D_{\vec{k}}$ is an anomalous Ohmic diffusivity due to diamagnetic fluid convection of magnetic flux. $\mathcal{A}_{\vec{k}}$ is a stabilizing (for negative $\Delta'_{\vec{k}''}$) Alfvén effect due to the

stress that magnetic turbulence exerts on the fluid motion. These terms have physical interpretations similar to their resistive MHD counterparts.

Although this renormalized one-point theory offers qualitative insights into saturation mechanism through evaluation of propagators, it is necessary to solve renormalized spectral energy equations to obtain spectra of the saturated m=1 fluctuations and to ensure the energy conservation. The magnetic and internal energy evolution equations can be derived using Eqs. (121) and (123), and the spectral equations are:

$$\frac{\partial}{\partial t}E^M_{\vec{k}} = -\int dx \tilde{J}_{-\vec{k}} k_\parallel \tilde{p}_{\vec{k}} - \eta \int dx \left|\tilde{J}_{\vec{k}}\right|^2 + \int dx \left\langle \tilde{J}\cdot\nabla\tilde{p} \times \tilde{b}\cdot\nabla\tilde{\psi}\right\rangle_{\vec{k}} \quad (153)$$

$$\frac{\partial}{\partial t}E^I_{\vec{k}} = i\int dx \tilde{p}_{-\vec{k}} k_\parallel \tilde{J}_{\vec{k}} - i\int dx \tilde{p}_{-\vec{k}} k_y \tilde{\psi}_{\vec{k}} \langle J_0\rangle' - \int dx \left\langle \tilde{p}\nabla\tilde{\psi}\times\hat{b}\cdot\nabla\tilde{J}\right\rangle_{\vec{k}}. \quad (154)$$

Defining the source term

$$S^0_{\vec{k}} = -\int dx \left\langle \tilde{p}_{-\vec{k}}\nabla_y\tilde{\psi}_{\vec{k}}\right\rangle \langle J_0\rangle', \quad (155)$$

the sink term

$$S^I_{\vec{k}} = \eta \int dx \left\langle \tilde{J}^2_{\vec{k}}\right\rangle \quad (156)$$

and nonlinear transfer (triplet) terms

$$T_{\vec{k}} = \int dx \left\langle \tilde{J}\cdot\nabla\tilde{p}\times\hat{b}\cdot\nabla\tilde{\psi}\right\rangle_{\vec{k}} - \int dx \left\langle \tilde{p}\cdot\nabla\tilde{\psi}\times\hat{b}\cdot\nabla\tilde{J}\right\rangle_{\vec{k}} \quad (157)$$

for wavenumber $\vec{k}$, the saturation condition for the mode $\vec{k}$ is given by

$$S^0_{\vec{k}} - S^I_{\vec{k}} + T_{\vec{k}} = 0. \quad (158)$$

Here, the triplets represent energy exchange between field and fluid and transfer in $\vec{k}$-space, and can be renormalized using a weak coupling closure as in the case of the one-point equations. The resulting renormalized triplets are:

$$T_{\vec{k}} = \int dx \sum_{\vec{k}'} \left(\frac{n^2}{n''^2}\right) \frac{\Delta'_{\vec{k}''} g(x'')}{\left[\Delta\omega_{\vec{k}''} + i\omega''_*\right]} \frac{(1/\pi W_c)}{\left[1 + \frac{x^2}{W_c^2}\right]}$$

$$\cdot \left\{ (k'_y)^2 \left|\tilde{p}_{\vec{k}'}\right|^2 \left|\frac{\partial \tilde{\psi}_{\vec{k}}}{\partial x}\right|^2 + k_y^2 \left|\frac{\partial \tilde{p}_{\vec{k}'}}{\partial x'}\right|^2 \left|\tilde{\psi}_{\vec{k}}\right|^2 \right\}$$

$$- \int dx \sum_{\vec{p},\vec{q}}^{\Delta} \frac{\Delta'_{-\vec{p}-\vec{q}}\, g(x)}{\left[\Delta\omega_{-\vec{p}-\vec{q}} + i\omega_*\right]} \frac{(1/\pi W_c)}{\left[1 + \frac{x^2}{W_c^2}\right]} \left\{ p_y^2 \left|\tilde{p}_{\vec{p}}\right|^2 \left|\frac{\partial \tilde{\psi}_{\vec{q}}}{\partial x}\right|^2 + q_y^2 \left|\frac{\partial \tilde{p}_{\vec{p}}}{\partial x}\right|^2 \left|\tilde{\psi}_{\vec{q}}\right|^2 \right\}$$

$$+ \int dx \sum_{\vec{k}'} \left(1 - \frac{n'^2}{n''^2}\right) \frac{\Delta'_{\vec{k}''} g(x'')}{\left[\Delta\omega_{\vec{k}''} + i\omega''_*\right]} \frac{(1/\pi W_c)}{\left[1 + \frac{x^2}{W_c^2}\right]}$$

$$\times \left\{ (k'_y)^2 \left|\tilde{\psi}_{\vec{k}'}\right|^2 \left|\frac{\partial \tilde{p}_{\vec{k}}}{\partial x}\right|^2 + k_y^2 \left|\frac{\partial \tilde{\psi}_{\vec{k}'}}{\partial x'}\right|^2 \left|\tilde{P}_{\vec{k}}\right|^2 \right\}. \tag{159}$$

Here, the first and third terms in the renormalized triplets, represent coherent scattering to larger-m mode and the second term represents incoherent emission effects. Using the steady-state condition, Eq. (158), saturation of m=1 mode occurs when

$$- \int dx \sum_{n} \left\langle \tilde{p} \nabla_y \tilde{\psi} \right\rangle_{1,n} \langle J_0 \rangle' \simeq \int dx \sum_{n,n'} \left|\Delta'_{2,n+n'}\right| \frac{g(x'')}{\left[\Delta\omega_{\vec{k}''} + i\omega''_*\right]} \frac{(1/\pi W_c)}{\left[1 + \frac{x^2}{W_c^2}\right]}$$

$$\cdot \left\{ \left\langle (\nabla_y \tilde{\psi})^2 \right\rangle_{1,n'} \left\langle (\nabla_x \tilde{p})^2 \right\rangle_{1,n} \right\} \tag{160}$$

i.e., when coupling (by interaction with neighboring m=1 modes) to stable m=2 modes ($\Delta'_{2,n+n'} < 0$) balances growth due to $\langle J_0 \rangle'$ relaxation. This process can be interpreted as a result of the nonlinear $\vec{J} \times \vec{B}$ force in multiple-helicity turbulence which opposes linear driving forces of current-gradient free-energy source. The nonlinear decorrelation rate $\Delta\omega$ is determined by the

Alfvénic eddy-turnover time (associated with $A_{\vec{k}}$ of Eq. (152)) and the related nonlinear characteristic time depends on the m=1 fluctuation level, and is $\Delta\omega \sim (\delta B/B_0)_{\rm rms}/|\Delta_2' a|^{1/2}$. Here, $(\delta B/B_0)_{\rm rms}$ is the rms-value of the m=1 fluctuation level in the RFP core. In order to obtain a quantitative estimate of the saturated m=1 fluctuation level, however, it is necessary to evaluate the left-side of Eq. (159) which represents the relaxation of the current-gradient and is the source of fluctuation. The evaluation of the source requires a (nonlinear) calculation of the phase-shift between the fields $\tilde{p}$ and $\tilde{\psi}$ and the inclusion of the effect of quasilinear flattening of the current-gradient without an assumption of the (linear) growth rate in calculating the driving term.

In the next section, we will propose one answer for these difficult questions by observing the relationship between flux transport process in the equilibrium magnetic energy evolution and the source of fluctuation energy evolution. This relationship is consistent with experimental evidence which links 'dynamo' processes to m=1 kink-tearing mode evolution.

B. Generalized Nonlinear Theory of the Turbulent Dynamo and Magnetic Relaxation

Experimental evidence has linked 'dynamo events' (increases in $|\langle B_z \rangle|$ near the wall) in RFP to m=1 MHD activity. Due to the large radial extent of m=1 modes and their comparatively high fluctuation levels, m=1 tearing modes can induce significant magnetic field profile modification and affect the evolution of the average toroidal field $\langle B_z(r) \rangle$ and $q(0)$, the safety factor on axis in an RFP. For these reasons, the quasilinear theory of m=1 tearing mode evolution has been utilized to estimate the electric field $\left\langle \tilde{v} \times \tilde{B} \right\rangle$, induced by turbulence. The required m=1 fluctuation level for maintaining the magnetic field configuration (reversal) against resistive diffusion was cal-

culated and has the rms-value $(\delta B/B_0)_{\rm rms} \sim S^{-1/3}$ which is consistent with the resistive MHD prediction for m=1 fluctuation levels in steady-state turbulence. Although the quasilinear theory is qualitatively consistent with the nonlinear MHD predictions and experimental observations in small machines, implementation of the theory requires using the rather dubious approximation that the relaxation time-scale for the average flux $\langle\psi\rangle$ is given approximately by the linear growth rate γ^ℓ. This difficulty also arises in the determination of the saturation amplitude, where the driving term is approximated by linear growth-rate $\left(\text{i.e.,} -\int dx \left\langle \tilde{p}\nabla_y\tilde{\psi}\right\rangle_{\vec{k}} \langle J_0\rangle' \longrightarrow \gamma^\ell_{\vec{k}} E_{\vec{k}}\right)$. Hence, it should be emphasized that quasilinear theory alone does not sufficiently characterize the saturated state of m=1 turbulence and it is necessary to develop a generalized theory which accomodates the required dynamical features.

In view of the fact that global m=1 modes convert poloidal magnetic field energy (tapped at the mode resonance surface in the core) into the toroidal field energy, the dynamo process in RFP can be explained as a redistribution of magnetic energy and current density. Here, we propose another approach to evaluate the phase-shift between $\tilde{v}_r$ and $\tilde{\psi}$, which is crucial for evaluation of the relaxation time-scale, by constructing spectral equations for flux transport and energy evolution. The relationship between energy relaxation and the dynamo process can be seen more clearly by constructing the evolution equations for the equilibrium magnetic energy and average magnetic flux, i.e.,

$$\frac{\partial}{\partial t} E^M_{\rm eq} = -\int dx \left\langle (\nabla_\perp \tilde{p})\tilde{\psi}\right\rangle \langle J_0\rangle' \tag{161}$$

$$\frac{\partial}{\partial t}\langle\psi\rangle = \langle E_\parallel\rangle = -\frac{\partial}{\partial r}\left\langle (\nabla_\perp\tilde{p})\tilde{\psi}\right\rangle. \tag{162}$$

These equations directly connect the configuration evolution (dynamo) to the fluctuation evolution. Hence, instead of approximating phase-shift between $(\nabla_\perp\tilde{p})$ and $\tilde{\psi}$ by the linear growth-rate, the phase shift can be determined by

solving the spectral equations for flux transport $\left\langle (\nabla_\perp \tilde{p})\tilde{\psi} \right\rangle$. Thus, it is natural this phase-shift depends on the correlation time τ_{cl} of the nonlinear coupling (triplet) process. This approach allows us to relate turbulent transport of flux to the energy relaxation and dynamo process.

The spectral equation for flux transport can be derived by defining the two-point correlation $\left\langle (\nabla_\perp \tilde{p})\tilde{\psi} \right\rangle$ by

$$\left\langle (\nabla_\perp \tilde{p})\tilde{\psi} \right\rangle = \left\{ \left\langle (\nabla_{\perp 1} \tilde{p}(1))\, \tilde{\psi}(2) \right\rangle + \left\langle (\nabla_{\perp 2} \tilde{p}(2))\, \tilde{\psi}(1) \right\rangle \right\}$$

where the indices 1 and 2 represent two different spatial positions, and using Eqs. (125)-(126). After symmetrizing, the resulting evolution equation for $\left\langle (\nabla_\perp \tilde{p})\tilde{\psi} \right\rangle$ is given by

$$\frac{\partial}{\partial t} \left\langle (\nabla_\perp \tilde{p})\tilde{\psi} \right\rangle - \eta \left\langle (\nabla_\perp \tilde{p})(\nabla_\perp^2 \tilde{\psi}) \right\rangle + \hat{T}_{12} = \hat{S}^0_{12} \tag{163}$$

where the triplet is

$$\begin{aligned} \hat{T}_{12} = & \left\langle (\nabla_{\perp 1} \tilde{p}(1)) \cdot (\nabla_{\perp 2} \tilde{p}(2)) \times \hat{z} \cdot \nabla_{\perp 2} \tilde{\psi}(2) \right\rangle \\ & + \alpha \left\langle \tilde{\psi}(2) \cdot \nabla_{\perp 1} \left(\nabla_{\perp 1} \tilde{\psi}(1) \times \hat{z} \cdot \nabla_{\perp 1} \tilde{J}(1) \right) \right\rangle + \langle 1 \longleftrightarrow 2 \rangle \end{aligned} \tag{164}$$

and the source is

$$\begin{aligned} \hat{S}^0_{12} = & -\alpha \langle J_0 \rangle' \left\langle \tilde{\psi}(2) \cdot \nabla_{\perp 1} \left(\nabla_{y1} \tilde{\psi}(1) \right) \right\rangle + \alpha \left\langle \tilde{\psi}(2) \cdot \nabla_{\perp 1} \left(\nabla^{(0)}_{\|1} \tilde{J}(1) \right) \right\rangle \\ & - \left\langle (\nabla_{\perp 1} \tilde{p}(1)) \cdot \left(\nabla^{(0)}_{\|2} \tilde{p}(2) \right) \right\rangle + \langle 1 \longleftrightarrow 2 \rangle . \end{aligned} \tag{165}$$

Here, the slow time-scale variations are described by the time derivatives, and $\langle 1 \longleftrightarrow 2 \rangle$ stands for term with indices 1 and 2 exchanged. Now, we can find the evolution operator for the $\left\langle (\nabla_\perp \tilde{p})\tilde{\psi} \right\rangle$ correlation using the spatial representation technique which has been developed to solve mode coupling equations

in the context of various fluid plasma systems.[52,53] The weak coupling closure with standard iteration scheme in the relative coordinate system $(\vec{x}_+, \vec{x}_-)$ is used to renormalize the triplets. Here, the average position is defined by $\vec{x}_+ = \frac{1}{2}(\vec{x}_1 + \vec{x}_2)$ and the relative position is defined by $\vec{x}_- = \frac{1}{2}(\vec{x}_1 - \vec{x}_2)$. After straightforward manipulation, the renormalized spectral equation for flux transport is given by

$$\frac{\partial}{\partial t}\left\langle(\nabla_\perp\tilde{p})\tilde{\psi}\right\rangle - (\eta+\eta^A)\frac{\partial^2}{\partial x_-^2}\left\langle(\nabla_\perp\tilde{p})\tilde{\psi}\right\rangle + \frac{\partial}{\partial x_-}a_-^x\frac{\partial}{\partial x_-}\left\langle(\nabla_\perp\tilde{p})\tilde{\psi}\right\rangle = \hat{S}_{12}^0 \tag{166}$$

where the average over the $\vec{x}_+$-coordinate has been performed and important relative radial diffusion effects have been retained. The renormalized triplet (from the diamagnetic convection term) approximates the fluid convection of magnetic flux as the scale-independent anomalous resistivity η^A which has the form of $D_{\vec{k}}$ in one-point theory, Eq. (151). However, the renormalized triplet from $\mathbf{J}\times\mathbf{B}$-torque approximates the Alfvénic effect as a scale-dependent anomalous dissipation which is defined by

$$a_-^x = \frac{\alpha}{2}\left(2\mathcal{A}_{\vec{k}} - \mathcal{A}_x^{(1,2)} - \mathcal{A}_x^{(2,1)}\right) \tag{167}$$

where the scale-independent piece $\mathcal{A}_{\vec{k}}$ is same as Eq. (152) which accounts for correlated diffusion and the scale-dependent piece is

$$\left(\mathcal{A}_x^{(1,2)} + \mathcal{A}_x^{(2,1)}\right) \simeq \sum_{\vec{k}'}\cos(\vec{k}'\cdot\vec{x}_-)\frac{(k_y')^2\left(1-\frac{n^2}{n'^2}\right)\left(\frac{\Delta'_{\vec{k}''}g}{\pi W_c\bar{x}_R^2}\right)}{\left[\Delta\omega_{\vec{k}''}+i\omega_*''\right]\left[1+\frac{x^2}{W_c^2}\right]}\left\langle\tilde{\psi}_{-\vec{k}''}\tilde{J}_{\vec{k}'}\right\rangle \tag{168}$$

which accounts for incoherent mode coupling processes. In order to estimate the characteristic time for the relaxation of the two-point correlation from evolution

equation Eq. (166), it is necessary to invert the evolution operator. The steady-state solution of Eq. (166) can be formally written as

$$\left\langle (\nabla_\perp \tilde{p})\tilde{\psi} \right\rangle = \tau_{\rm cl}(\vec{x}_-)\hat{S}^0_{12} \tag{169}$$

where the inverse operator $\tau_{\rm cl}(\vec{x}_-)$ describes the characteristic time associated with the relaxation of two-point correlation, and depends on the relative separation of the two points. Although obtaining an exact expression for $\tau_{\rm cl}(\vec{x}_-)$ using the Green's function method is possible, it is sufficient for our purposes to determine the characteristic time-scale associated with the moments of the Green's function for $\tau_{\rm cl}$. Following the same procedures given in Ref. 53, the life-time of the two-point correlation is given by

$$\tau_{\rm cl} = \left[-2\mathcal{A}_{\vec{k}}k^2_{0x}\right]^{-1} \ln\left\{1/\left[\left(k^2_{0x}x^2_- + k^2_{0y}y^2_- + k^2_{0z}z^2_-\right) - (\eta+\eta^A)/\mathcal{A}_{\vec{k}}\right]\right\} \tag{170}$$

where k_{0x}, k_{0y} and k_{0z} are the typical reciprocal scales or wavenumbers for the x, y and z directions, respectively. In particular, k_{0x} represents the radial correlation scale and k_{0y} (and k_{0z}) can be calculated by taking root-mean-square over the calculated wavenumber spectrum. As we discussed earlier in the context of one-point theory, the expression for the two-point correlation lifetime in Eq. (170) shows that the Alfvénic eddy-turnover time associated with $\mathcal{A}_{\vec{k}}$ (which has negative sign for $\Delta'_{\vec{k}''} < 0$) asymptotically determines the nonlinear time-scale, and leads to the logarithmic peaking of the correlation for small initial separation. At steady-state, these smaller scale correlations are removed by resistivity and scale independent anomalous resistive diffusion.

To complete the evaluation of the steady-state correlation $\left\langle (\nabla_\perp \tilde{p})\tilde{\psi} \right\rangle$, it is necessary to evaluate the source function $\hat{S}^0_{12}$ of fluctuations in Eq. (165). Because of the global nature of m=1 modes, the scale-independent source approximation which has been adopted for the case of localized modes,

is no longer applicable and the exact determination of the source function over the entire radial domain is extremely unlikely to be found analytically. (The linear eigenfunction for m=1 mode in an RFP plasma does not have a simple analytic form.) However, the existence of two disparate radial scales (regions) associated with resonant region (where $k_{||} \rightarrow 0$) and exterior region (where $\vec{B}\cdot\nabla J \rightarrow 0$) enable us to estimate the effective source of $\left\langle (\nabla_\perp \tilde{p})\tilde{\psi} \right\rangle$-correlation for each region. To illustrate the dynamical processes associated with the source in the two regions, the effective source for $\left\langle (\nabla_\perp \tilde{p})\tilde{\psi} \right\rangle$-correlation in $\vec{x}_1 \rightarrow \vec{x}_2$ limit can be written as

$$\hat{S}^0_{12}(x) \simeq \left[2\alpha \langle J_0 \rangle' \sum_{\vec{k}} k_y^2 \left| \tilde{\psi}_{\vec{k}} \right|^2 - 2\alpha \sum_{\vec{k}} \frac{(x_+ - 2x_s)}{L_s} k_y^2 \left(E^M_{\vec{k}} - E^I_{\vec{k}} \right) \right] \quad (171)$$

where L_s is the shear-length and x_s denotes the radial position of rational surface for mode $\vec{k}$. This source function has the characteristics of current-gradient relaxation in the first term and the ideal exterior dynamics in the second term.

Now, we need to examine the relationship between equilibrium magnetic energy relaxation and the evolution of average magnetic flux by rewriting the evolution equations of Eqs. (161)-(162) using the steady-state solution of Eq. (169), i.e.,

$$\frac{\partial}{\partial t} E^M_{\rm eq} = -\int dx \left\langle (\nabla_\perp \tilde{p})\tilde{\psi} \right\rangle \langle J_0 \rangle' = -\int dx \tau_{\rm cl} \hat{S}^0_{12} \langle J_0 \rangle' \quad (172)$$

$$\frac{\partial}{\partial t} \langle \psi \rangle = \langle E_{||} \rangle = -\frac{\partial}{\partial r} \left\langle (\nabla_\perp \tilde{p})\tilde{\psi} \right\rangle = -\frac{\partial}{\partial r} \left(\tau_{\rm cl} \hat{S}^0_{12} \right). \quad (173)$$

Using these related evolution equations for configuration and fluctuation, the dynamical processes associated with two different regions can be elucidated by taking two limits of the source function. For the resonant region where $k_{||} \rightarrow 0$,

hence $x_+ \to 2x_s$ limit in Eq. (171), the source function in the resonant region has the form given by

$$\hat{S}^0_{\mathrm{Res}} \simeq \sum_{\vec{k}} 2\alpha \langle J_0 \rangle' k_y^2 \left| \tilde{\psi}_{\vec{k}} \right|^2 = 2\alpha \langle J_0 \rangle' \sum_{\vec{k}} \left\langle \tilde{b}_r^2 \right\rangle_{\vec{k}}. \tag{174}$$

Using this resonance region contribution of the source function, we can calculate the time rate change of equilibrium magnetic energy due to resonant region as

$$\left(\frac{\partial}{\partial t} E^M_{\mathrm{eq}} \right)_{\mathrm{Res}} \simeq -2\alpha \int_{\mathrm{Res}} dx \left(\langle J_0 \rangle' \right)^2 \left(\sum_{\vec{k}} \tau_{\mathrm{cl}} \left\langle \tilde{b}_r^2 \right\rangle_{\vec{k}} \right). \tag{175}$$

Here, it is important to note that the time rate change of equilibrium magnetic energy due to the resonant region is negative definite and this represents the fact that the equilibrium magnetic energy stored in the current gradient has locally decreased in order to drive fluctuations within the resonant region. The related time evolution of the average flux in the resonant region is governed by

$$\frac{\partial}{\partial t} \langle \psi \rangle \simeq -\frac{\partial}{\partial r} \left[2\alpha \langle J_0 \rangle' \sum_{\vec{k}} \tau_{\mathrm{cl}} \left\langle \tilde{b}_r^2 \right\rangle_{\vec{k}} \right]. \tag{176}$$

The equilibrium magnetic energy relaxation rate Eq. (175), allows us to relate dynamical processes associated within the resonant region as follows:

i) the reduction of equilibrium magnetic energy stored in the current gradient drives fluctuations within the resonant region

ii) Along with the flattening of the current gradient, poloidal magnetic flux is expelled from the core region, resulting in an increase in safety factor at the magnetic axis $q(0)$.

The dynamics of the exterior region where the kink (Newcomb) structures prevail, can be examined by using an approximate source function

assuming the relation $\vec{B} \cdot \nabla J = 0$, i.e., $\tilde{B} \cdot \nabla \langle J_0 \rangle + \left\langle \vec{B} \right\rangle \cdot \nabla \tilde{J} = 0$. Then, the source function for the exterior region can be obtained from Eq. (171) and is given by

$$\hat{S}^0_{\text{Ext}} \simeq 2\alpha \sum_{\vec{k}} \tau_{\text{cl}} \frac{(x_+ - 2x_s)}{L_s} k_y^2 E^I_{\vec{k}}. \tag{177}$$

The time rate change of equilibrium magnetic energy due to this exterior source contribution can be obtained by

$$\left(\frac{\partial}{\partial t} E^M_{\text{eq}} \right)_{\text{Ext}} \simeq -2\alpha \int_{\text{Ext}} dx \, \langle J_0 \rangle' \sum_{\vec{k}} \tau_{\text{cl}} \frac{(x_+ - 2x_s)}{L_s} k_y^2 E^I_{\vec{k}}. \tag{178}$$

The sign of this rate depends on the safety factor profile shape through the sign of $k_{||}$ in the exterior region. For a normal RFP safety factor profile $(dq/dr) < 0$, the parallel wavenumber at the exterior has a positive sign $\left(\text{i.e.}, k_{||}\Big|_{\text{Ext}} > 0 \right)$, hence the time rate change of equilibrium magnetic energy in the exterior region has positive (definite) sign. This signature represents the fact that the fluctuation energy (driven at the resonant region) is absorbed into equilibrium magnetic energy, therefore the exterior kinking provides sink of fluctuation energy obtained from current gradient relaxation process. The related evolution of average magnetic flux associated with exterior dynamics is governed by

$$\frac{\partial}{\partial t} \langle \psi \rangle \simeq -\frac{\partial}{\partial r} \left\{ 2\alpha \sum_{\vec{k}} \tau_{\text{cl}} \frac{(x_+ - 2x_s)}{L_s} k_y^2 E^I_{\vec{k}} \right\}. \tag{179}$$

The dynamical processes associated with this average flux evolution can be examined for two different exterior regions, namely the outside of reversal surface $(r > r_{\text{rev}})$ and the core region $(r \simeq 0)$. For the outside of reversal surface, the average toroidal magnetic field evolves according to

$$\frac{\partial}{\partial t} \langle B_z \rangle \simeq \frac{\partial^2}{\partial r^2} \left\{ 2\alpha \sum_{\vec{k}} \frac{(x_+ - 2x_s)}{L_s} \tau_{\text{cl}} \, k_y^2 E^I_{\vec{k}} \right\}, \tag{180}$$

thus the sign of the time rate change of the average toroidal magnetic field at the outside of the reversal surface is negative (definite) for the $k_{\|}\Big|_{\text{Ext}} > 0$ condition of RFP plasma. This result represents the fact that the exterior dynamics (kinking) drives (aids) reversal of toroidal magnetic field. The dynamical processes associated with exterior dynamics can be summarized as follows:

i) the fluctuation energy is absorbed into the equilibrium magnetic energy, hence the exterior kinking provides sink of fluctuation energy

ii) the time rate change of average magnetic flux contributes to drive the reversal of toroidal magnetic field and contributes to raise the safety factor at the magnetic axis.

Having elucidated dynamical processes which connect the fluctuation evolution to the configuration evolution, and calculated the two-point correlation lifetime for $\left\langle (\nabla_{\perp}\tilde{p})\tilde{\psi} \right\rangle$-evolution which determines the phase-shift for flux transport, one can estimate the saturation level of m=1 fluctuations by noting that the Alfvénic eddy-turnover time associated with multiple helicity nonlinear $\vec{J}\times\vec{B}$ force determines nonlinear time scale, and also thus determines the saturation level. The renormalized nonlinear $\vec{J}\times\vec{B}$ force is represented by $\mathcal{A}_{\vec{k}}$ of Eq. (170). Balancing $\mathcal{A}_{\vec{k}}$ with the incoherent emission from driven current term determines cascading and the phase-shift in the transport of flux. The latter process is thus tied to the generation of smaller scales. In this approach, the inertia can be neglected ($\gamma \to 0$) and the source can be calculated using the phase-shift associated with correlation lifetime τ_{cl}. This notion indicates that the saturation level is independent of, or very weakly dependent on resistivity η. The magnetic fluctuation level has been estimated by using the scale

transformation method,[54] and is given by

$$\left(\frac{\delta B}{B_0}\right)_{\rm rms} \sim \left(\frac{B_\theta}{B_z}\right)^2 \frac{|\Delta'_{m=2}|}{\langle J_0\rangle'}.$$

This indeed shows the magnetic fluctuation level is independent of resistivity and the previous estimation $(\delta Br/B_0)_{\rm rms} \sim S^{-1/3}$ is actually too optimistic for future high-temperature experiments. However, since this theory predicts magnetic fluctuations even in the high temperature limit, these fluctuations will continue to support the very necessary turbulent dynamo which drives reversal and hence sustains a globally stable plasma in RFP configurations.

8.4 Summary and Conclusions

Observed low frequency magnetic turbulence in RFP is well correlated with anomalous heat conduction and dynamo activity. It is widely believed that resistive current gradient driven modes are responsible for driving magnetic fluctuations. Since the m=1 tearing modes appear to be the best candidate to explain these phenomena, the resistive MHD study of tearing mode turbulence was successful in predicting saturation levels which are consistent with experimental results. Here, we extend the previous work to high temperature regime by using a set of fluid equations for semi-collisional regime tearing modes, and propose a generalized nonlinear theory of the turbulent dynamo and magnetic relaxation.

The principal results of this chapter are:

(i) A set of fluid equations for a tearing mode in the semi-collisional regime is derived and is used to investigate current gradient driven m=1 magnetic turbulence in RFP. Using a standard iterative closure scheme, the renormalized spectral equations are derived and the stabilizing Alfvénic effects associated with the progressive current filamentation process (cascade) are identified as the saturation mechanism.

(ii) In order to calculate the source of fluctuation energy in the spectral energy equation without approximating the driving term by the linear growth rate, the two-point correlation equation for $\left\langle (\nabla_\perp \tilde{p})\tilde{\psi} \right\rangle$ is derived and the characteristic time scale τ_{cl} is calculated. The relaxation time τ_{cl} is shown to approach the Alfvénic eddy turnover time, asymptotically.

(iii) Using the relaxation time τ_{cl} of the two-point $\left\langle (\nabla_\perp \tilde{p})\tilde{\psi} \right\rangle$-correlation for the phase-shift between $\tilde{v}_r$ and $\tilde{\psi}$ in the source function, the source of fluctuation is calculated and the direct relationship between fluctuation evolution and configuration evolution is identified. The dynamical processes in the two separate regions of kink-tearing mode activity, i.e., the resonant region ($k_\parallel \rightarrow 0$) and the exterior region ($\vec{B} \cdot \nabla J \rightarrow 0$), are explored and the calculated magnetic fluctuation level is shown to be independent of, or very weakly dependent on the magnetic Reynolds number S. Thus, dynamo related heat transport even in the high temperature regime, is predicted. However, this magnetic fluctuation will provide the dynamo mechanism for sustaining the stable magnetic configuration in future experiments.

In this chapter, the effects of the electrostatic potential on the nonlinear evolution of semi-collisional tearing mode has been ignored for simplicity. The validity of this approximation is not rigorously established in the nonlinear regime. This will be discussed in future publications.

CHAPTER 4. CONCLUSIONS AND REMARKS

In this dissertation, two types of low frequency turbulence, related to anomalous plasma losses and relaxation phenomena in magnetically confined plasma, have been investigated. They include ion-temperature-gradient-driven electrostatic turbulence in tokamaks and electromagnetic current-gradient driven tearing mode turbulence in high-temperature current-carrying plasma. The results provide reasonable explanations for the experimentally observed anomalous transport processes and for the correlation between fluctuations and relaxation phenomena. Furthermore, the methods developed for theoretical anaysis of these nonlinear processes can be applied to other similar nonlinear systems.

In Chapter II, we studied ion-temperature-gradient-driven turbulence. By solving the energy-conserving, renormalized spectrum energy equations (mode-coupling equations) with the spatial representation technique, it is possible to calculate the wavenumber spectrum of stationary turbulence and the resultant anomalous transport coefficients in a self-contained manner. This study also serves to relate complicated nonlinear theory to experimentally observable (measurable) quantities.

Although little change in the basic conclusions is to be expected, the theory can be applied to the toroidal branch of the ion-temperature-gradient-driven mode using the large-n ballooning representation. Also, extensions of the present analysis to investigate the weak shear regime and parallel momentum transport associated with these electrostatic fluctuations, are worthwhile and feasible.

The second type of low frequency turbulence under investigation is current-gradient driven tearing mode turbulence. In Chapter III, we studied these electromagnetic fluctuations by extending previous resistive MHD studies of the $m = 1$ kink-tearing system to the high temperature RFP plasma regimes, by applying a similar renormalization approach which was developed in Chapter II. We were successful in relating fluctuation evolution to configuration evolution through the role of the source function in the two seperate regions of the kink-tearing mode. Hence, this study provides a theoretical interpretation of the experimental observation in several contemporary RFP's and a theoretical prediction for the future high temperature RFP experiments.

An extension of the present analysis can be applied to the relaxation phenomena associated with magnetic turbulence in general, and would be worthwhile.

Appendix A :

The Fourier Transform of the Radially Averaged Correlation Lifetime

Here, we provide the details of the derivation of Eq. (83),

$$
\begin{aligned}
F(k_y,k_z) &= -\frac{1}{\Delta_x}\int_0^{\Delta_x} dx_- \int dy_- \int dz_- e^{-ik_y y_- - ik_z z_-}\bar{\tau}_{\mathrm{cl}}(x_-,y_-,z_-) \\
&= -\frac{1}{\Delta_x}\int_0^{\Delta_x} dx_- \int dy_- \int dz_- e^{-ik_y y_- - ik_z z_-} \ln\left\{\left(\frac{\alpha}{\alpha+1}\right)\right. \qquad (A1)\\
&\quad \left. + C\left[(1+\alpha)k_{ox}^2 x_-^2 + k_{oy}^2 y_-^2 + k_{oz}^2 z_-^2\right]\right\}.
\end{aligned}
$$

Transforming to a polar coordinate system given by

$$
\begin{aligned}
u^2 &= \left[\frac{x_-^2}{\Delta_x^2}\right] \\
\rho^2 &= C\left(k_{oy}^2 y_-^2 + k_{oz}^2 z_-^2\right) \\
y_- &= \frac{\rho}{k_{oy}\sqrt{C}}\sin\theta \qquad (A2)\\
z_- &= \frac{\rho}{k_{oz}\sqrt{C}}\cos\theta,
\end{aligned}
$$

this yields

$$
\begin{aligned}
F(k_y,k_z) = \left[\frac{2}{k_{oy}k_{oz}C}\right]\int_0^{\sqrt{1-a^2}} \rho d\rho \int_0^{2\pi} d\theta e^{-i\frac{\rho}{\sqrt{C}}\left(\frac{k_y}{k_{oy}}\sin\theta + \frac{k_z}{k_{oz}}\cos\theta\right)} \\
\left[\sqrt{1-(a^2+\rho^2)} - \sqrt{a^2+\rho^2}\cos^{-1}\left(\sqrt{a^2+\rho^2}\right)\right], \qquad (A3)
\end{aligned}
$$

where $a^2 \equiv \frac{\alpha}{\alpha+1}$.

Using Jacobi-Anger expansion,[55] i.e.

$$\begin{aligned}&\int_0^{2\pi} d\theta e^{-i\rho/\sqrt{C}\left(\left(k_y/k_{oy}\right)\sin\theta+\left(k_z/k_{oz}\right)\cos\theta\right)}\\&=\sum_{m=-\infty}^{\infty}(-i)^m(2\pi)J_m\left(\frac{k_y\rho}{k_{oy}\sqrt{C}}\right)J_m\left(\frac{k_z\rho}{k_{oz}\sqrt{C}}\right),\end{aligned}\tag{A4}$$

and using Neumann's addition theorem for Bessel functions, i.e.

$$J_0\left(\frac{\beta}{\sqrt{C}}\rho\right)=\sum_{m=-\infty}^{\infty}(-i)^m J_m\left(\frac{k_y}{k_{oy}\sqrt{C}}\rho\right)J_m\left(\frac{k_z}{k_{oz}\sqrt{C}}\rho\right)\tag{A5}$$

where $\beta=\sqrt{\left(k_y/k_{oy}\right)^2+\left(k_z/k_{oz}\right)^2}$, we then arrive at the expression given in Eq. (83)

$$\begin{aligned}F\left(k_y,k_z\right)=&\left[\frac{4\pi}{Ck_{oy}k_{oz}}\right]\int_0^{\sqrt{1-a^2}}\rho d\rho J_0\left(\frac{\beta}{\sqrt{C}}\rho\right)\left[\sqrt{1-\left(a^2+\rho^2\right)}\right.\\&\left.-\sqrt{a^2+\rho^2}\cos^{-1}\left(\sqrt{a^2+\rho^2}\right)\right].\end{aligned}\tag{A6}$$

For the large Reynolds number regime, Eq. (A6) can be approximated by

$$F\left(k_y,k_z\right)=\left(\frac{4\pi}{k_{oy}k_{oz}}\right)\int_0^1\rho d\rho J_0(\beta\rho)\left[\sqrt{1-\rho^2}-\rho\cos^{-1}\rho\right].\tag{A7}$$

Integrating over k_z yields the poloidal wavenumber spectrum given in Eq. (84)

$$F\left(k_y\right)=\left(\frac{4\pi^2}{k_{oy}}\right)\left(\frac{k_{oy}}{k_y}\right)^2\left[1-J_0\left(\frac{k_y}{k_{oy}}\right)\right].\tag{A8}$$

Appendix B :
Fluid Equations for Impurity Gradient Effects

We outline the derivation of model equations of impurity gradient effects η_i-mode turbulence discussed in Section 2.4-B. The fluid model consists of equations for background ions, Eqs. (2)-(5), and equations for cold impurity ions. Using the same normalization as in Section 2.2 and the quasineutrality condition gives

$$\frac{\partial}{\partial t}\left(1-\frac{n_{oi}}{n_{oe}}\nabla_\perp^2\right)\tilde{\phi}+\frac{1}{n_{oe}}\left(\frac{n_{oi}}{L_{ni}}+\frac{Zn_{oI}}{L_{nI}}\right)\nabla_y\tilde{\phi}+\left(\frac{1+\eta_i}{\tau}\right)\frac{n_{oi}}{n_{oe}}\frac{1}{L_{ni}}\nabla_y\left(\nabla_\perp^2\tilde{\phi}\right)$$
$$-\frac{n_{oi}}{n_{oe}}\hat{b}\times\nabla\tilde{\phi}\cdot\nabla_\perp\left(\nabla_\perp^2\tilde{\phi}\right)+\frac{n_{oi}}{n_{oe}}\nabla_\parallel\tilde{v}_{\parallel i}+Z\frac{n_{oI}}{n_{oe}}\nabla_\parallel\tilde{v}_{\parallel I}=0 \qquad (B1)$$

$$\frac{\partial}{\partial t}\tilde{v}_{\parallel i}+\hat{b}\times\nabla\tilde{\phi}\cdot\nabla\tilde{v}_{\parallel i}-\mu_i\nabla_\parallel^2\tilde{v}_{\parallel i}=-\nabla_\parallel\tilde{\phi}-\nabla_\parallel\tilde{p}_i \qquad (B2)$$

$$\frac{\partial}{\partial t}\tilde{v}_{\parallel I}+\hat{b}\times\nabla\tilde{\phi}\cdot\nabla\tilde{v}_{\parallel I}-\mu_I\nabla_\parallel^2\tilde{v}_{\parallel I}=-Z\frac{m_i}{m_I}\nabla_\parallel\tilde{\phi} \qquad (B3)$$

$$\frac{\partial}{\partial t}\tilde{p}_i+\hat{b}\times\nabla\tilde{\phi}\cdot\nabla\tilde{p}_i+\left(\frac{1+\eta_i}{\tau}\right)\frac{1}{L_{ni}}\nabla_y\tilde{\phi}=-\frac{\Gamma}{\tau}\nabla_\parallel\tilde{v}_{\parallel i}, \qquad (B4)$$

where n_{oi}, n_{oe} and n_{oI} are background ion density, electron density and impurity density, respectively.

REFERENCES

1. M. Greenwald et al., *IAEA 10th International Conference on Plasma Physics and Controlled Nuclear Fusion Research*, London, Vol. I, 45 (1984).
2. S. M. Wolfe, M. Greenwald et al., MIT Report PFC/JA-85-31, (1985); submitted to Nuclear Fusion.
3. R. J. Groebner et al., GA Report GA-A17935, (1985).
4. B. Coppi, M. N. Rosenbluth, and R. Z. Sagdeev, Phys. Fluids **10**, 582 (1967); L. I. Rudakov and R. Z. Sagdeev, Dokl. Akad. Nauk. SSSR **138**, 581 (1961) [Sov. Phys. Dokl. **6**, 415 (1965)].
5. L. Garcia, P. H. Diamond, B. A. Carreras, and J. D. Callen, Phys. Fluids **28**, 2137 (1985).
6. T. Antonsen, B. Coppi, and R. Englade, Nucl. Fusion **19**, 641 (1979).
7. W. Horton, D.-I. Choi, and W. M. Tang, Phys. Fluids **24**, 1077 (1981).
8. W. Horton, R. D. Estes, and D. Biskamp, Plasma Physics **22**, 663 (1980).
9. P. N. Guzdar, Liu Chen, W. M. Tang, and P. H. Rutherford, Phys. Fluids **26**, 673 (1983).
10. S. I. Braginskii, in **Review of Plasma Physics**, (M. A. Leontovich, ed.) Consultants Bureau, NY, Vol. I, (1965).
11. F. L. Hinton and C. W. Horton, Phys. Fluids **14**, 116 (1971).
12. Y. K. Pu and S. Migliuolo, Phys. Fluids **28**, 1722 (1985); S. Migliuolo, Phys. Fluids **28**, 2778 (1985).

13. R. E. Waltz, W. Pfeiffer, and R. R. Dominguez, Nucl. Fusion **20**, 43 (1980).

14. G. S. Lee and P. H. Diamond, *Proc. of Annual Controlled Fusion Theory Conference*, Paper 1S24 (1985).

15. P. H. Diamond, R. D. Hazeltine, Z. G. An, B. A. Carreras, and H. R. Hicks **27**, 1449 (1984).

16. A. Hasegawa and K. Mima, Phys. Rev. Lett. **39**, 205 (1977).

17. T. H. Dupree, Phys. Fluids **15**, 334 (1972).

18. P. W. Terry and P. H. Diamond, Phys. Fluids **28**, 1419 (1985).

19. J. W. Connor, Culham Laboratory Report TPN/85/26 (1985); J. W. Connor and J. B. Taylor, Phys. Fluids **27**, 2676 (1984).

20. C. S. Chang and F. L. Hinton, Phys. Fluids **25**, 1493 (1982).

21. Z. G. An, G. S. Lee, and P. H. Diamond, Institute for Fusion Studies Report **196**, (1985).

22. G. Becker, *12th European Conference on Controlled Fusion and Plasma Physics*, Budapest, Vol. II, 454 (1985).

23. J. C. Adam, W. M. Tang, and P. H. Rutherford, Phys. Fluids **19**, 561 (1976).

24. B. Coppi and C. Spight, Phys. Rev. Lett. **41**, 551 (1978).

25. Yu. N. Dnestrovskii, S. V. Neudachin, and G. V. Pereverzev, Fiz. Plazmy **10**, 236 (1984) [Sov. J. Plasma Phys. **10**, 137 (1984)].

26. D. W. Ross and W. L. Rowan, Private Communication, (1985).

27. E. A. Lazarus et al., J. Nucl. Mater. **121**, 61 (1984).

28. G. H. Neilson et al., Nucl. Fusion **23**, 285 (1983).

29. D. W. Swain and G. H. Neilson, Nucl. Fusion **22**, 1015 (1982).

30. B. A. Carreras, P. H. Diamond, M. Murakami et al., Phys. Rev. Lett. **50**, 503 (1983).

31. P. H. Diamond, P. L. Similon, T. C. Hender, and B. A. Carreras, Phys. Fluids **28** 1116 (1985).

32. M. Murakami et al., *IAEA 10th International Conference on Plasma Physics and Controlled Nuclear Fusion Research*, London, Vol. I, 87 (1984).

33. B. Coppi, H. P. Furth, M. N. Rosenbluth, and R. Z. Sagdeev, Phys. Rev. Lett. **17**, 377 (1966).

34. W. M. Tang, R. B. White, and P. N. Guzdar, Phys. Fluids **23**, 167 (1980).

35. I.H. Hutchinson, et al., Nucl. Fusion **24**, 59 (1984).

36. G.A. Wurden, Phys. Fluids **27**, 554 (1984).

37. R.A. LaHaye, et al., Nucl. Fusion **21**, 1235 (1982).

38. R.G. Watt and R.A. Nebel, Phys. Fluids **26**, 1168 (1983).

39. E.J. Caramana, et al., Phys. Fluids **26**, 1305 (1983).

40. Z.G. An, et al., Plasma Physics and Controlled Nuclear Fusion Research (IAEA, London, England), Vol. 2, 231 (1984).

41. J.B. Taylor, Phys. Rev. Lett. **33**, 134 (1974).

42. H.R. Strauss, Phys. Fluids **19**, 134 (1976).

43. H.R. Strauss, Phys. Fluids **27**, 2580 (1984).

44. A. Hasegawa and M. Wakatani, Phys. Fluids **26**, 1770 (1983).

45. R.D. Hazeltine, Phys. Fluids **26**, 3242 (1983).

46. J.F. Drake and T.M. Antonsen, Jr., Phys. Fluids **27**, 898 (1984).

47. R.D. Hazeltine and J.D. Meiss, Phys. Reports **121**, 1 (1985).

48. A.B. Rechester and M.N. Rosenbluth, Phys. Rev. Lett. **40**, 38 (1978).

49. J.F. Drake and Y.C. Lee, Phys. Fluids **20**, 1341 (1977).

50. M.N. Rosenbluth, et al., Phys. Fluids **16**, 1894 (1973).

51. P.H. Diamond, et al., Phys. Fluids **27**, 1449 (1984).

52. P.W. Terry and P.H. Diamond, Phys. Fluids **28**, 1419 (1985).

53. G.S. Lee and P.H. Diamond, Institute for Fusion Studies Report #209 (1986), submitted to Phys. Fluids.

54. J.W. Connor and J.B. Taylor, Plasma Physics and Controlled Nuclear Fusion Research (IAEA, London, England), Vol. 2, 13 (1984).

55. G. N. Watson, **A Treatise on the Theory of Bessel Functions** (Cambridge, 1966).

VITA

Gyung Su Lee was born on June 7, 1956, in Taegu, Republic of Korea, the first son of Dae Whan Lee and Chunja (Kwon) Lee. He entered The Seoul National University, Seoul, Korea in March 1975, majoring in physics. In Feburary 1979, he received the degree of Bachelor of Science in Physics. After graduation, he entered The Graduate School of The Seoul National University and worked on theoretical particle physics. He moved to The Graduate School of The University of Chicago in September, 1980. In January, 1981, he entered The Graduate School of The University of Texas at Austin and has been employed as research assistant since then. On April 28, 1985 he was married to Kyesun Kim of Taegu, Korea.

Permanent Address: 186 Bi-San Dong, Seo-Gu
Taegu, Republic of Korea